UNIVERSIDADE FEDERAL DE PERNAMBUCO
CENTRO DE TECNOLOGIA E GEOCIÊNCIAS
DEPARTAMENTO DE ENGENHARIA CIVIL E AMBIENTAL
PROGRAMA DE PÓS-GRADUAÇÃO EM ENGENHARIA CIVIL

SAVANNA CRISTINA MEDEIROS D'AGUIAR

HYDROSTATIC COLLAPSE OF CORRODED SUBSEA PIPELINES UNDER EXTERNAL PRESSURE

Recife/PE
2025

SAVANNA CRISTINA MEDEIROS D'AGUIAR

HYDROSTATIC COLLAPSE OF CORRODED SUBSEA PIPELINES UNDER EXTERNAL PRESSURE

Tese apresentada ao Programa de Pós-Graduação Engenharia Civil da Universidade Federal de Pernambuco, como requisito parcial para obtenção do título de doutora em Engenharia Civil.
Área de concentração: Estruturas

Orientadora: Profª. Dra. Silvana Maria Bastos Afonso da Silva

Coorientador: Prof. Dr. Renato de Siqueira Motta

Recife/PE

2025

.Catalogação de Publicação na Fonte. UFPE - Biblioteca Central

D'aguiar, Savanna Cristina Medeiros.
Hydrostatic Collapse of Corroded Subsea Pipelines under External Pressure / Savanna Cristina Medeiros D'aguiar. - Recife, 2025.
120f.: il.

Tese (Doutorado) - Universidade Federal de Pernambuco, Centro de Tecnologia e Geociências, Programa de Pós-Graduação em Engenharia Civil, 2025.
Orientação: Silvana Maria Bastos Afonso da Silva.
Coorientação: Renato de Siqueira Motta.
Inclui referências.

1. Corrosion; 2. Subsea Pipelines; 3. Collapse Pressure; 4. Interacting defects; 5. Complex defects; 6. Finite Element Method. I. Silva, Silvana Maria Bastos Afonso da. II. Motta, Renato de Siqueira. III. Título.

UFPE-Biblioteca Central

SAVANNA CRISTINA MEDEIROS D'AGUIAR

HYDROSTATIC COLLAPSE OF CORRODED SUBSEA PIPELINES UNDER EXTERNAL PRESSURE

Tese apresentada ao Programa de Pós-Graduação Engenharia Civil da Universidade Federal de Pernambuco, como requisito parcial para obtenção do título de doutora em Engenharia Civil.
Área de concentração: Estruturas

Aprovada em 09/07/2025

Orientadora: Profª. Dra. Silvana Maria Bastos Afonso da Silva

Coorientador: Prof. Dr. Renato de Siqueira Motta

BANCA EXAMINADORA

Participação por videoconferência
Prof. Dr. Bernardo Horowitz (Examinador Interno)
Universidade Federal de Pernambuco (UFPE)

Participação por videoconferência
Engº Dr. Divino Jose da Silveira Cunha (Examinador externo)
PETROBRAS/CENPES (Centro de Pesquisas da Petrobras)

Participação por videoconferência
Prof. Dr. Evandro Parente Júnior (Examinador externo)
Universidade Federal do Ceará (UFC)

Participação por videoconferência
Profª. Dra. Juliana Von Schmalz Torres (Examinadora Externa)
Universidade Federal de Pernambuco (UFPE)

Participação por videoconferência
Prof. Dr. Ramiro Brito Willmersdorf (Examinador externo)
Universidade Federal do Pernambuco (UFPE)

AGRADECIMENTOS

A Deus, toda honra e glória.

Aos meus pais, Ana Santana e Sergio Henrique, por serem meu porto seguro, e ao meu esposo, Djanino Fernandes, pelo amor, companheirismo e incentivo. Nada disso teria sido possível sem o apoio incondicional de vocês.

Á minha família, sou eternamente grata pelo apoio em todas as etapas desta jornada. Em especial gostaria de agradecer a minha avó, Domerina Dantas, professora do ensino básico municipal, que me alfabetizou e despertou em mim o amor pelo conhecimento. Mesmo enfrentando o desafio da doença de Alzheimer, sua memória permanece viva em mim e continua a inspirar minha trajetória.

Á minha orientadora, professora Silvana Bastos, pela paciência, confiança e, principalmente, pela oportunidade de desenvolver este trabalho sob sua orientação. Agradeço também ao professor Renato Motta pelo conhecimento compartilhado e apoio na orientação deste trabalho. Com certeza, os considero referências acadêmicas fundamentais para minha formação.

Ao grupo de pesquisa PADMEC e seus integrantes, pelas trocas, parcerias e pela construção coletiva de ideias que fundamentaram este trabalho. Com menção especial para Álamo, Luccas e Paulo Sousa pela amizade e parceria durante este período.

Aos professores Bernardo Horowitz, Divino José da Silveira Cunha, Evandro Parente Júnior, Juliana Von Schmalz Torres e Ramiro Brito Willmersdorf, por gentilmente aceitarem compor a banca examinadora. Suas observações serão decisivas para o aprimoramento desta pesquisa e seus desdobramentos futuros.

Ao Professor Marcílio Nunes, meu orientador na graduação, registro minha profunda gratidão pela dedicação, paciência e incentivo ao longo daquela etapa tão importante da minha formação.

A todos os professores que marcaram minha formação — da graduação na Universidade Federal Rural do Semi-Árido, do mestrado na Universidade Federal do Ceará e do doutorado na Universidade Federal de Pernambuco —, minha sincera gratidão.

Aos amigos da graduação e da vida, Ruan, Jessyca, Ada, Sumaya, Michelle, Francisco e Cristiane pela amizade, incentivo e por sempre se alegrarem com minhas conquistas.

A todos os funcionários do Programa de Pós-Graduação em Engenharia Civil da Universidade Federal de Pernambuco (PPGEC/UFPE) pelo suporte ao longo do percurso.

À Fundação de Amparo à Ciência e Tecnologia do Estado de Pernambuco (FACEPE), ao Conselho Nacional de Desenvolvimento Científico e Tecnológico (CNPq), à Coordenação de Aperfeiçoamento de Pessoal de Nível Superior (CAPES), à Petrobras, ao Laboratório Integrado de Tecnologia em Petróleo, Gás e Biocombustíveis (i-LITPEG) e à Universidade Federal de Pernambuco (UFPE), pelo apoio institucional e financeiro que tornou esta pesquisa possível.

E a todas as pessoas que, mesmo não mencionadas nominalmente, sempre estarão guardadas em meu coração — aquelas que, direta ou indiretamente, contribuíram para a realização deste trabalho —, meu sincero agradecimento.

Savanna Cristina Medeiros D'Aguiar

RESUMO

Dutos submarinos são propensos a falhas que podem resultar em perdas econômicas e desastres ambientais catastróficos. A corrosão se destaca como um dos mecanismos de falha mais comuns em dutos offshore. A expansão de redes de dutos em águas profundas e ultraprofundas requer o aprimoramento dos métodos de avaliação do colapso hidrostático de dutos submarinos corroídos sob pressão externa. Apesar da crescente relevância do tema nos últimos anos, ainda existem lacunas significativas, especialmente na estimativa da pressão de colapso de dutos com defeitos de corrosão interativos ou complexos. Os métodos semiempíricos atualmente disponíveis na literatura dependem de simplificações que levam a estimativas excessivamente conservadoras. Por outro lado, a acurácia e a precisão das simulações numéricas via Método dos Elementos Finitos (MEF) exigem um alto custo computacional e tempo de processamento, inviabilizando sua aplicabilidade em larga escala. Diante disso, esta pesquisa tem como objetivo desenvolver uma metodologia mais acurada para avaliação da integridade de dutos submarinos corroídos. Inicialmente, a resposta ao colapso de dutos submarinos com dois ou mais defeitos de corrosão é analisada utilizando MEF. Novos fatores de ajuste são propostos para melhorar a precisão das previsões de colapso para defeitos isolados e interagentes. Posteriormente, este trabalho investigou o colapso hidrostático de dutos submarinos com perfis de corrosão reais, e os resultados permitiram o desenvolvimento de uma nova metodologia para estimar a pressão de colapso desses dutos. A metodologia é validada por meio de extensas simulações numéricas via MEF, confirmando sua aplicabilidade a diferentes cenários. Os resultados obtidos fornecem importantes contribuições para a avaliação da integridade de dutos submarinos corroídos, uma vez que os fatores de ajuste e a metodologia propostos apresentaram alta precisão e acurácia, podendo ser incorporados como ferramentas práticas para a indústria de petróleo e gás e para pesquisas.

Palavras-chave: Corrosão; Dutos submarinos, Pressão de Colapso; Defeitos Interagentes, Defeitos complexos; Método dos Elementos Finitos.

ABSTRACT

Subsea pipelines are prone to failures that can result in catastrophic economic losses and environmental disasters. Corrosion stands out as one of the most common failure mechanisms in offshore pipelines. The expansion of pipeline networks in deep and ultra-deep waters requires improving the methods for evaluating the hydrostatic collapse of corroded submarine pipelines under external pressure. Despite the topic's growing relevance in recent years, there are still significant gaps, especially in estimating the collapse pressure of pipelines with interactive or complex corrosion defects. The semi-empirical methods currently available in the literature rely on simplifications that lead to excessively conservative estimates. On the other hand, the accuracy and precision of numerical simulations via the Finite Element Method (FEM) require a high computational cost and processing time, making their applicability on a large scale unfeasible. In view of this, this research aims to develop a more accurate methodology for evaluating the integrity of corroded submarine pipelines. Initially, the collapse response of subsea pipelines with two or more corrosion defects is analyzed using FEM. New adjustment factors are proposed to improve the accuracy of collapse predictions for isolated and interacting defects. Subsequently, this work investigated the hydrostatic collapse of subsea pipelines with real corrosion profiles, and the results allowed the development of a new methodology to estimate the collapse pressure of these pipelines. The methodology is validated through extensive numerical simulations via FEM, confirming its applicability to different scenarios. The results obtained provide important contributions to evaluating the integrity of corroded subsea pipelines since the proposed adjustment factors and methodology presented high precision and accuracy and can be incorporated as practical tools for the oil and gas industry and research.

Keywords: Corrosion; Subsea pipelines, Collapse Pressure; Interacting defects; Complex defects; Finite Element Method.

FIGURE LIST

INTRODUCTION

LITERATURE REVIEW

AN INVESTIGATION ON THE COLLAPSE RESPONSE OF SUBSEA PIPELINES WITH INTERACTING CORROSION DEFECTS

NOVEL APPROACH OF COLLAPSE PRESSURE PREDICTION OF SUBSEA PIPELINES WITH REALISTIC CORROSION DEFECTS

ADVANCES IN RESEARCH

TABLE LIST

AN INVESTIGATION ON THE COLLAPSE RESPONSE OF SUBSEA PIPELINES WITH INTERACTING CORROSION DEFECTS

NOVEL APPROACH OF COLLAPSE PRESSURE PREDICTION OF SUBSEA PIPELINES WITH REALISTIC CORROSION DEFECTS

ADVANCES IN RESEARCH

LIST OF ABBREVIATIONS

ANP	Brazilian National Agency of Petroleum, Natural Gas and Biofuels
CoV	Coefficient of Variation
DNV	Det Norske Veritas
FE	Finite Element
FEA	Finite Element Analyses
FEM	Finite Element Method
MEF	Método dos Elementos Finitos
PADMEC	High-Performance Processing in Computational Mechanics
PCL	Patran Command Language
PIP	Pipe-In-Pipe
RBP	River Bottom Profile
RCA	Renewed Classical Approach
RO	Ramberg-Osgood
UFPE	Universidade Federal de Pernambuco
UK	United Kingdom
USA	United States of America

TABLE OF CONTENTS

1 INTRODUCTION

This thesis is part of the research line focused on the evaluation of the integrity and safety of submarine pipelines subjected to corrosion, a topic of great relevance for the safe and efficient operation of offshore infrastructure.

1.1 SUBSEA PIPELINE

In recent years, the operation of subsea pipelines has become essential for economic development associated with the exploration of petroleum resources. In this context, pipelines play a crucial role in the offshore production infrastructure, functioning as indispensable routes for continuously and safely transporting hydrocarbons extracted from the seabed (Bai; Bai, 2005)

Offshore pipelines can be classified according to their functionality within the production infrastructure (Guo *et al.*, 2014). Figure 1.1 shows the schematic of the components and infrastructure of the offshore production system.

Figure 1.1 - Schematic of offshore system components

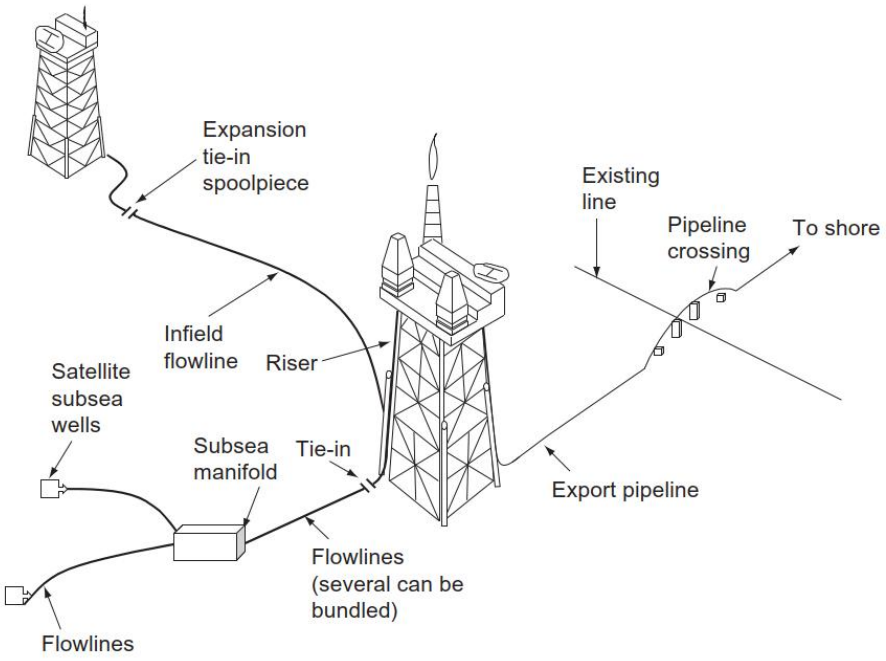

Source: Guo *et al.* (2014).

According to Kaiser (2020), Flowlines in Figure 1.1 transport unprocessed raw fluids, while Export pipelines transport processed oil and gas from platforms to the coast (Guo *et al.*, 2014). Each category contributes to the economic and operational viability of offshore oil and gas exploration and production activities.

Subsea pipelines can be categorized not only by their function but also by their structure. There are three main types: rigid pipelines, flexible lines, and pipe-in-pipe (PIP) systems. Although all configurations are used in offshore operations, rigid and flexible pipelines are the most common (Kaiser, 2020).

Rigid pipelines are made of carbon steel or a high-performance steel alloy, with additional coatings that provide corrosion protection. Flexible lines, on the other hand, are composed of multiple layers of steel wires and polymer coatings, which provide greater flexibility (Kaiser, 2020).

Advances in drilling and installation equipment have enabled the construction of wells and production infrastructures at depths greater than 3,000 meters, where the technological challenges are significantly more complex (Bruschi *et al.*, 2015). However, the authors emphasize that rigid pipelines, known for their reliability, remain the leading choice for transporting fluids in offshore systems.

Thus, this study highlights the assessment of rigid pipelines under external pressure, given their significance in offshore infrastructure, particularly in ultra-deepwater submarine settings.

1.2 MOTIVATION

According to the most recent data from the Brazilian National Agency of Petroleum, Natural Gas and Biofuels (ANP, 2023), offshore fields account for 97.6% of national oil and 87.2% of national natural gas production. In 2019, the network of submarine pipelines in Brazilian jurisdictional waters covered approximately 20,000 kilometers (ANP, 2019). However, the extension of the country's submarine pipeline network is expected to continue growing, especially with the advancement of pre-salt exploration.

Bruschi *et al.* (2015) emphasize that developing deepwater offshore fields has been a well-established industrial practice for over two decades. They point out that the primary regions involved in these activities are in the Atlantic Ocean, emphasizing the Gulf of Mexico, West Africa, and Brazil — an area known as the Golden Triangle.

In the international scenario, more recent research shows that the total length of the subsea pipeline network in the Gulf of Mexico region, located in the United States of America (USA), is approximately 37,000 kilometers (Xie; Meng; Chen, 2022). The United Kingdom (UK) Offshore Operators Association estimates that the North Sea

has 1,567 submarine pipelines, totaling around 25,000 kilometers in length (Eastvedt; Naterer; Duan, 2022).

However, subsea pipelines may be prone to failures that could result in economic losses for the oil and gas industry and trigger environmental disasters of catastrophic proportions. Sulaiman and Tan (2014) suggest that the distribution of causes of failures in offshore pipelines can be grouped into four main categories. As shown in Figure 1.2, corrosion is one of the most frequent causes of failures in subsea pipelines, accounting for 36% of the total.

Figure 1.2 - Cause of failures in subsea pipelines

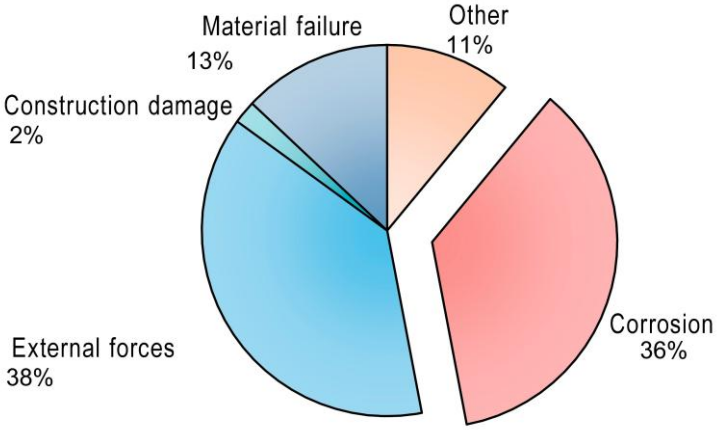

Source: Adapted from Sulaiman and Tan (2014)

Corrosion can occur on the external surface of the pipeline due to the loss of external coating caused by environmental agents and on the internal surface of the pipeline due to the action of the components of the transported fluid and its speed (Bhardwaj; Teixeira; Guedes Soares, 2022).

Figure 1.3 shows the incidents related to corrosion in onshore and offshore pipelines recorded in the USA over the last few years. In general, the frequency of incidents increases with the pipeline's age, showing that corrosion, as a time-dependent process, gradually reduces the pipeline's resistant capacity (Mahmoodian; Li, 2017). The slight decrease in incident frequency for pipelines older than 50 years may be associated with the decommissioning of older assets, which are progressively removed from operation as they reach the end of their service life.

Figure 1.3 - Incidents caused by corrosion in onshore and offshore pipelines (2012-2021)

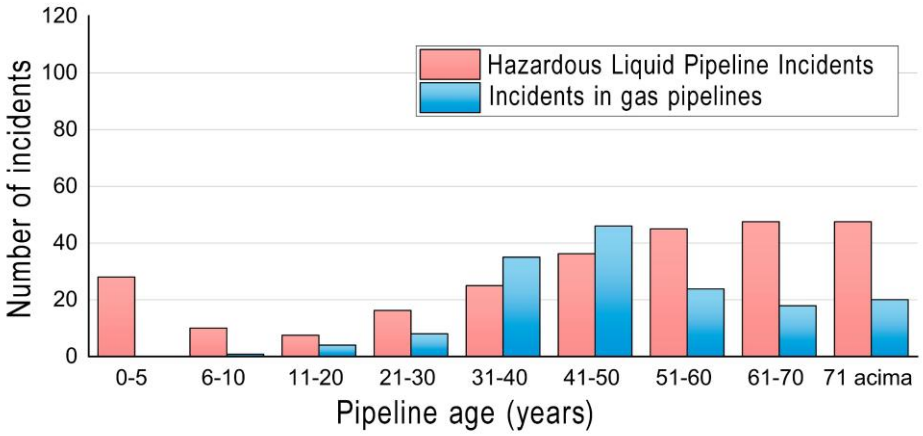

Source: Adapted from PHMSA (2022).

According to Muthukumar (2014), the cost of corrosion of gas and liquid transmission pipelines in the United States exceeds $7 billion. Although major oil-producing countries in the Gulf region do not publicly disclose specific data, the cost is estimated to be very high due to the corrosive environment in the region.

In this context, assessing the structural integrity of pipelines affected by corrosion is essential to determine the residual resistance of these components. This allows the formulation of an appropriate maintenance policy, ensuring these pipelines operate safely, helping to prevent catastrophic accidents and economic losses for industry.

Hydrostatic collapse is one of the leading design criteria for offshore pipelines, especially for lines installed in deep waters (Sakakibara; Kyriakides; Corona, 2008). Therefore, predicting the collapse pressure of corroded pipelines in deep waters is of paramount importance to ensure these structures' safety and efficiency (Gong *et al.*, 2021).

This thesis is part of a long-standing research initiative developed by the High-Performance Computing Group in Computational Mechanics (PADMEC) at the Federal University of Pernambuco (UFPE), in collaboration with the Petrobras Research and Development Center (CENPES). Over the past decade, this partnership has advanced methodologies for evaluating the structural performance of corroded pipelines under internal pressure. One key outcome is the PIPEFLAW system — an automated tool for modeling and numerical analysis of corroded pipelines using the finite element method (FEM). Several studies have validated the effectiveness of this tool in

assessing the integrity of corroded pipelines (Bruère *et al.*, 2019; Ferreira *et al.*, 2021; Motta *et al.*, 2021, 2017; Pimentel *et al.*, 2020; Soares *et al.*, 2019).

Currently, literature lacks comprehensive methods for estimating the hydrostatic collapse pressure of corroded subsea pipelines under external pressure (Tian et al., 2024). To address this gap — and building upon the research foundation established by the PADMEC group — this work investigates the hydrostatic collapse behavior of corroded subsea pipelines using the Finite Element Method (FEM).

1.3 PROBLEM STATEMENTS

This research is mainly aimed at addressing the following main problems:

- Corrosion is one of the leading causes of structural failures in submarine pipelines, compromising their integrity and operational safety.
- The hydrostatic collapse of subsea pipelines can cause severe environmental disasters and result in high costs for the offshore industry.
- Hydrostatic collapse analysis is a complex process, which involves the consideration of several factors, such as material properties, loading conditions, geometric imperfections and interactions with the underwater environment.
- Multiple corrosion defects in proximity can significantly reduce the pipeline's collapse capacity.
- Current codes and semi-empirical approaches to assessing the hydrostatic collapse of corroded subsea pipelines under external pressure are based on simplified assumptions.
- Conservative corrosion assessment methods impose premature repair or replacement of pipelines, which can lead to significantly increased operating costs for the oil and gas industry.

1.4 OBJECTIVES

1.4.1 Main objective

The main objective of this study is to evaluate the hydrostatic collapse behavior of corroded subsea pipelines and to develop an integrity assessment approach for subsea pipelines with realistic corrosion geometries.

1.4.2 Secondary objectives

- Investigate the interaction of multiple idealized corrosion defects in subsea pipelines under external pressure, exploring the effects of different parameters, such as defect geometry, spacing between defects, initial ovality, and the influence of temperature change.
- Propose new adjustment factors for predicting the collapse pressure of subsea pipelines with idealized single and multiple corrosion defects, considering the initial ovality and the influence of temperature change.
- Utilizes a sub-defect mapping approach to enhance the prediction of collapse pressure of pipes with realistic corrosion defects.
- Introduces a novel approach for evaluating the collapse pressure of pipelines with realistic corrosion defects.

1.5 THESIS SCOPE AND ORGANIZATION

This thesis is structured into six chapters, including this introduction chapter. Chapters 3 and 4 are presented in the format of fully published for publication journal papers. Details on selected journals, authors, and bibliographical information are provided on section 1.6. Each Chapter is described as follows:

- **Chapter 2** provides a literature review of related research, focusing on the key findings regarding the collapse response of subsea pipelines. In addition, this chapter explores the fundamental theoretical principles of the hydrostatic collapse prediction of intact and corroded subsea pipelines.

- **Chapter 3** presents the first article that studies the collapse response of subsea pipelines with multiple corrosion defects using nonlinear FE analysis and presents new adjustment factors to introduce the effect of initial ovality and temperature variation in the collapse response of subsea pipelines. These findings enhance our understanding of subsea pipeline collapse and provide practical insights for the industry.

- **Chapter 4** presents que second article that introduces a novel approach to assessing the structural integrity of subsea pipelines with realistic corrosion defects. The proposed method's accuracy is validated through FE analyses, demonstrating its robustness and reliability.

- **Chapter 5** discusses some advances following the development and validation of the novel semi-analytical approach described in Chapter 4. It includes an extensive parametric study to assess the impact of the metal volume loss on realistic corrosion defects using the novel approach. Additionally, in this chapter, the applicability of the proposed approach is tested to predict the collapse pressure of subsea pipelines with interacting corrosion defects.

- **Chapter 6** summarizes the final conclusions of this thesis and offers recommendations for future research.

1.6 PUBLICATIONS OF THIS RESEARCH

Chapter 3 of this research has been published in the following journal article:

- D’Aguiar, S. C. M; Motta, R. de S.; Afonso, S. M. B. (2024) An investigation on the collapse response of subsea pipelines with interacting corrosion defects. **Engineering Structures**, v. 321, p. 118911. DOI: https://doi.org/10.1016/j.engstruct.2024.118911

Chapter 4 of this research has been published in the following journal article:

- D’Aguiar, S. C. M; Motta, R. de S.; Ferreira, A. D. M.; Afonso, S. M. B. (2025) Novel approach of collapse pressure prediction of subsea pipelines

with realistic corrosion defects. **Ocean Engineering,** v. 337, p. 121895. DOI: https://doi.org/10.1016/j.oceaneng.2025.121895

Moreover, research related to this thesis has also been presented in the proceedings of the following international conferences:

- D'Aguiar S. C. M, Motta, R. de S; Afonso, S. M. B. (2023) Collapse of subsea pipelines: Numerical study on the interaction of corrosion defects with different geometrical properties. **27th COBEM – International Congress of Mechanical Engineering**. Florianópolis, Brasil.
  This paper was recognized for its contribution to the field and was awarded the **Springer Best Paper Award** in the category of Fracture, Fatigue, and Structural Integrity at the 27th International Congress of Mechanical Engineering - COBEM 2023, organized by ABCM.

- D'Aguiar S. C. M, Motta, R. de S; Ferreira, A. D. M., Afonso, S. M. B. (2024) An investigation on the collapse pressure prediction of subsea pipelines with realistic corrosion defects. **XLV Ibero-Latin American Congress on Computational Methods in Engineering**. Maceió, Brasil. Doi: https://doi.org/ 10.55592/cilamce.v6i06.8138

2 LITERATURE REVIEW

This chapter presents fundamental concepts on the collapse behavior of subsea pipelines and reviews previous research conducted on the collapse assessment of intact and corroded pipelines. The literature review focuses on basic principles, experimental and numerical investigations, semi-empirical approaches, and key findings.

Initially, a thorough review of the existing theoretical framework follows, focusing on determining the collapse pressure of intact pipelines — those without corrosion defects. Subsequently, the analysis then delves into the study of the hydrostatic collapse of corroded pipelines, which constitutes the main contribution of this work.

2.1 HYDROSTATIC COLLAPSE IN INTACT SUBSEA PIPELINES

According to Nogueira and Mckeehan (2005), offshore pipelines generally operate under conditions where the external pressure exceeds the internal pressure, resulting in differential pressure across the pipeline wall. In deepwater and ultra-deepwater, the external hydrostatic pressure becomes the dominant load condition and is the main factor determining the minimum pipeline wall thickness (Novitsky; Gray, 2003; Torselletti *et al.*, 2003).

As a result, the design of subsea pipelines in deep and ultra-deep waters is primarily focused on ensuring resistance to collapse. Figure 2.1 illustrates the cross-section of a collapsed pipeline.

Offshore oil pipelines are usually installed empty to minimize the stress caused by their weight. Additionally, these pipelines undergo periodic depressurization during operation for maintenance purposes (Kyriakides; Corona, 2007). So, the collapse criterion is based on the empty pipeline condition. This approach ensures that structural integrity is evaluated under the most severe conditions.

Figure 2.1 - Hydrostatic collapse in pipelines: (a) Cross section of intact pipeline subjected to external pressure (P_{ex}) and (b) Cross section of collapsed pipeline.

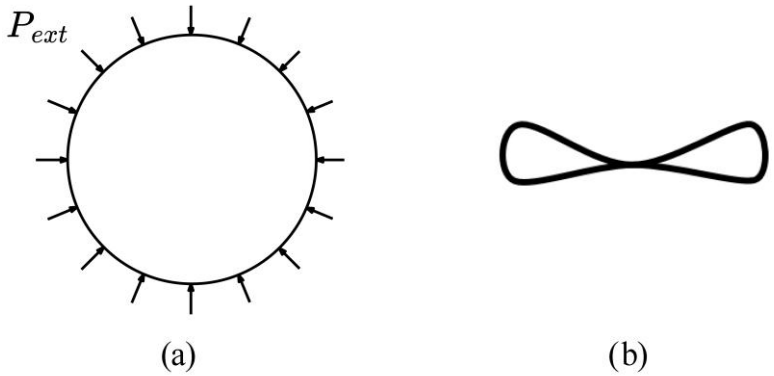

Source: The Author (2025).

Many factors influence the collapse response of subsea pipelines, including the diameter-to-thickness ratio (D/t), the material properties, initial geometric imperfection, the existence of the inner pipe, and the bending moment (Yu *et al.*, 2016). The authors highlight that the D/t ratio has been extensively studied, and the results indicate that the collapse pressure decreases if the D/t ratio increases. So, increasing the wall thickness can enhance the collapse strength for a certain radius of the pipe (Li; Chen; Guedes Soares, 2021).

Among the factors mentioned, initial ovality stands out as a critical geometric imperfection, which significantly influences the response to the collapse of pipelines subjected to external pressure (Fan *et al.*, 2017; Gong *et al.*, 2018; Li; Chen; Soares, 2022).

Novitsky and Gray (2003) define ovality as a second-order effect resulting from the cross-section deformation due to the longitudinal stress generated by curvature variations during the pipeline installation. Figure 2.2 illustrates a typical ovalization of a cross-section of the pipe. The ovality, represented by Δ, can be modeled by an ellipse with the semi-major axis of $R(1+\Delta)$ and the semi-minor axis of $R(1-\Delta)$, respectively (Zhang; Pan, 2020).

Figure 2.2 – Ovality of the cross-section of the pipe

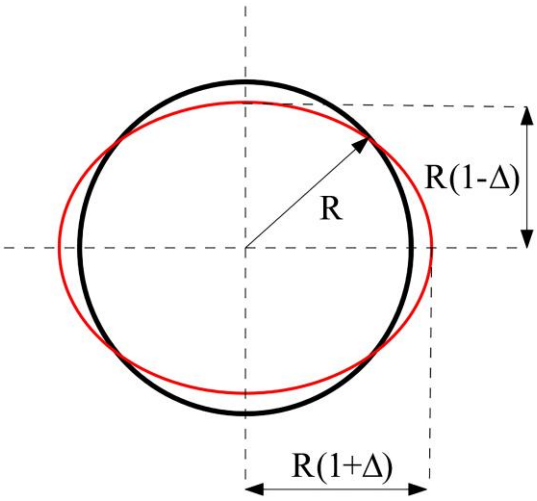

Source: The Author (2025).

One of the initial landmarks in the research on the hydrostatic collapse of metal pipelines was the classical formulation proposed by Gere and Timoshenko (1961), from which the collapse pressure of thin-walled pipelines is estimated. To this end, the authors simplified the modeling of infinitely long pipelines, representing them as two-dimensional rings composed of an ideal elastic-plastic material.

The elastic collapse pressure (P_{el}) can be calculated using the equation from classical formulation (Gere; Timoshenko, 1961):

$$P_{el} = \frac{2E}{(1-\nu^2)}\left(\frac{t}{D_{ave}}\right)^3 \tag{1}$$

where E is Young's modulus of the material, ν is the Poison's ratio, t and D_{ave} are, respectively, wall thickness and the average diameter of the pipe $(D_{ave} = D_{ext} - t)$.

Considering an initial imperfection (Δ_o), the hydrostatic collapse pressure (P_{co}) can be calculated according to the equation below (Gere; Timoshenko, 1961):

$$P_{co} = \frac{1}{2}\left\{\left(P_y + \mu P_{el}\right) - \left[\left(P_y + \mu P_{el}\right)^2 - 4P_y P_{el}\right]^{\frac{1}{2}}\right\} \tag{2}$$

which P_y is the yielding pressure given by:

$$P_y = 2\sigma_y \frac{t}{D} \tag{3}$$

where σ_y is the yield stress and D is the nominal outside diameter of the pipe.

The variable μ, shown in Eq. (2), depends on the geometric parameters of the pipe and the initial ovality and can be described as (Gere; Timoshenko, 1961):

$$\mu = 1 + 3\Delta_0 \frac{D}{t} \tag{4}$$

where Δ_0 is the ovality parameter, calculated using the equation below:

$$\Delta_0 = \frac{D_{max} - D_{min}}{D} \tag{5}$$

which D_{max} is the greatest measured inside or outside diameter, and D_{min} is the smallest measured inside or outside diameter.

The classic formulation of Gere and Timoshenko (1961) does not fully consider the nonlinear properties of the material and geometry of the subsea pipes, which limits its use to pipelines that undergo elastic buckling. Nevertheless, this formulation and other classic approaches have served as a foundation for improving design methodologies and defining operational limits for offshore pipelines.

Advancements in subsea engineering have led to the development of numerous methods to estimate the collapse pressure of intact metal pipelines, incorporating nonlinear effects, geometric imperfections, and material property variations (Benjamin; Cunha, 2012b; DNV, 2013; Haagsma; Schaap, 1981; He; Duan; An, 2014; Kamalarasa; Calladine, 1988; Murphey; Langner, 1985; Zhang; Pan, 2020).

The design code Det Norske Veritas (DNV, 2013) defines the collapse pressure (P_{co}) of a subsea pipeline under external pressure based on the method initially proposed by Haagsma; Schaap (1981). The formula is derived from elastic capacity, plastic capacity, and ovality, as detailed below:

$$(P_{co} - P_{el}) \cdot \left(P_{co}^2 - P_p^2\right) = P_{co} \cdot P_{el} \cdot P_p \cdot \Delta_o \cdot \frac{D}{t} \tag{6}$$

where P_{el} is the elastic collapse pressure, calculated according to Eq. (1), and P_p represents the plastic collapse pressure given by Eq. (3).

Notably, DNV (2013) specifies that the maximum ovality permitted in pipelines is 3%. This applies to the pipeline according to its installed condition. The standard also highlights that the minimum ovality to consider for the system collapse check is 0.5%.

The prediction of the plastic collapse pressure (P_p) can be calculated by using the yield stress of the material (f_y) and the manufacturing factor (α_{fab}):

$$P_p = f_y \cdot \alpha_{fab} \cdot \frac{2t}{D} \tag{7}$$

The standard DNV (2013) was replaced by the new standard DNV (2021), but the formula remains unchanged. Hydrostatic collapse can occur in the elastic regime or the plastic regime. The plastic regime occurs when D/t values are minimal.

Benjamin and Cunha (2012b) stated that deepwater oil pipelines typically exhibit diameter-to-thickness (D/t) ratios below 20, and for D/t ratios smaller than 15, the DNV method becomes excessively conservative. For this reason, the authors developed the Renewed Classical Approach (RCA). The RCA method is a modified version of the DNV method based on several nonlinear Finite Element Analyses (FEA) results. They concluded that the RCA method is more accurate than the DNV method for predicting the collapse pressure of subsea pipelines.

In an additional study, Benjamin and Cunha (2012a) reviewed the main classical approaches used to evaluate the hydrostatic collapse of submarine pipelines. They also compared results obtained using Finite Element (FE) models and those predicted by classical approaches, including the methods described in this section.

According to Benjamin and Cunha (2012a), the RCA method presented the collapse pressure predictions closest to the values obtained in the numerical analyses. However, this method has as its main limitation the lower limit of the ovality parameter (f_o). For $\Delta_0 < 0.5\%$, the method conventionally adopts $\Delta_0 = 0.5\,\%$, restricting its applicability under certain conditions.

Subsequently, Benjamin and Cunha (2015) developed a new version of the RCA method to include smaller values of Δ_0 and higher D/t ratios. The proposed reformulation is based on extensive numerical results that led to new equations for calculating the parameter and extending the applicable range of Δ_o to 0.25%. Benjamin and Cunha (2015) conducted a comparative study with a specific set of finite element results. They found that the new RCA method presented collapse pressure predictions closer to those obtained by finite element (FE) models. This performance was superior to the first version of RCA and the DNV method.

He, Duan and An (2014) investigated the collapse behavior for long and moderately thick-walled submarine pipelines under external hydrostatic pressure. Through numerical analysis via FEA, the authors developed a predictive formula to estimate the collapse pressure of pipelines with D/t ratios greater than 12.5. The results showed that the D/t ratio, initial ovality, and yield stress significantly impact the pipeline collapse responses. In addition, the proposed equation showed good

agreement with the numerical and experimental results, confirming its accuracy in predicting the critical collapse pressure.

More recently, Zhang and Pan (2020) evaluated the collapse responses of thick-walled subsea pipelines with geometric imperfections, i.e., initial ovality and thickness eccentricity. The thickness eccentricity, shown in Figure 2.3, can be defined as the variation in the thickness of the pipeline wall along its circumference, as described in the equation below (Yeh; Kiriakides, 1986):

$$\Xi = \frac{t_{max} - t_{min}}{t_{max} + t_{min}} \tag{8}$$

where Ξ is the thickness eccentricity and t_{max} and t_{min} are the maximum and the minimum wall thicknesses, respectively.

Figure 2.3 - Thickness eccentricity of the cross-section of the pipe.

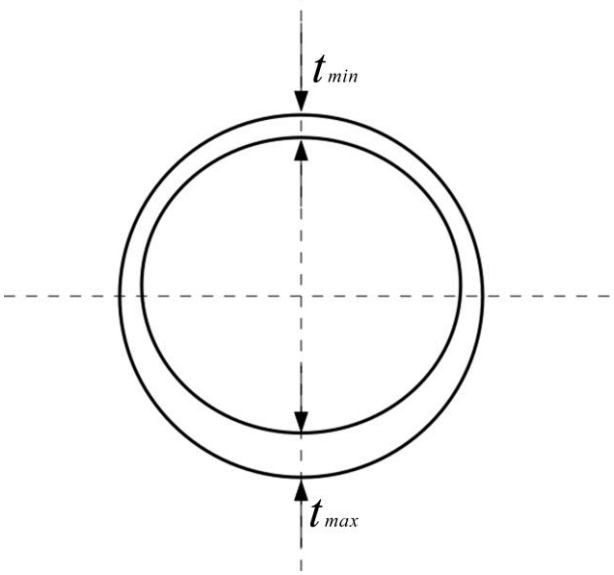

Source: The Author (2025).

Zhang and Pan (2020) noted that ovality becomes the main factor influencing the collapse response when the thickness eccentricity is less than 10%. The findings also indicate that the DNV method exhibits significant errors in cases of high thickness eccentricity, as the DNV formulation does not include this parameter.

Additionally, based on He, Duan and An (2014) study, Zhang and Pan (2020) developed a new equation to estimate the collapse pressure of subsea pipelines, incorporating the initial ovality and thickness eccentricity parameters. The proposed formulation demonstrated high accuracy compared against the FE results.

This section provided an overview of research on the hydrostatic collapse of intact subsea pipelines. In summary, the study of the collapse response of subsea pipelines has undergone significant development over the decades, starting from the

classical formulations by Gere and Timoshenko (1961) to more advanced approaches incorporating nonlinear effects from imperfect geometries and material properties. Extensive research and increasingly precise semi-empirical methods indicate the scientific maturity of this topic.

2.2 HYDROSTATIC COLLAPSE OF CORRODED SUBSEA PIPELINES

As discussed in the previous chapter, corrosion is also a critical factor influencing the response to the collapse of subsea pipelines, as it can significantly compromise their structural integrity over time. According to Bardal (2004), corrosion in the oil industry is a global concern, especially in offshore production. Structures installed in marine environments face extremely aggressive conditions in deep waters, where inspection and control are complex and challenging.

Corrosion is the degradation of a metal by its electrochemical reaction with its environment. A primary cause of corrosion is due to an effect known as galvanic corrosion. All metals have different natural electrical potentials. When two metals with different potentials are electrically connected in an electrolyte (e.g., seawater), current will flow from the more active metal to the other, causing corrosion (Bai; Bai, 2005).

Corrosion defects can be categorized into three types: general corrosion, local corrosion, and stress corrosion cracking. General (or uniform) corrosion affects the over entire exposed metal surface uniformly. In contrast, local corrosion affects only specific areas or parts of the metal surface, including pitting, galvanic, erosion, and hydrogen corrosion (Xu *et al.*, 2023). Stress corrosion cracking occurs when the effects of applied stress and corrosion effects are combined (Duret-Thual, 2014).

This research focuses on subsea pipelines with localized corrosion defects. Because localized corrosion is more common, it poses a greater risk in pipelines than general corrosion. Additionally, the propagation rate of localized corrosion can be higher under specific environmental conditions (Sun, 2020). Tan (2023) highlights that localized corrosion may be due to a single form or multiple changing forms, whose processes and mechanisms vary significantly over time and location.

DNV (2017) also classifies corrosion defects into three categories: single defect, interacting defect, and complex-shaped defect. A single defect is defined as one that does not interact with neighboring defects. An interacting defect occurs when nearby defects interact, either in the longitudinal or circumferential direction. Finally, a

complex-shaped defect results from the combination of colonies of interacting defects or a single defect for which its real detailed profile is available.

Figure 2.4 illustrates the three types of pipeline corrosion defects according to DNV (2021). The parameters S_l and S_c are the longitudinal and circumferential distances between adjacent defects.

Figure 2.4 - Three types of pipeline corrosion defects: (a) Single defect, (b) Dual corrosion defects, and (c) Combination of colonies of interacting defects (Adapted from DNV (2017)).

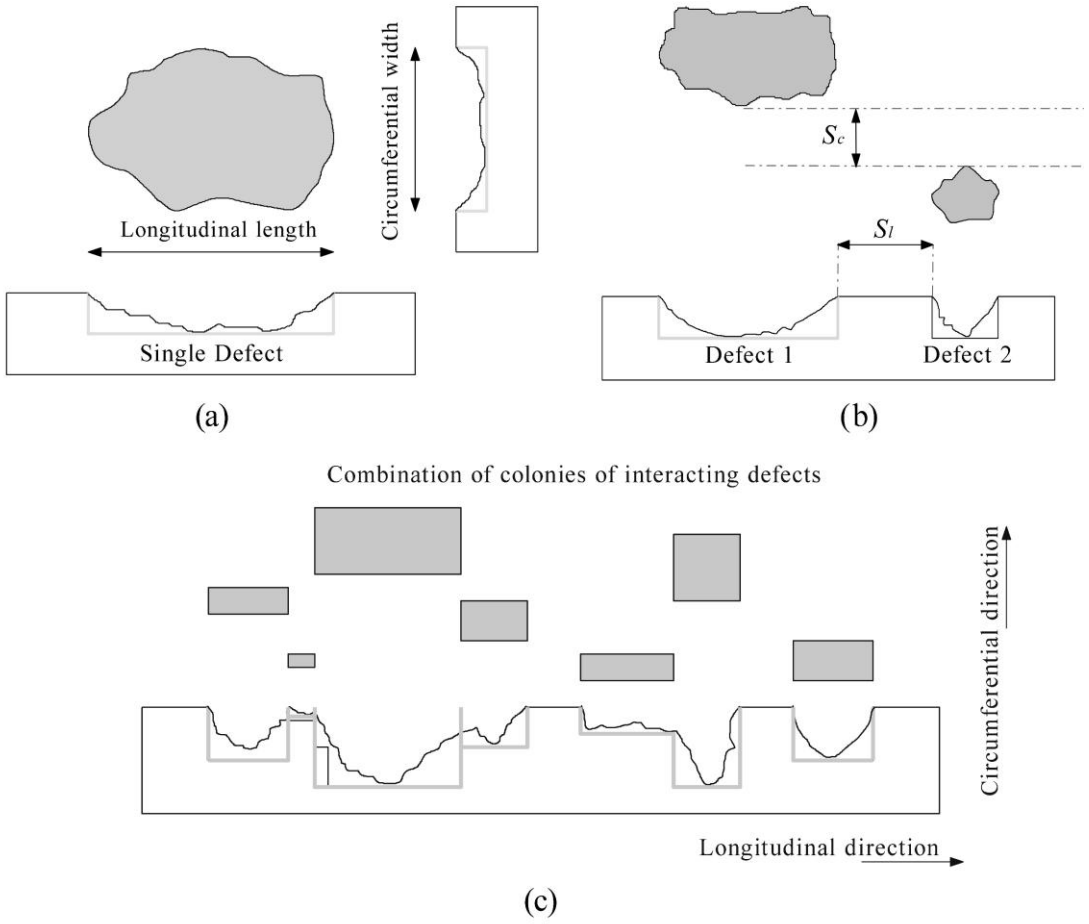

Source: The Author (2025).

Corrosion defects typically exhibit irregular and complex geometries. To enable practical and efficient assessment, especially in the early stages of integrity evaluation, it is common to simplify these defects by representing them with idealized shapes. This approach is aligned with Level 1 integrity assessment methods, which act as preliminary screening tools using simplified criteria for pass/fail decisions. In such methods, non-uniform corrosion profiles are often idealized using constant-depth (rectangular), elliptical, or parabolic shapes, as illustrated schematically in Figure 2.5. These simplifications allow for the application of empirical or semi-empirical formulas

which, although less precise, offer conservative estimates suitable for preliminary assessments.

Figure 2.5 - Schematic diagrams of different idealized shapes

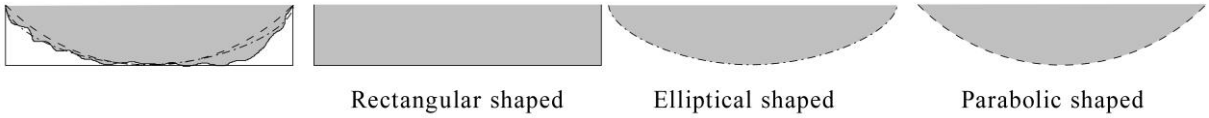

Source: The Author (2025).

Next, following the classification of corrosion defects delineated in DNV (2017), a literature review will be presented on the hydrostatic collapse of corroded subsea with single, interacting and complex corrosion defects.

2.2.1 Single corrosion defect

Bai and Hauch (1998) conducted a pioneering milestone study on the behavior of corroded subsea pipelines under external pressure. They extended the classic analytical model of Gere and Timoshenko (1961) to incorporate the effects of corrosion defects. Their approach assumed that the thickness of the shell element is equivalent to the thickness of the corroded region — however, the results are excessively conservative, mainly for deep defects.

In early research, similar studies were conducted by Xue and Hoo Fatt (2005). They presented analytical solutions for evaluating the elastic buckling of non-uniform, long cylindrical shells subjected to external hydrostatic pressure. Buckling analysis is essential for predicting collapse failure of long-pressure vessels and pipelines when exposed to external overpressure.

In this study, Xue and Hoo Fatt (2005) represented the corroded pipeline as a non-uniform shell divided into two regions, as illustrated in Figure 2.6. In this model, based on elastic principles, t denotes the nominal thickness of the pipeline, d represents the corrosion depth, and β indicates the angular extension of the corrosion (Region 1).

Figure 2.6 - Cross-section of non-uniform pipeline

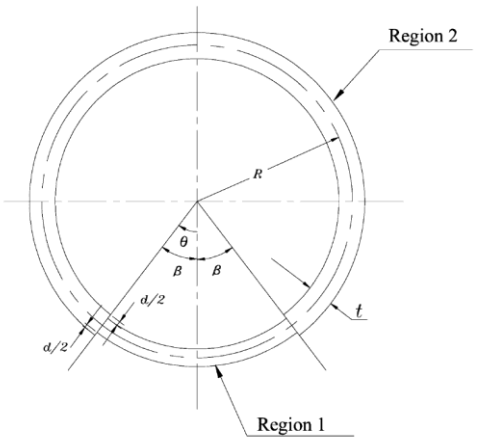

Source: Xue and Hoo Fatt (2005).

According to Xue and Hoo Fatt (2005), the buckling pressure decreased with thickness reduction and angular extension of the corrosion region. Additionally, the authors noted that the bounds between symmetric or antisymmetric buckling mode depend on the degree of corrosion.

Over the years, extensive studies have evaluated the collapse behavior of subsea pipelines with a single corrosion defect, including two- and three-dimensional nonlinear FE models. Sakakibara, Kyriakides, and Corona (2008) performed experimental and numerical studies to evaluate the influence of internal grooves caused by corrosion on the collapse behavior of the subsea pipes. Their results show that the collapse pressure decreased with the groove depth increasing, reducing by nearly 50% when the groove depth was 40 % of the wall thickness of the pipe.

Netto, Ferraz, and Botto (2007) and Netto (2010) combined small-scale experimental and numerical efforts to investigate the collapse response of subsea pipelines with single corrosion defects. They pointed out that the geometry of the corrosion defect, its localization in the surface of the pipeline (internal or external), and its position relative to the ovalized cross-section influence the collapse capacity.

Netto (2009, 2010) include a procedure for estimating collapse pressure based on experimental data and numerical results. The procedure focused on the most practical range of geometric parameters, specifically narrow and long defects. This methodology yielded the following equation:

$$\frac{P_{cor}}{P_{co}} = \left[\frac{1-\frac{d}{t}}{1-\frac{d}{t}\left(1-\left(\frac{c}{\pi D}\right)^{0.4}\left(\frac{l}{10D}\right)^{0.4}\right)}\right]^{2.675} \quad (9)$$

where P_{cor} is the collapse pressure of the corroded pipe, and P_{co} is the collapse pressure of the intact pipe, *D* is the nominal outer diameter, *t* is the thickness of the pipe, *d* is the corrosion depth, *c* is the corrosion circumferential width, and l is the corrosion length.

This procedure can be used as an effective tool to predict the collapse pressure of subsea pipelines with single corrosion defects. However, the key parameters must not deviate considerably from the range of values used by Netto (2009, 2010). The application range and further details can be found in Section 4.2.

Fan *et al.* (2017) combined experimental and numerical analyses to assess the effects of ovality axial length parameters on the corroded collapse subsea pipeline. The collapse pressure is significantly affected by the straight (l_s) and the transition length (l_t) of the maximum ovality. For this reason, they extended the empirical formula proposed by Netto (2009, 2010) that considers the axial characteristics of local maximum ovality, and the results showed good agreement with numerical and experimental data.

Benjamin and Cunha (2014a, 2014b) developed a method for the assessment of the hydrostatic collapse pressure of corroded deepwater pipelines. This method, named BCA (Based on Classical Approach), is based on the results of a large number of nonlinear FE analyses and assumes that the pipeline has a single idealized corrosion defect. The level of conservatism demonstrated by the BCA method is considered satisfactory for level 1 evaluation methods, which consider the idealized geometry of the corrosion defect.

Afterward, Cunha *et al.* (2020) provided experimental data from full-scale tests for the collapse response of pipes with metal loss defects and subjected to external pressure. The authors used the test results to verify the accuracy and conservatism of semi-empirical methods employed to predict the collapse of pipes with a single idealized corrosion defect. The BCA method positively reflected the trends observed in experimental results, showing reasonable conservatism.

Zhang, Chen and Guedes Soares (2020) studied the effects of non-symmetrical corrosion defects on the collapse response of subsea pipelines using the Finite

Element Method (FEM). Their study also evaluated how ovality interacts with corrosion effects. They found that the corrosion location angle, width, and depth affect the collapse response. Furthermore, the results indicate that the interaction between ovality and corrosion can increase the collapse pressure when the corrosion length, width, or depth increases, mainly if the corrosion location angle is small.

More recently, Gong *et al.* (2021) used experimental tests and Finite Element Analyses (FEA) to investigate the collapse performance of subsea corroded pipelines. They proposed an empirical formula to estimate the collapse pressure with a single elliptical corrosion defect. The formulation proposed by Gong *et al.* (2021) provides a reliable estimate for subsea pipes with elliptical corrosion defects. It is important to highlight that the previously mentioned formulations consider corrosion defects as being idealized in a rectangular shape (constant-depth, shown in Figure 2.5).

Chen *et al.* (2021a) investigated the buckling failure of subsea pipelines with corrosion defects idealized as rectangular, elliptical, and parabolic shapes. They revealed that corrosion shape primarily affects pipelines' buckling mode. Additionally, their results indicate that the idealization of actual corrosion geometry to a constant depth, as is often done in the available literature, underestimates the buckling pressure for subsea pipelines. It is noteworthy that this simplification aligns with Level 1 integrity assessment procedures.

Tian *et al.* (2024) used FE numerical analysis to establish a collapse pressure prediction model based on corrosion shape, length, and depth. They introduced shape coefficients for constant depth, elliptical corrosion, and parabolic corrosion. The prediction models show good reliability compared to results obtained using the formula proposed by Netto (2009, 2010).

2.2.2 Overview interacting and complex corrosion defects

Corrosion defects are distributed randomly by nature (Chen *et al.*, 2015), leading to interactions between neighboring defects in axial and circumferential directions. These interactions play an important role in predicting the collapse pressure of corroded subsea pipelines.

Studies on interacting corrosion defects in pipelines have established interaction rules that define the critical spacing between corrosion defects (Sun;

Cheng, 2018). The critical spacing is the distance at which the interaction is weak enough that defects are considered isolated (Benjamin *et al.*, 2016a).

DNV (2017) specifies that the minimum information required to define interaction rules includes the angular position of each defect around the circumference of the pipe, the axial spacing between adjacent defects, the location of defects (internal or external surface), and the length, depth, and width of each single defect.

According to Benjamin *et al.* (2016a), the distance between defects, the pipe outer diameter, the pipeline wall thickness, and the defects' geometry influence the interaction. However, the most relevant factor is the distance between defects. As mentioned previously, these distances can be longitudinal (S_l) and circumferential (S_c) direction.

Yu *et al.* (2017) evaluate the effects of local random cluster corrosion on the collapse pressure of a 2D ring under external pressure. Subsequently, (Wang *et al.*, 2018b, 2018a) carry out extensive experimental tests and three-dimensional nonlinear FE models are established to study the effect of the random corrosion defects on the collapse response of the subsea pipelines. These studies focus on pitting corrosion defects, and the interaction rules between these different corrosion defects have not been explored.

Gong *et al.* (2020) investigated the evolution of the collapse of subsea pipes with dual elliptical defects on the external surface. They performed small-scale experiments and developed FE models to reproduce the collapse response. Three defect arrangements are considered: longitudinally, circumferentially, and diagonally positioned, respectively. Their study highlighted that the geometric features—such as the diameter-to-thickness ratio of the pipe, initial ovality, and defect size—significantly influence the interaction between defects.

Wu *et al.* (2022) studied the collapse of subsea pipelines with interacting corrosion defects based on nonlinear finite element models. They provide the formulation for the collapse prediction of pipelines with identical dual corrosion defects. Their expression is a function of the geometric features and the axial and circumferential defect spacing, as described below:

$$\frac{P_{cor}}{P_{co}} = g\left(\frac{d}{t}, \frac{c}{\pi D}, \frac{L}{10D}\right) \cdot h\left(\frac{S_l}{D}, \frac{S_c}{\pi D}\right) \tag{10}$$

where P_{cor} is the collapse pressure of the corroded pipe, and P_{co} is the collapse pressure of the intact pipe. Based on finite element analyses, the functions related to the geometry of corrosion defects $g\left(\frac{d}{t},\frac{c}{\pi D},\frac{L}{10D}\right)$ can be expressed as:

$$g\left(\frac{d}{t},\frac{c}{\pi D},\frac{L}{10D}\right)=\left(b_1+b_2\left(\frac{d}{t}\right)^{b_3}\cdot\left(\frac{c}{\pi D}\right)^{b_4}\cdot\left(\frac{l_c}{10D}\right)^{b_5}\right)^{b_6} \tag{11}$$

where $b_1 = 1.29$, $b_2 = 14.9$, $b_3 = 1.73$, $b_4 = 0.56$, $b_5 = 0.6$, and $b_6 = -0.99$.

Subsequently, the function to the axial and circumferential defect spacing $h(\frac{S_l}{D},\frac{S_c}{\pi D})$ in Eq. (10) can be obtained:

$$h\left(\frac{S_l}{D},\frac{S_c}{\pi D}\right)=\frac{\left(c_1+c_2\left(\frac{S_l}{D}\right)+c_3\left(\frac{Sc}{\pi D}\right)+c_4\left(\frac{S_c}{\pi D}\right)^2\right)}{\left(1+c_5\left(\frac{S_l}{D}\right)+c_6\left(\frac{S_c}{\pi D}\right)+c_7\left(\frac{S_c}{\pi D}\right)^2\right)} \tag{12}$$

where $c_1 = 0.9$, $c_2 = 0.42$, $c_3 = -7.08$, $c_4 = 19.65$, $c_5 = 0.44$, $c_6 = -8.25$, and $c_7 = 22.87$.

Equation (10) is applied only to a specific range of parameters: $d/t \leq 0.6$, $c/\pi D \leq 0.6$, $L/10D \leq 1$, $S_l/D \leq 5$, and $S_c/\pi D \leq 0.4$. Furthermore, Wu *et al.* (2022) assessed the accuracy of this formulation for the collapse pressure of pipelines with multiple corrosion defects. They used equivalent parameters and obtained results with acceptable conservatism.

Recently, Wu *et al.* (2023) proposed an equation to predict the collapse response of subsea pipes with irregular corrosion defects under external pressure. The irregular defect is the two overlapping idealized defects, which combine a top-layer defect (small defect) and a bottom-layer defect (large defect). The main findings indicate that the angle of the bottom-layer defect (large defect) has a more pronounced effect on the interaction than the angle of the top-layer defect (small defect).

Advances in inspection techniques have made it possible to detect complex corrosion geometries (Chen *et al.*, 2021b). For example, ultrasonic waves can detect the shape and volume of corrosion defects with high accuracy and precision (Pengchao, 2025). Despite that, the effect of the actual morphology of corrosion defect on the collapse response of subsea pipelines has yet to be investigated.

Only one study in the current literature has considered the effect of non-uniform corrosion defects on the collapse response of these pipes. Li, Xie and Liu (2023) used

a reverse inversion modeling method to reconstruct the numerical model of pipes with non-uniform surface corrosion defects. They found a good correlation between numerical and experimental results. However, there are still no results that are more conducive to engineering applications.

2.3 FINAL REMARKS

The reviewed literature consolidates the state of knowledge for assessing intact subsea pipeline collapse, providing a solid basis for understanding this phenomenon. However, the collapse of subsea corroded pipelines still lacks clear insight.

Firstly, the influence of the interaction between corrosion defects on the collapse pressure is not yet fully understood. Few studies evaluate the remaining bearing capacity of pipelines affected by interacting defects, and the governing rules for these interactions remain unclear, especially when combined with external factors.

Furthermore, most experimental tests and numerical models employ idealized forms of corrosion defects, diverging from the actual conditions observed in pipelines in operation. As a result, existing methods for assessing the collapse of subsea pipelines are excessively conservative, highlighting the need for more improved approaches to assess the structural integrity of these pipes.

This research advances the understanding of structural integrity in subsea pipelines by proposing an integrated approach to assess collapse in pipes with complex or interacting corrosion defects. In contrast to previous studies that often consider isolated factors or rely on overly conservative assumptions, it introduces a predictive methodology that improves collapse pressure estimates by balancing accuracy and computational efficiency. Together, these contributions form a framework aligned with the demands of offshore engineering and support more consistent technical decisions in pipeline integrity assessments.

3 AN INVESTIGATION ON THE COLLAPSE RESPONSE OF SUBSEA PIPELINES WITH INTERACTING CORROSION DEFECTS

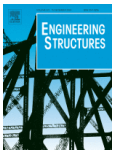

D'Aguiar, S. C. M; Motta, R. de S.; Afonso, S. M. B. (2024) An investigation on the collapse response of subsea pipelines with interacting corrosion defects. **Engineering Structures**, v. 321, p. 118911.
DOI: https://doi.org/10.1016/j.engstruct.2024.118911

Abstract

Subsea pipelines are usually affected by corrosion. Corrosion defects can occur anywhere along the pipeline and may interact with each other. The interaction between corrosion defects is pivotal in determining the response of subsea pipes subjected to external pressure. This work uses nonlinear Finite Element (FE) analyses to evaluate the collapse of subsea pipelines containing multiple corrosion defects. The computer system called PIPEFLAW is used to automatically generate and analyze corroded pipeline models. The FE-based solutions are validated against experimental results in the literature and achieved good agreement. Then, extensive parametric analyses are conducted to assess whether an interaction exists between adjacent longitudinal and circumferential defects with different geometries. The results from parametric study suggest that defect arrangements play a fundamental role in the interaction rules. The longitudinal critical spacing at which defects can be considered isolated was found to be 50 times the pipeline thickness, and the circumferential defects should always be considered interacting. Additionally, based on the FE simulation data, this study introduces expressions for adjustment factors for predicting the collapse pressure, considering the effect of the initial ovality (factor f_o) and temperature variation (factor f_t). The proposed adjustment factors are valuable tools for predicting the collapse pressure of pipelines. So, these findings expand our understanding of corroded subsea pipeline collapses and offer practical insights for the industry.

Keywords: Collapse response, Failure analysis, Corrosion, Interaction rules, Ovalization, Temperature.

3.1 INTRODUCTION

Subsea pipelines are crucial for efficient and safe oil and gas transportation. As the pipeline ages, corrosion defects commonly occur on internal and external surfaces. Corrosion is responsible for 36% pipeline failures (Liu *et al.*, 2018) and can cause accidents with far-reaching economic, environmental, and human impacts. In ultra-deepwater scenarios, pipelines are subject to higher pressures and temperatures (Haq; Kenny, 2013), and the pipe thickness metal loss due to corrosion can cause it to collapse under external pressure rather than burst under internal pressure (Drumond *et al.*, 2018).

The behavior of subsea pipes with single corrosion defects subjected to external pressure has been extensively studied in the last 15 years (Benjamin; Cunha, 2015; Fan *et al.*, 2017; Fraldi *et al.*, 2011; Fraldi; Guarracino, 2011; Gong; Wang; Yuan, 2020; Kara; Navarro; Allwood, 2010; Kyriakides; Corona, 2007; Netto; Ferraz; Botto, 2007; Papadakis, 2008; Sakakibara; Kyriakides; Corona, 2008; Xue; Gan, 2014; Yan; Shen; Jin, 2015; Ye; Yan; Jin, 2016).

Fan *et al.* (2017) investigated the performance of corroded subsea pipelines and found that the axial length of the ovalized region plays a crucial role in the collapse pressure. Meanwhile, Gong *et al.* (2021) highlighted that defect depth exerts a more pronounced unfavorable effect on collapse pressure than other geometric parameters of the defect.

In the above-referred studies, the submarine pipelines present a single corrosion defect with idealized geometry. However, corrosion defects are frequently manifested in clusters, and the interaction between the defects can significantly influence failure mode and collapse capability (Li *et al.*, 2016).

Interaction rules can identify a critical spacing between corrosion defects, above which the defects can be considered isolated. So, the interaction effect on the analysis can be ignored if the spacing between defects exceeds this critical value (Qin; Cheng, 2021).

DNV (2017) presents interaction rules that classify the defects as isolated or under interaction. However, these rules should be used to determine whether an interaction existed between adjacent corrosion defects for pipes subject to internal pressure only. In the available literature, the research on interacting defects focuses mainly on pipelines under internal pressure, and numerous papers can be found on this topic (Al-Owaisi; Becker; Sun, 2016; Benjamin *et al.*, 2005, 2016b; Chouchaoui; Pick, 1996; Idris *et al.*, 2021; Li *et al.*, 2016; Mondal; Dhar, 2017; Motta *et al.*, 2017; Silva; Guerreiro; Loula, 2007; Sun; Cheng, 2021; Zhou *et al.*, 2022) .

Zhou *et al.* (2022) analyzed the influence of depth, length, and group spacing of corrosion defects on the failure of corroded pipelines subjected to internal pressure. Their numerical results showed that the corrosion defect depth is the main factor affecting the failure pressure in pipelines containing group corrosion defects.

Based on FE analyses, Li *et al.* (2016) proposed a new interaction rule to identify the interaction effect between defects on the failure pressure of corroded thin-walled pipelines with colonies of defects under internal pressure. Subsequently, Sun and

Cheng (2021) developed a model based on Finite element (FE), and a new interaction criterion was created for corrosion defects on an X46 steel pipe under axial tensile stresses.

Conversely, the study of pipe interaction mechanisms under external pressure is still insufficient. It is important to emphasize that the pipeline's structural behavior under internal pressure is different under external pressure, especially when exposed to corrosion. Few studies present detailed interaction rules for use in these cases, especially when considering combined loads. Gong *et al.* (2020) conducted experimental and numerical analyses to evaluate collapse evolution considering pipelines with two identical idealized geometry defects on the external surface. They reported that the geometric characteristics of the pipe and the defect parameters significantly influence the interaction rules.

Recently, extensive finite element analyses were performed by Wu *et al.* (2022) to evaluate the influence of corrosion defect dimensions on the interaction. They found that the longer the corrosion length, the greater the influence of the defect spacing on the collapse pressure. In addition, Wu et al (2022) developed a formula based on the critical external pressure formula of an intact thin-walled pipeline to predict the collapse pressure of pipelines with dual corrosion defects. The proposed equation can be applied to multiple corrosion defects. However, only external loading was considered in Gong *et al.* (2020) and Wu *et al.* (2022) in the studies cited.

This paper aims to provide new insights into the existing recommended practice by adding interaction rules for subsea pipelines with multiple corrosion defects. Furthermore, this study presents new adjustment factors, including the effect of initial ovality and temperature variation on the collapse response of these pipes.

3.2 FINITE ELEMENT MODELING

3.2.1 General

In this work, finite element (FE) based models were generated by the PIPEFLAW automatic modeling tool, developed by the PADMEC (High-Performance Processing in Computational Mechanics) research group at the Federal University of Pernambuco (UFPE, Brazil). PIPEFLAW is a computational tool based on

MSC.PATRAN (Patran, 2012) software integrates several tools for automatic FE model generation and FE analysis via ANSYS software (Ansys, 2020).

The PIPEFLAW program has a set of functions implemented in the PCL language (Patran Command Language) for the automatic generation of pipeline models with single or multiple corrosion defects with rectangular, elliptical, or complex geometry (Cabral *et al.*, 2007, 2017). The most significant advantage of using PIPEFLAW is the speed, accuracy and efficiency it brings to the process. Several studies have been developed considering this tool and have presented accurate and reliable results for evaluating the integrity of corroded pipelines (Bruère *et al.*, 2019; Cabral *et al.*, 2007, 2017; Ferreira *et al.*, 2021; Motta *et al.*, 2021, 2017; Pimentel *et al.*, 2020; Soares *et al.*, 2019).

The meshes used in this paper consider 3D hexahedral solid elements generated by the PIPEFLAW system. The discretization pattern used is described in detail by Cabral *et al.* (2007, 2017). Overall, a refined mesh is used in the defect region, followed by less refined meshes in the regions away from the defect, including transition regions along the thickness, transition regions along the surface, and mesh expansion regions. A typical mesh following such rules can be seen in Figure 3.1 for an isolated rectangular defect.

The distribution and refinement of the elements varied depending on the defect geometry. However, defects generated by the PIPEFLAW always have four elements along the wall thickness (Cabral *et al.*, 2017). Besides, there is a thickness mesh transition from four to two (Thickness transition) in the outside area to the defect, illustrated in Figure 3.1 (b).

Figure 3.1 - Mesh automatically generated by PIPEFLAW for a single defect: (a) External discretization and (b) Cross section of the middle of the pipe (center of the corrosion defect).

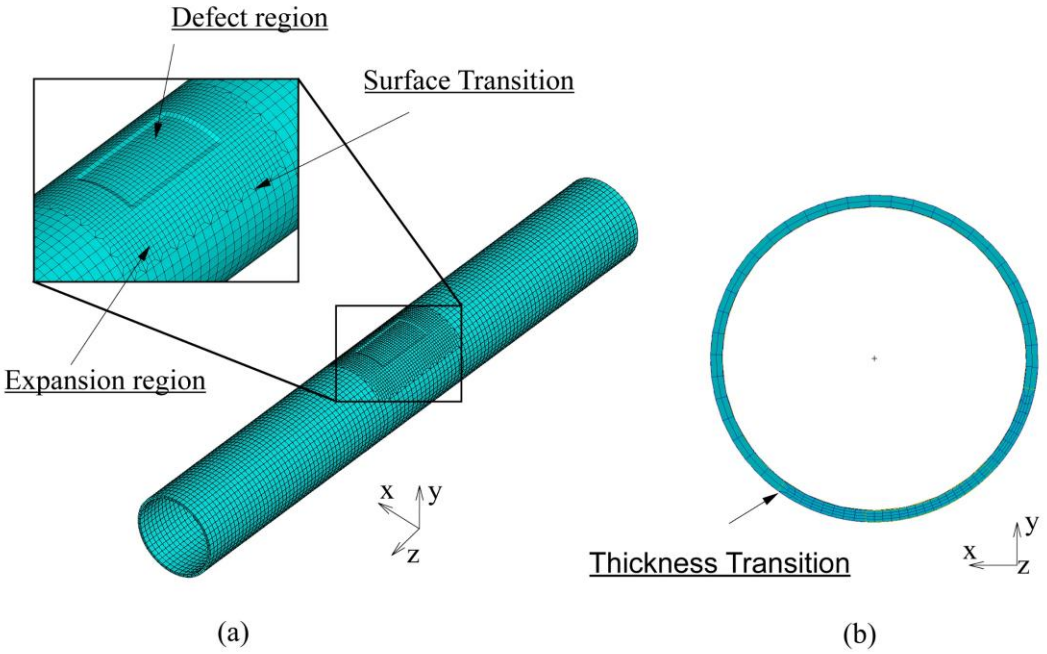

Source: The Author (2024).

3.2.2 Material Properties

The steel material properties used in the validation examples were obtained from the uniaxial tension tests performed by Gong *et al.* (2020). The average engineering stress-strain relationships tested in Gong *et al.* (2020) and represented in Figure 3.2 are used in the current calculations. The basic mechanical properties of the material considered are E = 200 GPa, σ_y = 198.2 MPa, n = 8.9, E' = 2400 MPa, $\sigma_{0.5}$ = 252.8 MPa (yield stress at a strain of 0.5%).

In the finite element analysis, the modified Ramberg-Osgood was used to define the hardening behavior of steel (Gong; Wang; Yuan, 2020):

$$\varepsilon = \frac{\sigma}{E}\left(1 + \frac{3}{7}\left|\frac{\sigma}{\sigma_y}\right|^{n-1}\right) \tag{13}$$

where ε, σ, E, σ_y and n are the uniaxial strain, the uniaxial stress, the elastic modulus, the effective yield stress, and the strain hardening parameter, respectively. The modified Ramberg-Osgood model of the material is also plotted in Figure 3.2.

According to Gong, Wang and Yuan (2020), Eq. (13) is used only for strain values less than 0.015. For strain levels greater than 0.015, the stress-strain response exhibits a linear relationship, whose slope is given by:

$$E' = \left.\frac{d\sigma}{d\varepsilon}\right|_{\varepsilon=0.015} = E\left(1 + \frac{3}{7}n\left|\frac{\sigma}{\sigma_y}\right|^{n-1}\right)^{-1} \quad (14)$$

where E' is the material's modulus of hardening.

Figure 3.2 - Stress-strain material curve considered.

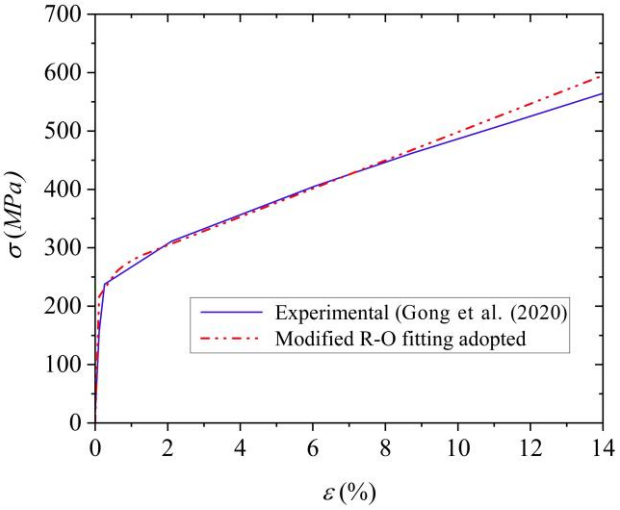

Source: Adapted by Gong, Wang and Yan (2020).

3.2.3 Boundary conditions and load

The loads and boundary conditions are shown in Figure 3.3. Appropriate boundary conditions are applied to fix the displacements in the longitudinal direction (Fix Z) at the ends of pipes. The displacement at θ direction (angular cylindrical coordinate) is also restricted (Fix θ) in two nodes to avoid rigid body motion (rotation).

Figure 3.3 - Loads and boundary conditions in the pipeline allowed by PIPEFLAW. In the present work, internal pressure, axial force, and bending moment are set to zero.

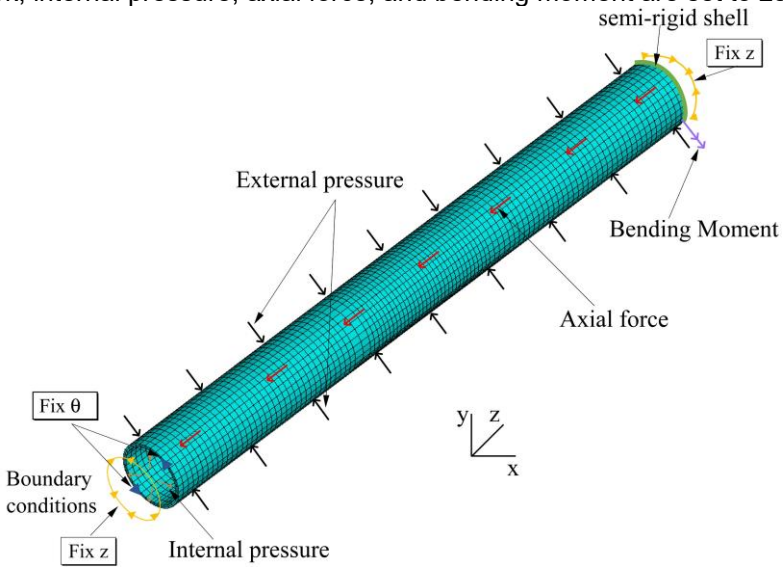

Source: The Author (2024).

The PIPEFLAW system accurately assesses the collapse pressure of corroded pipe submitted to combined loads (internal pressure, external pressure, axial loads, and bending moment).

According to DNV (2013), gas pipelines can experience almost zero internal pressure in the operational phase, and the collapse pressure becomes even more critical when internal pressure is minimal. For this reason, the external pressure is typically the primary loading parameter that governs the design of ultra-deep pipelines (Kyriakides; Lee, 2021). In the current study, only ultra-deep pipelines are considered and therefore, here, the generated models are subject only to external pressure, and the other loads are set to zero.

3.2.4 Ovalization

The initial ovality in the pipe section is unavoidable due to manufacturing limitations and the installation process. So, the ovality of the cross-section of the pipeline segment (initial geometric imperfection) is considered here. Ovality increases with the application of external pressure. According to DNV (2013), the initial ovality (Δ_0) is defined as:

$$\Delta_0 = \frac{D_{max} - D_{min}}{\frac{D_{max} + D_{min}}{2}} = 2 \cdot \frac{D_{max} - D_{min}}{D_{max} + D_{min}} \tag{15}$$

where D_{max} and D_{min} are the maximum and minimum outer diameters of the pipeline, respectively.

In this paper, the initial ovality is inserted using coordinate transformation after the model generation. A customized Python function was created to introduce the initial ovality into the numerical model. The new radius R_n of the nodes along the cross-section is obtained in the following form (Motta *et al.*, 2021):

$$R_n = R_o \frac{(1 - \Delta_o^2/4)}{\sqrt{(1 - \Delta_0/2)^2 + 2 \cdot \Delta_0 \sin^2(\theta)}} \tag{16}$$

where R_o is the original radius of the node and the mean radius of the ovalized section, and Δ_o is the ovalization defined in Eq. (15). Figure 3.4 illustrates typical original and ovalized cross-sections. More details of this procedure can be seen in Motta *et al.* (2021).

Figure 3.4 - Difference between the original (circular) and the ovalized pipeline cross-sections

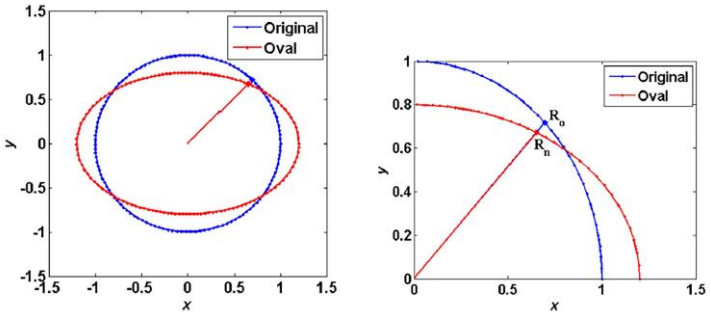

Source: Motta *et al.* (2021).

When the ovalized pipeline is subjected to external pressure, the fibers of the material show membrane and bending deformations. Bending and membrane strains depend on the curvature radius of the ovalized surface. At the lowest curvature part of the oval section, maximum compression occurs on the outer surface. On the other hand, in the part of greater curvature, the bending deformation compresses the inner surface. Considering these observations, it is important to study the effect of the location of the defect in relation to the curvature of the cross-section. The most severe situations arise when a defect coincides with the most compressed fibers of the collapsed cross-section without the presence of the defect (Netto; Ferraz; Botto, 2007). In Section 3.5.3, the relationship between ovality and the collapse response of subsea pipelines with multiple corrosion defects is analyzed in detail.

3.3 NON-LINEAR ANALYSIS

The automatic tools to control non-linear analysis are carried out by scripts developed in (Python, 2011) (PIPEFLAW system) in which the FE analyses are processed by ANSYS solver (Ansys, 2020). The analysis management is performed by automatic control algorithms where the convergence criteria and pre-defined load increments are processed and applied (Cabral *et al.*, 2017; Soares *et al.*, 2019).

The collapse response of thick and thin-walled subsea pipelines is an unstable nonlinear problem related to severe geometric nonlinearities and structural instability (Gong *et al.*, 2020). In simulations, the hydrostatic collapse pressure is the maximum pressure the pipeline reaches in a geometric non-linear elastoplastic analysis. Riks method (modified arc length method) (Riks, 1972) was adopted here to follow the loading history.

Section 3.5.4 evaluates the effect of temperature change on the collapse response of pipes with corrosion defects. For thermal analyses, the uniform temperature will be assigned to all nodes using the TUNIF command, available in ANSYS (Ansys, 2020).

3.4 VALIDATION OF NUMERICAL SIMULATIONS

The experimental and numerical results obtained in Gong *et al.* (2020) were used to validate the automatic procedure and the FE models proposed here. The numerical results of Gong *et al.* (2020) were obtained from FE models generated manually.

Gong *et al.* (2020) evaluated three types of external corrosion defect arrangements composed of two elliptical defects in longitudinal, circumferential, and diagonal directions, respectively.

Table 1 presents the dimensions of the studied pipeline, the outer diameter (D) and the wall thickness (t), and the geometric defects parameters, where l, c, and d are the defect's length, circumferential width, and depth, respectively. The pipeline length adopted is ten times the pipe diameter to avoid the influence of boundary conditions on the accuracy of the collapse pressure. The defect orientation and the initial ovality ($\Delta_o = 0.1\ \%$) agree with the experimental tests by Gong *et al.* (2020).

Table 3.1 - Dimensions of the pipe and the geometric parameters of defects.

D (mm)	t (mm)	l (mm)	c (mm)	d (mm)
83	4	83	13.04	2.4

Source: The Author (2024).

FE models were automatically generated by PIPEFLAW to simulate the cases from experimentally tested (Gong *et al.*, 2020). In the reference models, the real geometric parameters of the experimental tests are used, i.e., elliptical geometry illustrated in Figure 3.5 (a). In the simplified models, the defect geometry is idealized with constant length, width, and thickness, i.e., rectangular geometry as illustrated in Figure 3.5 (b).

Figure 3.5 - Cross section of two types of corrosion shapes: (a) elliptical geometry, and (b) rectangular geometry.

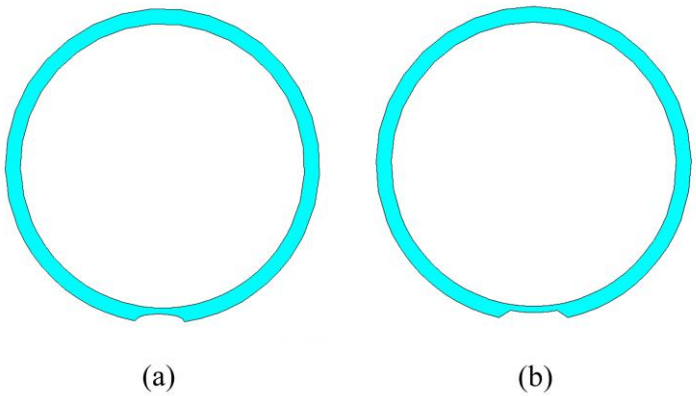

Source: The Author (2024).

FE models with rectangular geometry are commonly used in industry and adopted in technical standards. Moreover, simplified models typically provide conservative estimates for the collapse pressure of corroded pipes (Netto; Ferraz; Botto, 2007). Figure 3.6 presents the rectangular model adopted in this study for the three types of defect arrangements. In Figure 3.6, S_l and S_c are the longitudinal and circumferential distances between adjacent defects, respectively.

Figure 3.6 - Finite element mesh at different defect arrangements: (a) Longitudinal, (b) Circumferential, and (c) Diagonal.

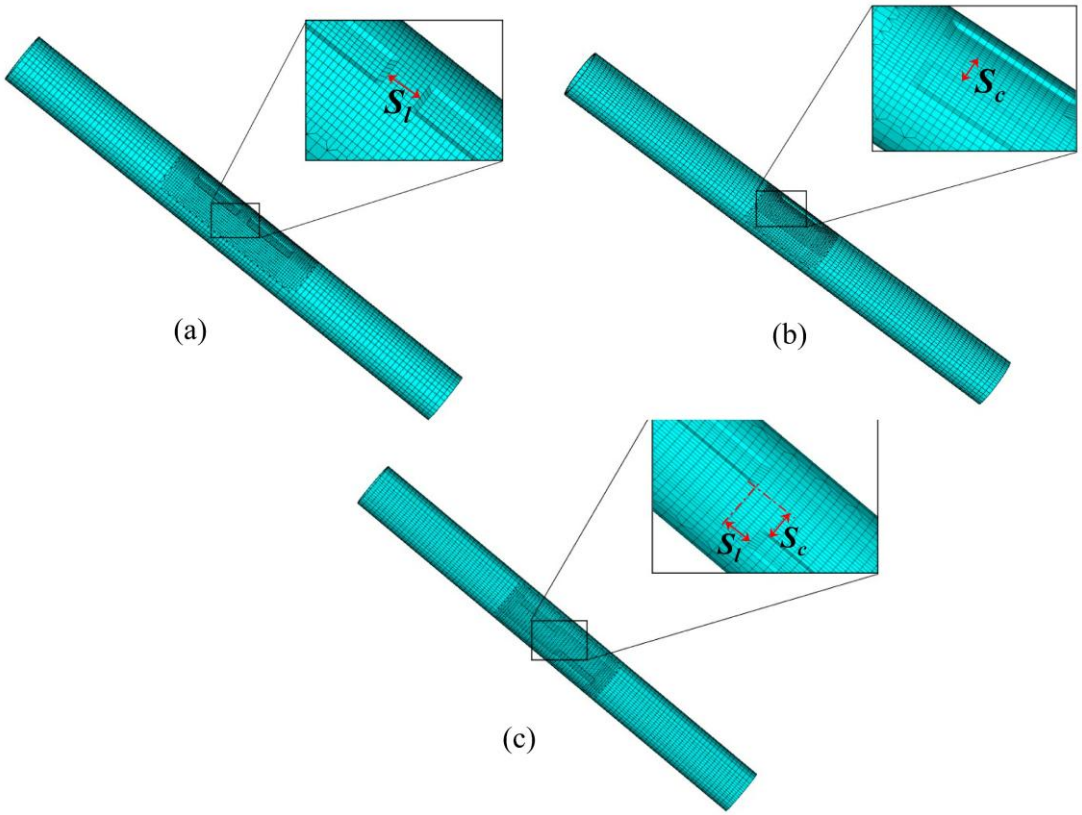

Source: The Author (2024).

Table 3.2 and Figure 3.7 present a comparison result to the collapse pressures (P_c) obtained experimentally (P_c^{test}) and numerically (P_c^a) by Gong *et al.* (2020) and predicted by the PIPEFLAW FE based system using elliptical (P_c^b) and rectangular (P_c^c) geometries.

Table 3.2 - Comparison of collapse pressure between the finite element analysis and tests.

Specimen	Aligned type	S_l *(mm)*	S_c *(mm)*	P_c^{test} (MPa)	P_c^a (MPa)	P_c^b (MPa)	P_c^c (MPa)	P_c^a/P_c^{test}	P_c^b/P_c^{test}	P_c^c/P_c^{test}
TSA1	Longitudinal	0.00	-	16.12	16.50	16.59	13.02	1.02	1.03	0.81
TSA2	Longitudinal	20.00	-	16.78	16.80	17.02	14.24	1.00	1.01	0.85
TSA3	Longitudinal	55.00	-	17.45	17.12	17.29	14.44	0.98	0.99	0.83
TSA4	Longitudinal	80.00	-	17.70	17.24	17.39	14.49	0.97	0.98	0.82
TSC1	Circumferential	-	0.00	16.52	16.48	16.62	11.86	1.00	1.01	0.72
TSC2	Circumferential	-	20.00	18.78	18.05	18.25	14.95	0.96	0.97	0.80
TSC3	Circumferential	-	55.00	17.39	17.47	17.46	14.83	1.00	1.00	0.85
TSC4	Circumferential	-	80.00	16.90	16.94	17.20	14.55	1.00	1.02	0.86
TSD1	Diagonal	0.00	0.00	17.01	17.54	16.88	13.18	1.03	0.99	0.77
TSD2	Diagonal	20.00	20.00	19.34	18.77	17.56	14.47	0.97	0.91	0.75
TSD3	Diagonal	80.00	80.00	18.87	18.32	17.45	14.76	0.97	0.92	0.78
							Mean:	1.00	0.99	0.81
							CoV (%):	2.29	3.84	5.58

NOTE: [test] Experimental results - elliptical geometry (Gong *et al.*, 2020). [a] Numerical results - elliptical geometry (Gong *et al.*,2020). [b] Numerical results present work – elliptical geometry. [c] Numerical results present work – rectangular geometry.

Source: The Author (2024).

Figure 3.7 - Summary of the collapse pressure (P_c) results for three aligned types: (a) Longitudinal, (b) Circumferential, and (c) Diagonal.

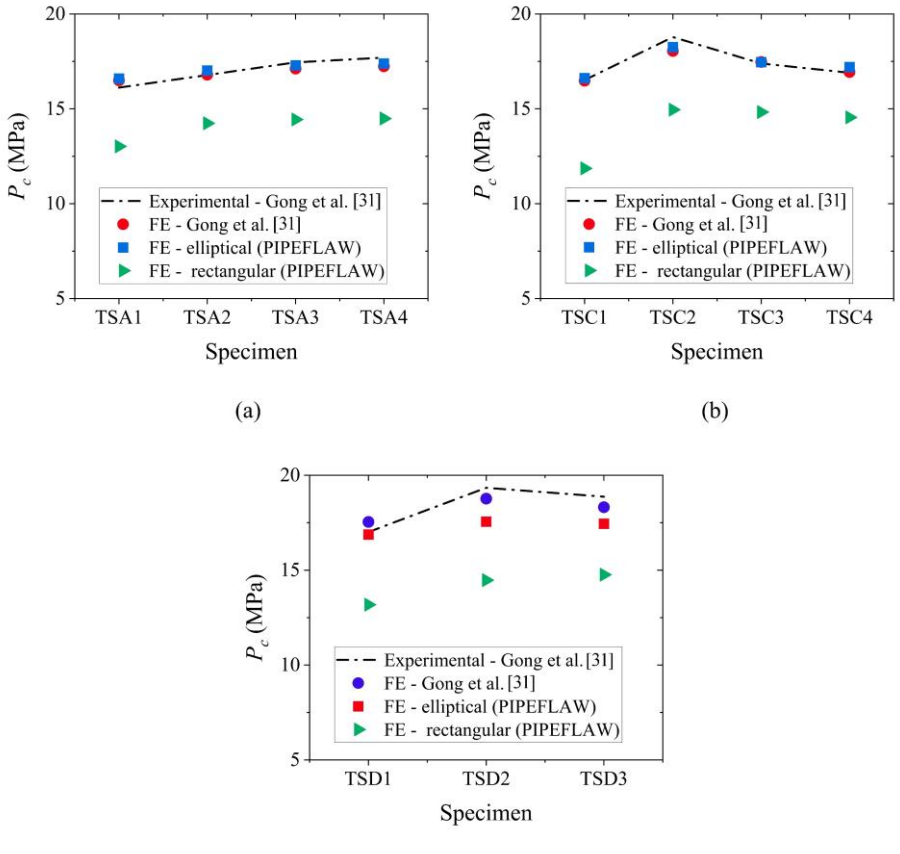

Source: The Author (2024).

The mean and coefficient of variation (CoV) of P_c^b/P_c^{test} (FE elliptical – PIPEFLAW), presented in Table 3.2, are 0.99 and 3.84 %, respectively, indicating that the collapse pressures of the FE-predicted and experimental tests are in good agreement. The most notable differences are observed in the cases of diagonally aligned defects. However, the PIPEFLAW system generally provides collapse pressure values that favor safety.

On the other hand, the mean and coefficient of variation (CoV) of P_c^c/P_c^{test} (FE rectangular geometry – PIPEFLAW), are 0.81 and 5.58 %, respectively. As expected, the simplified model is shown to be more conservative than the elliptical idealization. Netto, Ferraz and Botto (2007) suggest that the degree of conservatism of the rectangular model varies with the defect's dimensions, which justifies the increase in the coefficient of variation (CoV). The authors justify that as more material is removed from the pipe in the simplified geometry, the bigger the difference in comparison to the real defect results. This behavior was previously described in Xue and Hoo Fatt (2002).

Figure 3.8 to 3.10 illustrate the deformed configurations and von Mises stress contour after the collapse of different specimens (TSA1, TSC2, TSD2, respectively) obtained using PIPEFLAW. The deformed configurations (collapsed shape) and the von Mises stress contours are consistent with those obtained numerically and experimentally by Gong *et al.* (2020). Therefore, the results show that the PIPEFLAW system can reliably predict the collapse behaviors of corroded pipelines with various corrosion defects.

Figure 3.8 - FE results for specimen TSA2 (elliptical geometry) obtained using PIPEFLAW: (a) Deformed configuration after collapse and (b) Von Misses stress distribution after collapse.

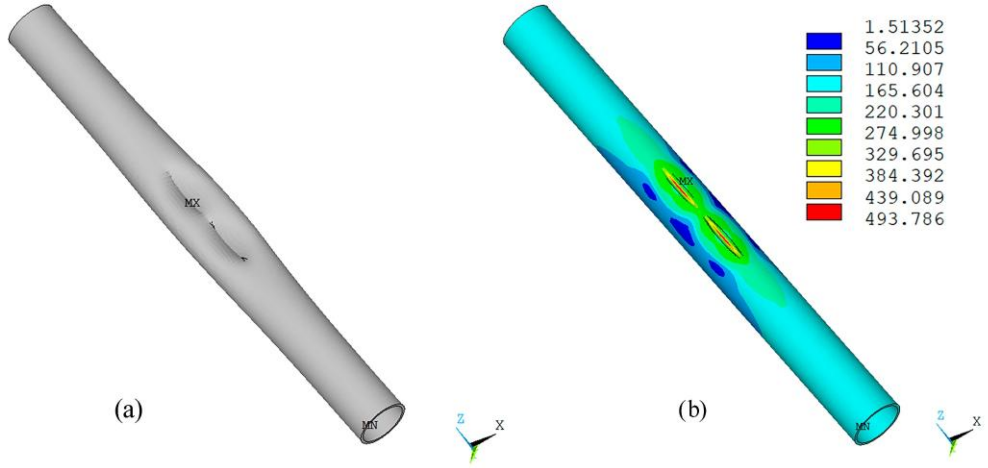

Source: The Author (2024).

Figure 3.9 - FE results for specimen TSC2 (elliptical geometry) obtained using PIPEFLAW: (a) Deformed configuration after collapse and (b) Von Misses stress distribution after collapse.

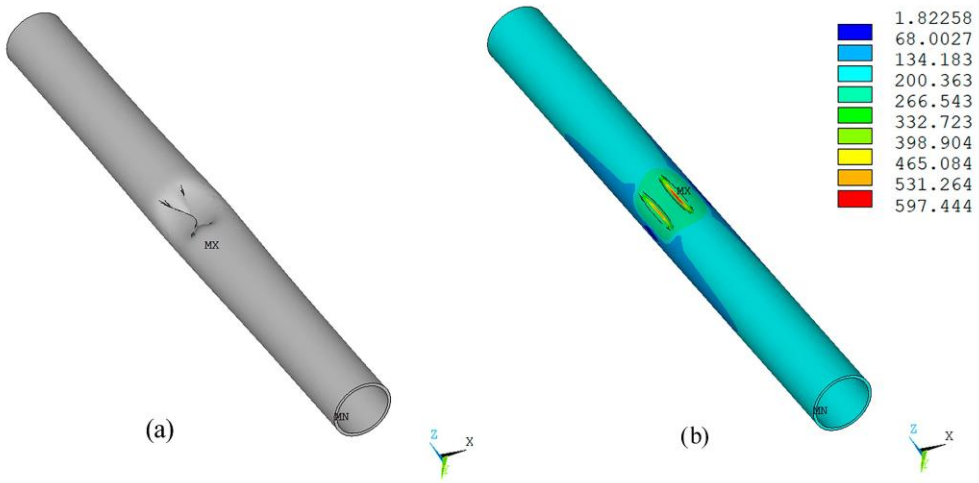

Source: The Author (2024).

Figure 3.10 - FE results for specimen TSD2 (elliptical geometry) obtained using PIPEFLAW: (a) Deformed configuration after collapse and (b) Von Misses stress distribution after collapse.

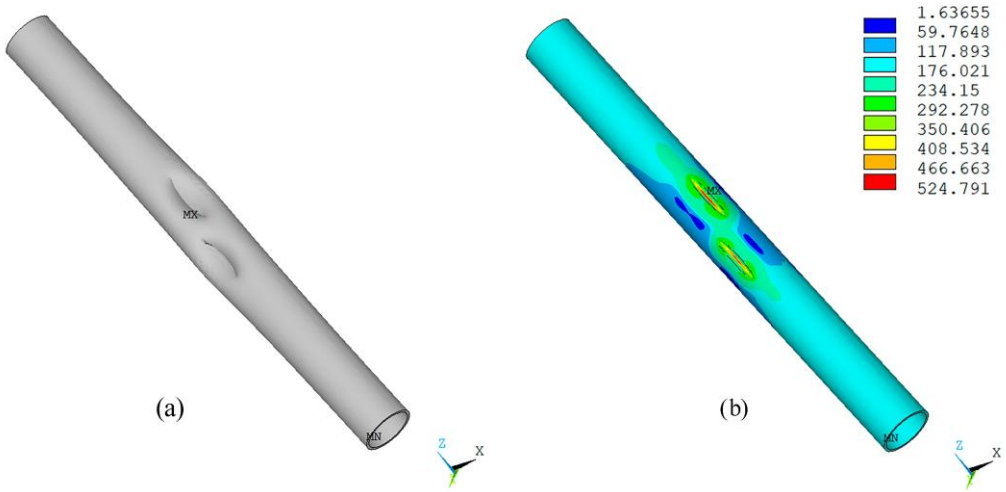

Source: The Author (2024).

3.5 PARAMETRIC STUDY

Given the results described in Section 3.4, an extensive parametric analysis to investigate the interaction effects between two or more corrosion defects is conducted. The attributes of the pipeline considered in the current study, and the geometric parameters of defects, are summarized in Table 3.3. A representative pipe steel grade

(i.e., X65) is selected for the parametric analysis. Gong *et al.* (2020) have reported that the steel grade has a minor influence on the defect interaction.

Table 3.3 - Pipe attributes and the geometric parameters of defects.

E (GPa)	E' (MPa)	σ_y (MPa)	$\sigma_{0.5}$ (MPa)	N	D (mm)	D/t	Δ_o (%)	l/D	$c/\pi D$	d/t
207	3047	410	450	13	323.85	20.4	0.1	1.0	0.05	0.3

Source: Adapted by Gong *et al.* (2020).

In all cases, the rectangular idealization (simplified model) is used to obtain a conservative prediction of the collapse pressures.

Next, the parameter J is used to quantify the interaction between adjacent corrosion defects (Wu *et al.*, 2022). This parameter is defined as the ratio $P_{c,multiple}/P_{c,single}$ (normalized collapse pressure). $P_{c,multiple}$ is the collapse pressure of multiple defects, and $P_{c,single}$ is the collapse pressure of a single-defect case.

The interaction exists between the defects when $P_{c,multiple}$ is smaller than $P_{c,single}$. The lower the ratio, the more significant the effect of interaction. So, when J reaches the value of 0.99, we define the spacing between defects as critical spacing (Gong *et al.*, 2020; Idris *et al.*, 2021; Wu *et al.*, 2022).

3.5.1 Interaction of longitudinally aligned defects

Previous studies have evaluated the effect of geometric defect parameters on the collapse response of pipelines with two corrosion defects aligned longitudinally (Feng; Wu; Li, 2022; Gong *et al.*, 2020). However, it is worth evaluating how these parameters affect the collapse behavior when considering two non-identical corrosion defects.

For this purpose, this section studies the interaction between two non-identical corrosion defects. Figure 3.11 shows the detailed layout of the corrosion defects evaluated in this section. In these cases, the corrosion defects are positioned on the compression side of the ovalized cross-section of the pipeline.

Figure 3.11 - Schematic diagram of longitudinally aligned defects: (a) top view and (b) longitudinal view.

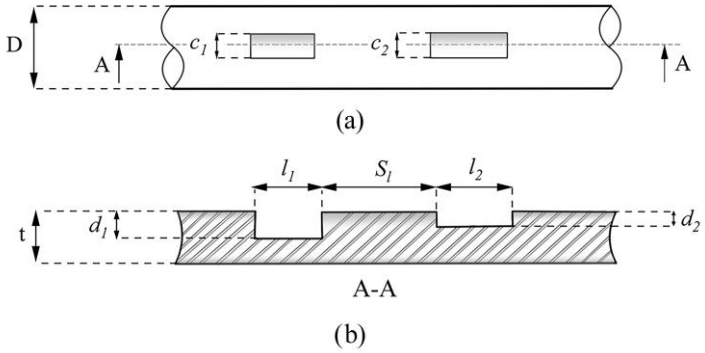

Source: The Author (2024).

3.5.1.1 Effect of corrosion defect length

Based on numerical analyses, the effect of the length of defect 2 (l_2) variation on the collapse response is investigated by considering the increase in the longitudinal distances between adjacent edges of the defects (S_l). The length of defect 1 (l_1) and the other geometric parameters are kept constant.

Figure 3.12 (a) presents the collapse pressure as a function of the normalized longitudinal spacing, and Figure 3.12 (b) shows the variation of the interaction evaluation parameter (J). As mentioned, this parameter is the ratio of $P_{c,multiple}/P_{c,single}$, where $P_{c,multiple}$ is the collapse pressure of pipes containing more than one corrosion defects. In cases where defects are not identical, $P_{c,single}$ was considered equal to the collapse pressure of the most critical defect.

Figure 3.12 - Collapse response against longitudinal spacing for different defect lengths: (a) Collapse pressure – $P_{c,multiple}$, and (b) Normalized collapse pressure – J.

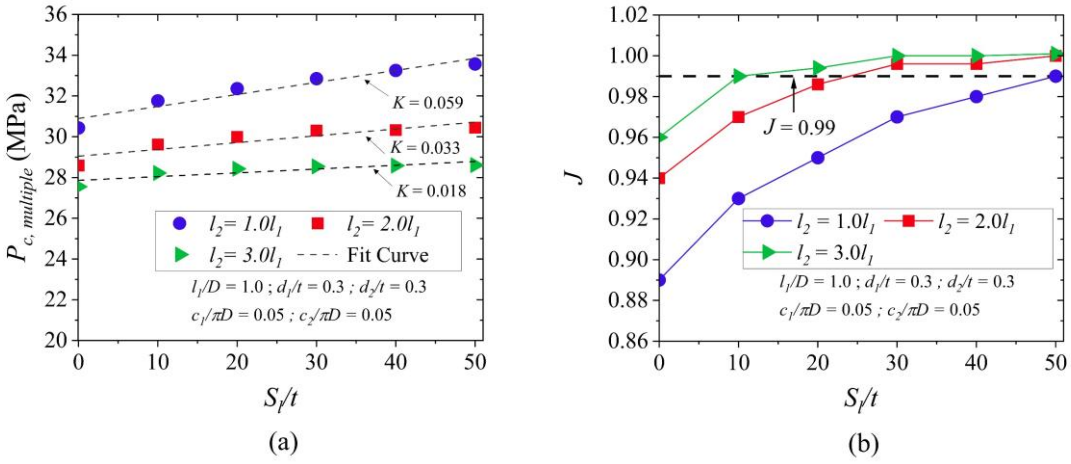

Source: The Author (2024).

The parameter K, shown in Figure 3.12 (a), is the steepness of a line obtained by the linear regression analysis and it is used to measure the relationship between the collapse pressure ($P_{c,multiple}$) and the normalized longitudinal spacing. It is noted that as the l_2 increases, the absolute value of the slope K decreases. Thus, when defect 2 becomes longer, the variation in collapse capacity becomes smaller as the longitudinal spacing between defects increases.

In summary, as expected, the collapse capacity, shown in Figure 3.12 (a), decreases with increasing l_2, but after normalization, the parameter J, shown in Figure 3.12 (b), exhibited an inverse direction (i.e., approaching to one for increasing l_2). So, the increase of l_2 leads to a reduction in the collapse capacity; however, the unfavorable influence resulting from the interaction between the defects became less significant.

A critical value for the longitudinal spacing is set when J reaches 0.99. As it was possible to observe in Figure 3.12 (b), the critical spacing between defects (S_l) decreases with increasing l_2, and the critical case occurs when the two defects are identical ($l_2 = l_1$). For this case, the critical spacing between defects is approximately $50t$.

3.5.1.2 Effect of corrosion defect depth

According to reference Gong *et al.* (2020), the defect depth of corrosion defects significantly impacts the collapse pressure of pipelines. In this section, to assess the impact of this variable, the depth of defect 2 (d_2) is varied and the collapse response is evaluated by considering the increase in the longitudinal distances between defects. The other variables are kept constant.

Figure 3.13 (a) shows the collapse pressure versus normalized longitudinal spacing, and Figure 3.13 (b) shows the interaction evaluation parameter (J), for different defect depths.

Figure 3.13 - Collapse response against longitudinal spacing for different defect depths: (a) Collapse pressure – $P_{c,multiple}$, and (b) Normalized collapse pressure – J.

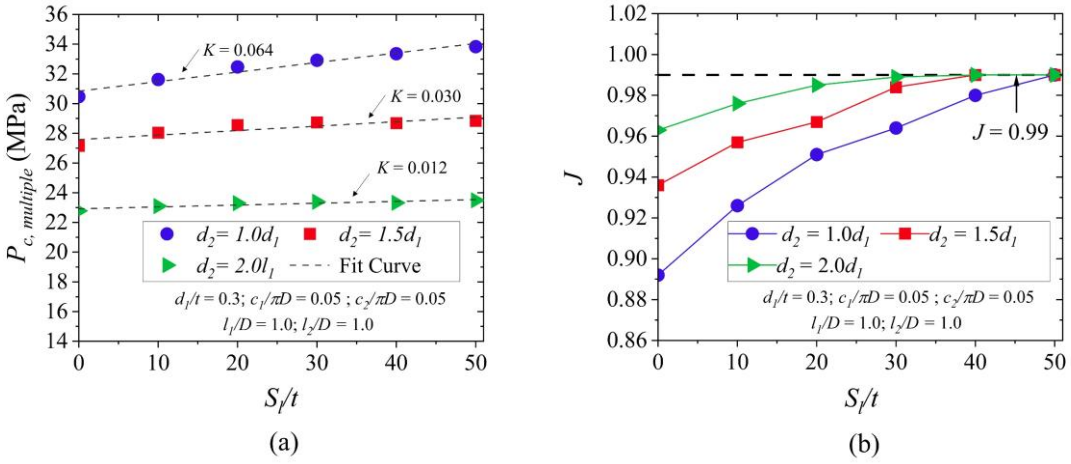

Source: The Author (2024).

As can be seen in Figure 3.13 (a), the collapse pressure decreases with increasing d_2. However, the J parameter exhibited an inverse order again, increasing with increasing d_2. In addition, as the depth of the defect increases, the absolute value of slope K decreases. Note that when $d_2 = 2.0d_1$ there is a minor variation in the collapse capacity.

As previously noted, the maximum interacting spacing between the defects decreases with increasing d_2, and the critical case occurs when the two defects are identical. For this case, the critical spacing between defects is approximately $50t$.

3.5.1.3 Effect of corrosion defect width

FE models were developed to determine the effect of the width of defect 2 (c_2) on the collapse response by considering the increase in the longitudinal distances between adjacent edges of the defects (S_l).

Figure 3.14 - Collapse pressure as a function of the longitudinal spacing for different defect widths: (a) $d_1/t = d_2/t = 0.3$ and (b) $d_1/t = d_2/t = 0.6$.

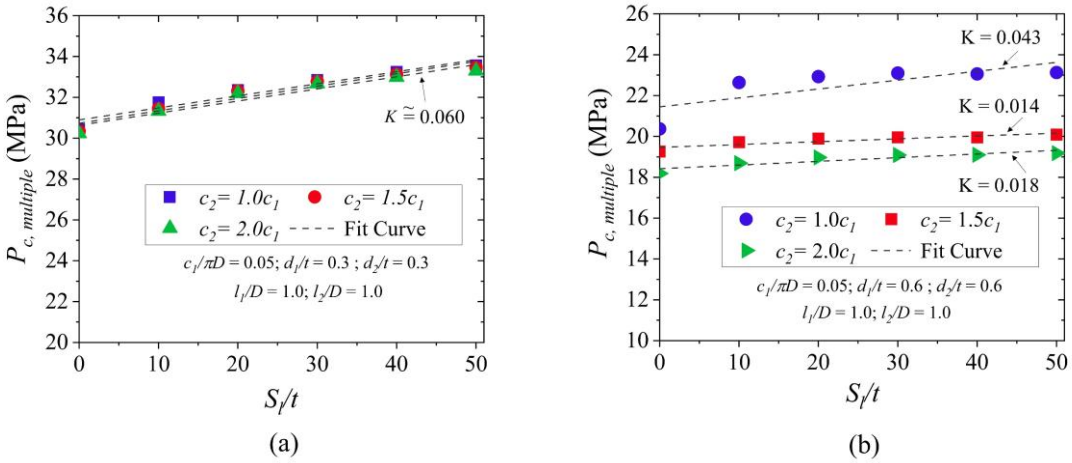

Source: The Author (2024).

Figure 3.14 (a) shows the effect of corrosion defect width on collapse pressure when $d_1/t = d_2/t = 0.3$. As observed, the increase in c_2 does not affect the collapse response significantly. The absolute value of slope K remained approximately equal to 0.060 for all cases. Additionally, Figure 3.14 (b) presents the effect of corrosion defect width on collapse pressure when $d_1/t = d_2/t = 0.6$. It is evident that the greater the defect depth, the more significant the effect of variations on parameter c_2.

Figure 3.15 (a) and (b) show the effect of corrosion defect width on J interaction factor, when $d_1/t = d_2/t = 0.3$, and $d_1/t = d_2/t = 0.6$, respectively. The trajectories of the curves presented show the same behavior observed previously, i.e., the *J* parameter exhibited an inverse order again, increasing with increasing c_2.

Figure 3.15 - Normalized collapse pressure as a function of the longitudinal spacing for different defect widths: (a) $d_1/t = d_2/t = 0.3$ and (b) $d_1/t = d_2/t = 0.6$.

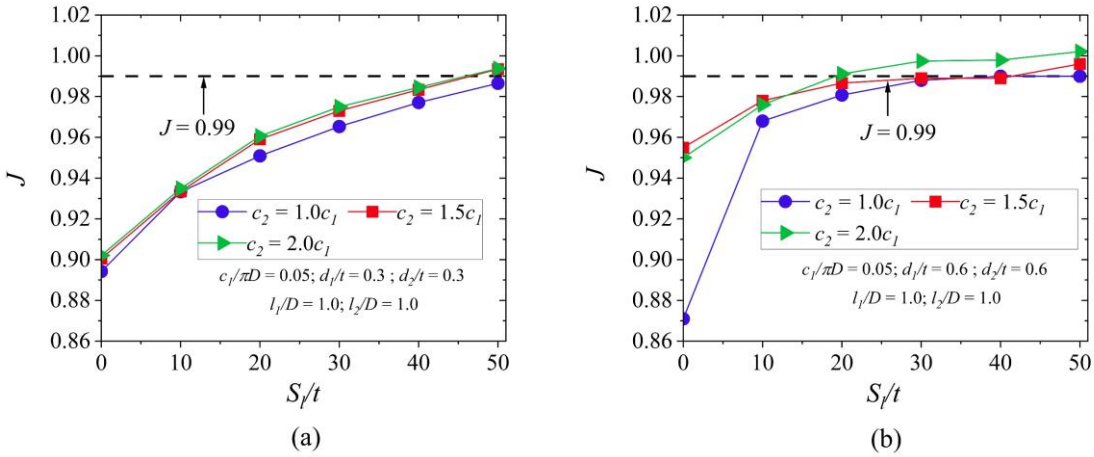

Source: The Author (2024).

In addition, it is possible to observe in Figure 3.15 (a) and (b) that the maximum interacting spacing between the defects decreases with increasing c_2. However, for

the pipeline with a smaller defect depth ($d_1/t = d_2/t = 0.3$), the effect of c_2 on the critical spacing is greater than that with a larger defect depth ($d_1/t = d_2/t = 0.6$).

3.5.2 Interaction of multiple corrosion defects

Corrosion defects arise randomly and in a wide variety of arrangements. Herein, to complete earlier studies, a parametric analysis was conducted on the configuration model shown in Figure 3.16, varying the distance between corrosion defects in the circumferential direction (S_c).

Figure 3.16 - Multiple defect configuration model.

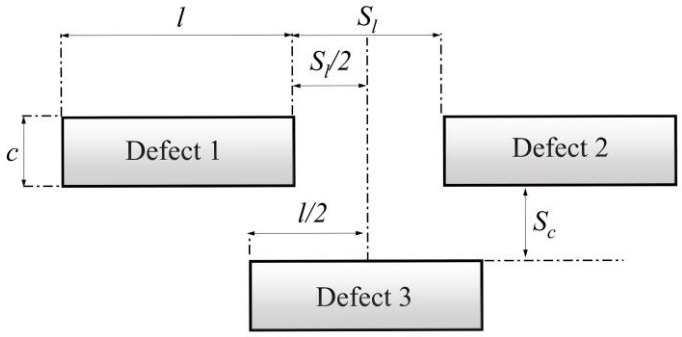

Source: The Author (2024).

In section 3.5.1, the critical spacing at which defects do not interact was found to be approximately $50t$. Therefore, for all cases in this section, $S_l = 50t$ was considered to ensure that Defects 1 and 2 are sufficiently spaced not to interact. In contrast, Defect 3 is positioned longitudinally in the center, between defects 1 and 2, and its angular position ranges from 0º to 180º concerning the other defects ($S_c/\pi D =$ 0, 0.05, 0.1, 0.2, 0.3, 0.4, 0.45). The angular position range corresponds to that used by Gong *et al.* (2020). However, in Gong *et al.* (2020), the study focused only on two corrosion defects.

Figure 3.17 schematically illustrates the position of defects concerning the ovalized cross-section. In Figure 3.17, the signs $(+)$ and $(-)$ represent the tensile and compressed surfaces, respectively. In these cases, defects 1 and 2 are positioned on the compression side of the ovalized cross-section of the pipeline. However, the position of defect 3 with respect to the ovalized cross-section varies from point A to B.

Figure 3.17 - Position of the defects with respect to the ovalized cross-section.

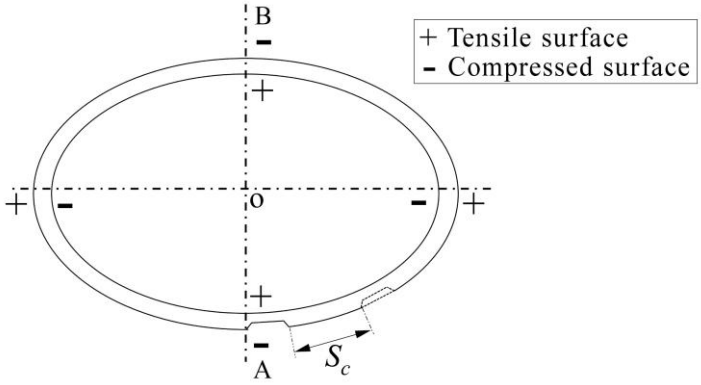

Source: The Author (2024).

As an illustration, Figure 3.18 depicts the finite element models for two representative pipes varying the circumferential spacing between adjacent corrosion defects. In Figure 3.18 and the following results, circumferential spacing is normalized by the pipeline diameter (D).

Figure 3.18 - Solid FE mesh varying the circumferential spacing between adjacent corrosion defects: (a) $S_c/\pi D = 0$, and (b) $S_c/\pi D = 0.1$.

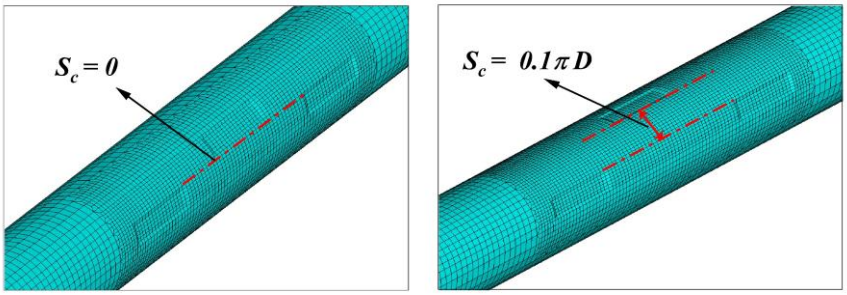

Source: The Author (2024).

Figure 3.19 shows some examples of the von Mises equivalent stress contour plots for the FE model, with the normalized circumferential spacing distance between defects of 0 and 0.1, respectively. The highest von Mises stress concentration is in the region of the defects. Also, stress concentration is high at the adjacent regions to the defects due to interaction, especially when $S_c/\pi D$ = 0.

Figure 3.19 - Von Misses stress distribution for the FE models with: (a) $S_c/\pi D = 0$, and (b) $S_c/\pi D = 0.1$.

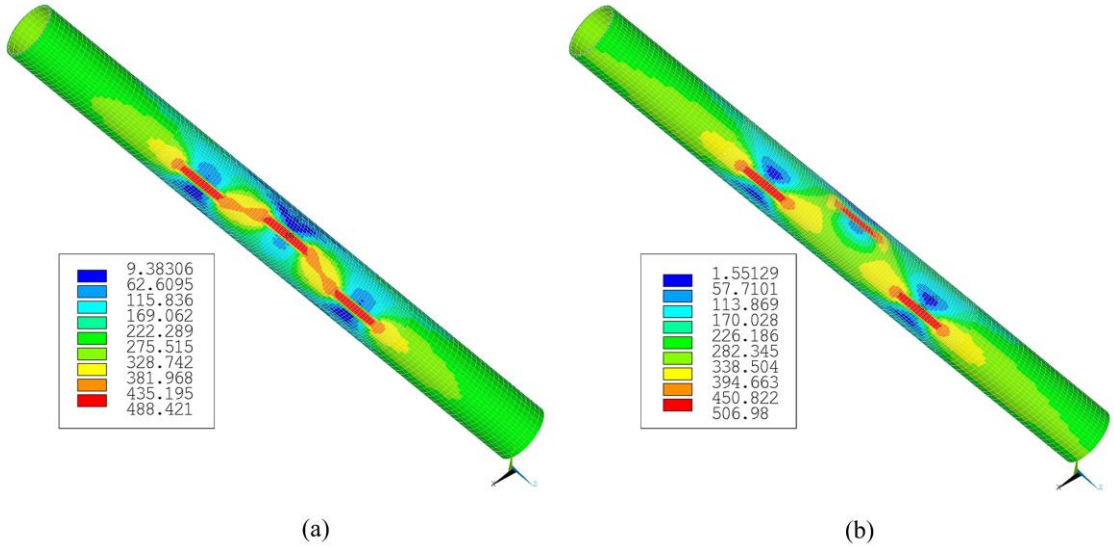

Source: The Author (2024).

The collapse modes for the normalized circumferential spacing distance between defects equal to 0, 0.1, 0.3, and 0.45, respectively, are shown in Figure 3.20. It is possible to observe that with the increase in circumferential spacing (S_c) between defects, the collapse mode tends to change.

Figure 3.20 - Collapse modes for the FE models with: (a) $S_c/\pi D = 0$, (b) $S_c/\pi D = 0.1$, (c) $S_c/\pi D = 0.3$, and (d) $S_c/\pi D = 0.45$

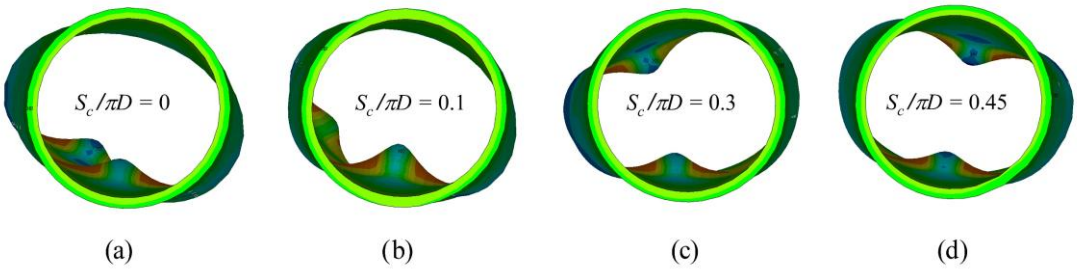

Source: The Author (2024).

Figure 3.21 (a) indicates that increasing the circumferential distance until 0.1 ($S_c/\pi D \leq 0.1$) causes a linear rise in the collapse pressure of the pipeline. However, for $S_c/\pi D > 0.2$ values, increasing the circumferential distance results in a continuous decay of the collapse pressure.

Figure 3.21 - Collapse response of multiple defects of corrosion plotted against circumferential spacing: (a) Collapse pressure – $P_{c,multiple}$, and (b) Normalized collapse pressure – J.

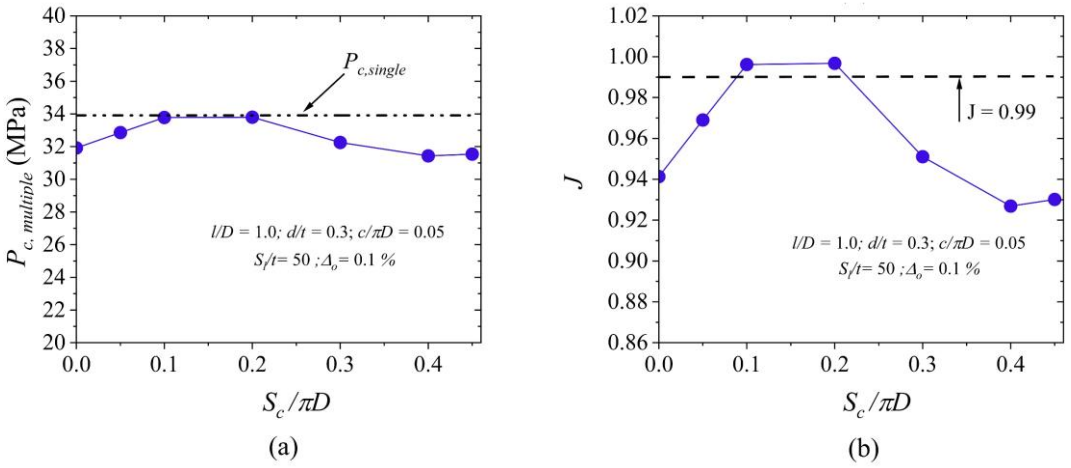

Source: The Author (2024).

In Figure 3.21 (b), the interaction evaluation parameter (J) follows the same behavior as the collapse pressure. The results show that for $S_c/\pi D = 0.1$ and $S_c/\pi D = 0.2$, J exceeds 0.99 and remains practically constant. Figure 3.21 (a) shows that $P_{c,multiple}$ was approximately equal to $P_{c,single}$ when $S_c/\pi D = 0.1$ and $S_c/\pi D = 0.2$. In these cases, there is a collapse mode transition, as for $S_c/\pi D > 0.2$, the order reverses, and the collapse pressure tends to decrease. The dominating collapse mode changed from a U-shaped mode to a semi-ovalization mode.

In summary, no critical angular spacing was found when adding a third circumferentially aligned defect, i.e., defects in the circumferential critical range should always be considered interacted. However, it is observed that the most critical cases occur for $S_c/\pi D = 0.0$ and $S_c/\pi D \geq 0.4$ (defects separated by almost 180°).

3.5.3 Effect of initial ovality on the defects interaction

Ovalization is a factor that significantly affects the mechanical behavior of pipes. This section presents a parametric study with to obtain the relationship between ovality and the collapse response for the scenario studied.

According to DNV (2013), the initial ovality tolerance of the pipeline manufacturing process should not exceed 3 %. Here, a study is carried out to up to an initial ovality of 4 % for a better curve fitting. Five initial ovalities, 0.1 %, 1.0 %, 2.0 %, 3.0 %, and 4.0 %, were considered. The effect of initial ovality is evaluated for different circumferential distances.

In Figure 3.22 (a), the collapse pressure was plotted against the variation of normalized circumferential spacing between the defects. As expected, the $P_{c,multiple}$ decreases with increasing initial ovality. Increasing ovality from 0.1% to 4.0% reduced the collapse pressure by more than 30%, regardless of the spacing between defects. This indicates the importance of considering the ovalization.

The response of the interaction evaluation parameter (J) is shown in Figure 3.22 (b). For the most critical cases ($S_c/\pi D = 0.0$ and $S_c/\pi D \geq 0.4$), J increases with increasing ovalization, and its trajectory as a function of circumferential spacing is similar for all cases.

Figure 3.22 - Collapse response plotted against circumferential spacing with different initial ovality: (a) Collapse pressure – $P_{c,multiple}$, and (b) Normalized collapse pressure – J.

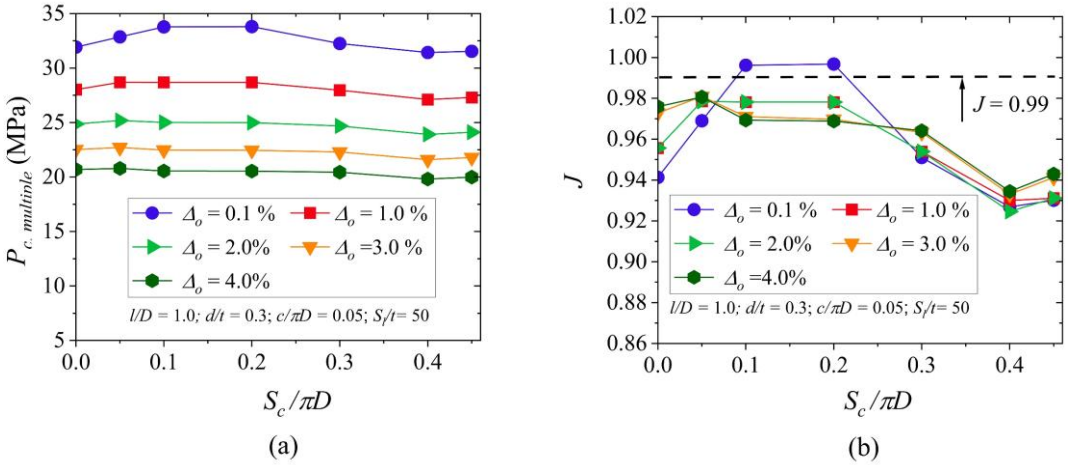

Source: The Author (2024).

Based on the numerical simulations conducted, Figure 3.23 shows the collapse pressure reduction factor against the variation of initial ovality. The reduction factor f_o, defined here, corresponds to the ratio between the collapse pressure of the ovalized pipeline ($P_{c,ovality}$) and the collapse pressure of the pipeline without ovalization (P_c). In this way, $P_{c,ovality}$) can be expressed as:

$$P_{c,ovality} = f_o \times P_c \tag{17}$$

Figure 3.23 - Reduction factor f_o against initial ovality for single and multiple defects with different circumferential spacing.

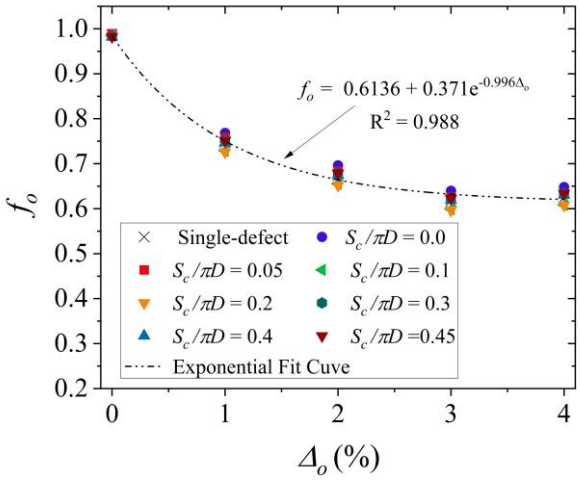

Source: The Author (2024).

As can be seen in Figure 3.23, the changing rates of the curves are almost the same in all cases (single and multiple defects). So, for the arrangement of analyzed defects, the results suggest that regardless of the number of defects, the effect of initial ovality has a similar impact on reducing the collapse pressure.

Additionally, an equation for the reduction factor f_o is developed based on numerical data, by fitting the exponential function, described in Eq. (18).

$$f_o = y_0 + Ae^{R_0\Delta_o} \tag{18}$$

where y_0, A, and R_0 are the tuning parameters.

So, using the Levenberg-Marquardt curve fitting method (Marquardt, 1963), the reduction factor f_o can be expressed as:

$$f_o = 0.6136 + 0.371e^{-0.996\Delta_o} \tag{19}$$

in which the range of Δ_o is 0-4%.

The R-Square (R^2), shown in Figure 3.23, is a statistical measure to qualify the fitting curve. The closer the R-Square value is to 1, the better the fitted curve fits your data. As can be seen in Figure 3.23, the fitted curve presents a good approximation (R^2 = 0.988). However, further research is required to determine the applicability of the proposed adjustment factor to other geometries and different types of steel.

Furthermore, it is essential to emphasize that subsea pipelines should not be subject to excessive ovalization. Here, from the observed results, regardless of the number of defects, there is no significant variation in the reduction factor when the initial ovality increases from 3% to 4%.

3.5.4 Effect of temperature change on the defects interaction

This section presents the results obtained from FE simulations to evaluate the influence of thermal load on the collapse response for the scenario studied, illustrated in Figure 3.16. Four temperatures changes (ΔT) of the pipe were studied: 0 ºC (reference), 50 º C, 75 ºC, 100 ºC and 120 ºC.

Figure 3.24 (a) presents the collapse pressure versus the normalized circumferential spacing between the defects. As expected, the $P_{c,multiple}$ decreases with increasing ΔT. However, the differences observed are not very significant. Increasing temperature change from 0 ºC to 120 ºC reduced collapse pressure by less than 7 %, regardless of the spacing between defects.

In addition, the response of the interaction evaluation parameter (J) is shown in Figure 3.24 (b). Note that J became larger with increasing temperature. Thus, despite the increase in temperature change leading to a reduction in the collapse capacity, the interaction between the defects became less pronounced with this increase.

Figure 3.24 - Collapse response against circumferential spacing for different ΔT: (a) Collapse pressure – $P_{c,multiple}$, and (b) Normalized collapse pressure – J.

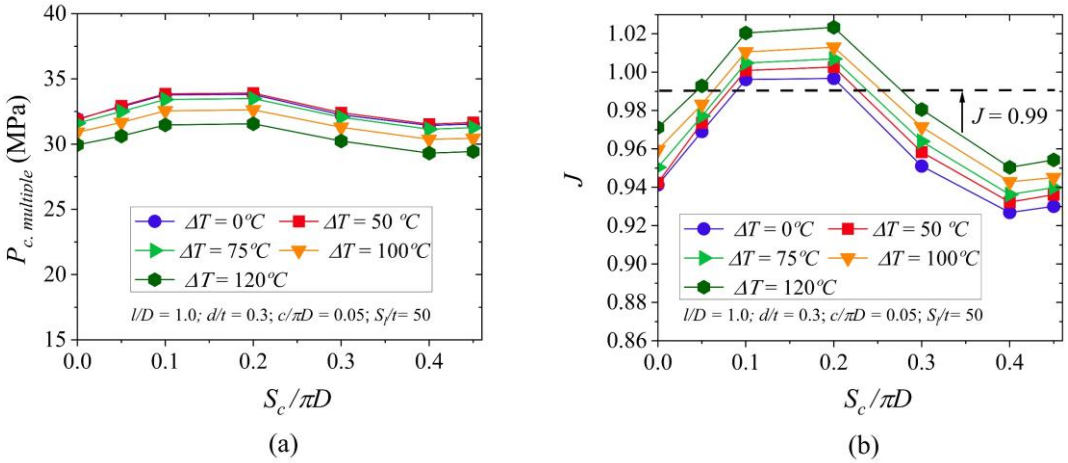

Source: The Author (2024).

Based on the numerical simulation conducted, Figure 3.25 shows the relationship between the collapse pressure reduction factor and temperature variation. The reduction factor f_T, defined here, is the ratio between the collapse pressure of the pipeline with thermal conditions ($P_{c,T}$) to the collapse pressure of the pipeline when $\Delta T = 0º$ (P_c). Thus, $P_{c,T}$ can be expressed as:

$$P_{c,T} = f_T \times P_c \tag{20}$$

Figure 3.25 - Reduction factor f_T against ΔT for single and multiple defects with different circumferential spacing

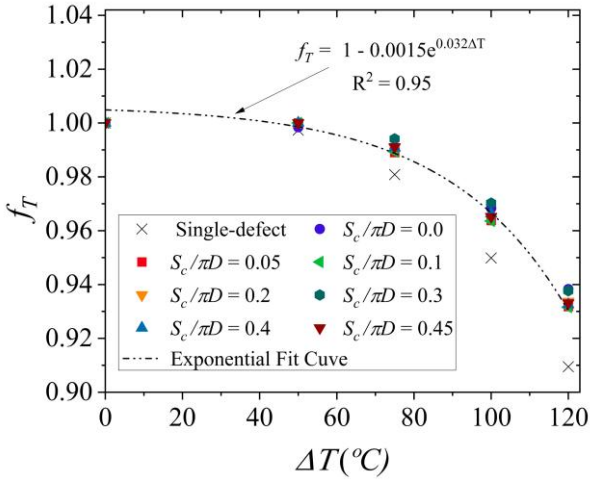

Source: The Author (2024).

Figure 3.25 shows that for small temperature changes, the reduction factor (f_T) is approximately equal to 1, i.e., ΔT effect does not affect the collapse response. However, for temperatures greater than 50°C, the increase in temperature variation causes a decrease of f_T, indicating a reduction in the collapse capacity of the pipeline for all cases (single and multiple defects).

Additionally, it is also possible to observe in Figure 3.25 that the effect of temperature was more prevalent in the case of a single defect. For this case, when increasing the temperature from 0°C to 120°C, the collapse capacity reduces by approximately 9 %. As seen previously, for multiple defects cases, this reduction was less than 7 %.

Based on the numerical data, an equation for the reduction factor f_T is proposed by fitting the exponential function described in Eq. (18). In the same way as the previous section, the Levenberg-Marquardt curve fitting method (Marquardt, 1963) is used to obtain the reduction factor f_T, described as:

$$f_T = 1 - 0.0015e^{0.032\Delta T} \quad (21)$$

in which the range ΔT is 0-120 ºC.

As can be seen in Figure 3.25, the fitted curve presents a good approximation (R^2 = 0.95). However, more studies are necessary to extend the applicable range of the proposed adjustment factor to other geometries and different types of steel.

3.6 CONCLUSIONS

This paper studies corroded subsea pipeline collapses employing finite element models automatically generated by the PIPEFLAW system. The PIPEFLAW system makes it possible to rapidly and accurately assess the collapse pressure of corroded pipelines subjected to combined loads with different geometric configurations.

Extensive parametric analysis of corroded subsea pipelines was conducted to assess the interaction of corrosion defects, considering varied geometries and arrangements. Finally, investigations include the effect of ovality and temperature on the collapse resistance of pipelines with single and multiple corrosion defect scenarios. Two collapse pressure adjustment factors were proposed. The main conclusions of this paper are as follows:

- The sizes of defects, i.e., length, width, and depth, significantly impact the collapse response and interaction rules in subsea pipelines with two longitudinally aligned corrosion defects. An increase in defect size is associated with decreased collapse pressure. In contrast, an increase in defect size tends to increase the interaction between defects. However, this interaction becomes less pronounced as the longitudinal distance between the defects increases.
- Increasing the longitudinal spacing between defects significantly reduces the effect of interaction. In this study, the critical longitudinal spacing necessary to consider isolated defects was found to be $50t$. The interaction rule based on the critical longitudinal spacing for non-identical defects proved consistent with the results found by Gong *et al.* (2020) for identical defects.
- For multiple defects, the interaction between circumferential defects is more significant when the defects are close or almost 180º apart from each other, i.e., there is no critical angular spacing. Therefore, given the observed complexity, the interaction between circumferential defects should always be considered (in favor of safety).
- The collapse pressure decreases significantly with increasing initial ovality for all cases. However, regardless of the number of defects, the effect of initial ovality has a similar impact on the collapse response.
- The temperature change negatively affects the collapse pressure, but the interaction between the defects became less pronounced with temperature

increase. Additionally, it was also observed that the effect of temperature change had more impact in the single defect case.

- The proposed adjustment factors lead to a good prediction of the collapse pressure of pipelines, considering the effect of initial ovality and temperature variation. However, these factors have a limited range of applications, and additional studies must be carried out to assess their applicability to other geometries and different types of steel.

4 NOVEL APPROACH OF COLLAPSE PRESSURE PREDICTION OF SUBSEA PIPELINES WITH REALISTIC CORROSION DEFECTS

D'Aguiar, S. C. M; Motta, R. de S.; Ferreira, A. D. M.; Afonso, S. M. B. (2025) Novel approach of collapse pressure prediction of subsea pipelines with realistic corrosion defects. **Ocean Engineering**, v. 337, p. 121895. DOI: https://doi.org/10.1016/j.oceaneng.2025.121895

Abstract.

Corrosion defects represent a significant risk to the structural integrity and operational safety of subsea pipelines. Advances in inspection technologies enable precise characterization of these defects through detailed mapping of corroded zones. This work introduces a novel approach to evaluate the collapse of pipelines with realistic corrosion defects. The proposed method is based on mapping the corroded surface into equivalent sub-defects, allowing for a more accurate estimation of the collapse pressure. The effectiveness of this approach is validated through comparisons with finite element analysis (FEA) results and benchmarked against traditional semi-empirical methods based on maximum and average defect depths. The findings indicate that traditional methods yield excessively conservative predictions, exhibiting an approximately 68% average relative error for 100 analyzed cases. In contrast, the novel approach significantly lowers this average relative error to 11.9 %. Furthermore, the standard deviation of the average error decreased from 20 % to approximately 7 %. These numbers demonstrate a substantial improvement in the precision and accuracy of the estimates considering the presented approach. Moreover, the strategy is highly computationally efficient, enabling the rapid analysis of numerous cases in a significantly shorter time. This makes it a valuable tool for pipeline shutdown decisions in the oil and gas industry.

Keywords: Subsea pipelines; Corrosion; Realistic shaped; Collapse Response.

4.1 INTRODUCTION

Subsea pipeline networks are the most effective and economical means of transporting oil and gas to offshore platforms or onshore terminals (Bhardwaj; Teixeira; Soares, 2020). Corrosion defects are significant imperfections influencing the collapse capacity of these pipelines (Chen *et al.*, 2021b; Gong *et al.*, 2021). As such, evaluating the collapse response of subsea pipes with corrosion defects is essential to ensuring offshore systems' integrity, safety, and efficiency.

Corrosion defects aging in pipelines vary widely in size, shape, location, and orientation (Zhu, 2021, 2018). Typically, real corrosion defects have an irregular depth profile and extend in an irregular pattern in both longitudinal and circumferential directions of the pipeline (Cosham; Hopkins; Macdonald, 2007). The assessment

guideline for corroded pipelines, DNV (2017), classifies corrosion defects into three categories: single, interactive, and irregular.

Subsea pipelines with single and idealized corrosion defects subjected to external pressure have been extensively studied (Chen *et al.*, 2021b; Fan *et al.*, 2017; Gong *et al.*, 2021; Li; Chen; Soares, 2022; Netto, 2009, 2010; Netto; Ferraz; Botto, 2007; Sakakibara; Kyriakides; Corona, 2008; Zhang; Chen; Guedes Soares, 2020; Zhou *et al.*, 2024). Also, detailed guidelines exist regarding the influence for such situations of corrosion defects on collapse pressure.

Netto, Ferraz, and Botto (2007) evaluated the effect of corrosion defects on the collapse pressure of offshore pipelines by combining laboratory experiments and nonlinear numerical analyses based on the Finite Element (FE). It was found in Netto, Ferraz, and Botto (2007) that the collapse mechanisms are complex and are affected by the geometry of the defect, its type (internal or external), and its position in the ovalized cross-section. Subsequently, Netto (2009, 2010) developed a method to estimate the collapse pressure of pipelines with long and narrow corrosion idealized defects.

Zhang, Chen, and Soares (2020) evaluated the effects of non-symmetrical corrosion defects and the influence of the angular location and the ovality on the collapse response for subsea corroded pipes. The effect of the location angle of the corrosion defect is not considered in the equations proposed by Netto (2009, 2010).

Gong *et al.* (2021) conducted small-scale experimental tests and FE analyses of subsea pipes with elliptical and rectangular corrosion defects, and they developed a simple empirical equation to estimate the collapse pressure of pipelines with a single elliptical corrosion defect. Afterward, Chen *et al.* (2021b) used FE models and studied the collapse behavior of pipelines with constant-depth, elliptical, and parabolic corrosion shapes. In the research by Chen *et al.* (2021b), expressions for predicting the collapse pressure of pipelines with constant-depth, elliptical, and parabolic corrosion shapes were developed, respectively. As expected, pipelines with elliptical or parabolic corrosion geometries withstand greater collapse capacity than those with constant-depth corrosion shape.

Over the past years, research on the behavior of subsea pipelines with interacting corrosion defects has also been highlighted (D'Aguiar; Motta; Afonso, 2024; Gong *et al.*, 2020; Wu *et al.*, 2022, 2023). Gong *et al.* (2020) investigated experimentally and numerically the influence of the interaction between two elliptical

corrosion defects on collapse response. The results indicated that the defect size, i.e., the length, width, depth, and geometry of the pipe are prominent parameters in the defect interaction rules.

D'Aguiar, Motta, and Afonso (2024) evaluated the interaction effects between two non-identical corrosion defects based on FE simulation data. The interaction rule based on the critical longitudinal spacing for non-identical defects, as presented in D'Aguiar, Motta, and Afonso (2024), proved consistent with the findings of Gong *et al.* (2020) for identical defects.

Wu *et al.* (2022) studied the interaction rules of corroded pipelines under external pressure considering several numerical analyses. They proposed a formula for estimating the collapse pressure of a pipeline with interacting corrosion defects based on the critical external pressure formula of an intact, thin-walled pipeline.

Few studies for the collapse response of corroded pipelines under external pressure have considered non-uniform corrosion defect shapes. Wu *et al.* (2023) proposed a method for the critical buckling pressure of pipelines with irregular corrosion defects (two idealized defects overlapping), presenting excellent accuracy to the numerical and experimental results.

On the other hand, the current literature includes many investigations into burst failure under the internal pressure of corroded pipelines with complex-shaped defects (Cabral *et al.*, 2022; Motta; Ferreira; Afonso, 2024; Ferreira *et al.*, 2021; Ferreira; Willmersdorf; Afonso, 2024; Li *et al.*, 2024; Pimentel *et al.*, 2020). Pimentel *et al.* (2020) introduced a methodology to automatically construct a smooth FE geometric representation of the realistic corroded pipe shape based on data provided by field inspection. This procedure was validated to evaluate the failure of corroded pipes under internal pressure and showed excellent results. Posteriorly, Ferreira *et al.* (2024, 2021) used a similar methodology for automating the generation of FE models and predicting the burst pressure of pipelines with synthetic corrosion defects with realistic properties.

Advances in inspection technologies, such as smart pigs, enable precise mapping of remaining wall thickness and captures complex corrosion defects in submarine pipelines. Despite these advancements, more research is needed on the collapse behavior of submarine pipelines with realistic corrosion defects under external pressure. Figure 4.1 illustrates the real corrosion defect morphology of subsea pipeline.

Figure 4.1. Morphology of a corroded subsea pipeline.

Source: Li, Xie, and Liu (2023).

Li, Xie, and Liu (2023) used a reverse inversion modeling method to reconstruct the numerical model of pipes with non-uniform surface corrosion defects. They found a good correlation between numerical and experimental results. However, no semi-empirical solution that explicitly accounts for the non-uniformity of real corrosion defects is currently available.

To fill this gap, this work introduces a novel approach to predicting the collapse pressure of subsea pipelines with realistic corrosion defects. The main contribution of this study is that the methodology proposed achieves results with high accuracy and reliability with a computationally efficient outcome, achieving a speed approximately 120 times faster than traditional 3D finite element simulations.

4.2 SEMI-EMPIRICAL METHOD

Netto (2009, 2010) developed a semi-empirical method based on experimental data and numerical results to instantly evaluate the effect of a single idealized corrosion defect, considering the most practical range of geometric parameters. The methodology proposed by Netto (2009, 2010) yielded the Eq. (21):

$$\frac{P_{cor}}{P_{co}} = \left[\frac{1 - \frac{d}{t}}{1 - \frac{d}{t}\left(1 - \left(\frac{c}{\pi D}\right)^{0.4} \left(\frac{l}{10D}\right)^{0.4}\right)} \right]^{2.675} \tag{21}$$

where P_{cor} is the collapse pressure of the corroded pipe, and P_{co} is the collapse pressure of the intact pipe, D is the nominal outer diameter, t is the thickness of the pipe, d is the corrosion depth, c is the corrosion circumferential width, and l is the corrosion length. The defect parameters c e d presented in Eq. (21) have the limits indicated in Table 4.1 (Netto, 2010).

Table 4.1 - Combination of parameters

Categories	d/t	$c/\pi D$
Shallow defects	$0.1 \leq \frac{d}{t} \leq 0.2$	$\frac{c}{\pi D} \leq 0.1$
Moderately deep defects	$0.2 \leq \frac{d}{t} \leq 0.4$	$\frac{c}{\pi D} \leq 0.1$
Deep and very narrow defects	$0.4 \leq \frac{d}{t} \leq 0.6$	$\frac{c}{\pi D} \leq 0.2 - 0.25\frac{d}{t}$

Source: Adapted by Netto (2010).

For moderately deep defects, the maximum $\frac{c}{\pi D}$ value to be considered is $(0.15 - 0.25\frac{d}{t})$, and for deep and very narrow defects, this value is $(0.1 - 0.125\frac{d}{t})$. Additionally, in all cases, $\frac{l}{D}$ shall be fixed as 10 if $\frac{l}{D}$ > 10. More details are available on Netto (2009, 2010).

The design code Det Norske Veritas (DNV, 2021) defines the collapse pressure of the intact pipe (P_{co}). The formula is derived from elastic capacity, plastic capacity, and ovality, as detailed below:

$$(P_{co} - P_{el}) \cdot \left(P_{co}^2 - P_p^2\right) = P_{co} \cdot P_{el} \cdot P_p \cdot \Delta_o \cdot \frac{D}{t} \tag{22}$$

where P_{el} is the elastic collapse pressure, P_p represents the plastic collapse pressure, and Δ_o is the ovality parameter.

The elastic collapse pressure (P_{el}) can be calculated using the equation from classical formulation (Gere; Timoshenko, 1961):

$$P_{el} = \frac{2E}{(1-\nu^2)}\left(\frac{t}{D_{ave}}\right)^3 \tag{23}$$

where E is Young's modulus of the material, ν is the Poison's ratio, t and D_{ave} are, respectively, wall thickness and the average diameter of the pipe ($D_{ave} = D - t$).

The prediction of the plastic collapse pressure (P_p) can be calculated by using the yield stress of the material (f_y) and the manufacturing factor (α_{fab}):

$$P_p = f_y \cdot \alpha_{fab} \cdot \frac{2t}{D} \tag{24}$$

Notably, DNV (2021) specifies that the maximum ovality permitted in pipelines is 3%. This applies to the pipeline according to its installed condition. The standard also highlights that the minimum ovality to consider for the system collapse check is

0.5%. In present study, the collapse pressure of the intact pipe (P_{co}) is obtained from FE analysis by the PIPEFLAW system.

4.3 FINITE ELEMENT ANALYSES

4.3.1 General

In the present work, the finite element analysis (FEA) is performed using the PIPEFLAW computational tool, developed by the PADMEC (High-Performance Processing in Computational Mechanics) research group at the Federal University of Pernambuco (UFPE, Brazil). The PIPEFLAW program integrates several tools for automatic FE model generation based on MSC.PATRAN (Patran, 2012) and FE analysis via ANSYS software (Ansys, 2020).

Numerous studies have used this tool, demonstrating its effectiveness in predicting accurate and reliable assessments of the integrity of pipelines for either idealized or realistic corrosion defects (Bruère *et al.*, 2019; D'Aguiar; Motta; Afonso, 2024; Ferreira *et al.*, 2021; Motta *et al.*, 2021, 2017; Pimentel *et al.*, 2020; Soares *et al.*, 2019).

The pipelines are modeled using 3D hexahedral solid elements. The FE models generated by the PIFEFLAW system present four elements along the wall thickness in the defect region (Cabral *et al.*, 2017). To optimize the computational cost and avoid small elements in the region far from the defect, the PIPEFLAW introduces mesh transitions. Thus, the number of elements in the thickness is reduced to two in the region outside the defect.

The size of the elements along the thickness is used as a parameter to automatically calculate the number of elements along the surface (Ferreira *et al.*, 2021), including mesh transitions and expansion regions around the defect region. Previous research provides more details of the model generation process (Cabral *et al.*, 2017; Ferreira *et al.*, 2021; Pimentel *et al.*, 2020).

The mesh density is defined based on sensitivity studies and convergence analysis previously conducted by the PETROBRAS R&D Center, ensuring the accuracy and efficiency of the simulations (Cabral *et al.* 2007).

Figure 4.2 shows typical meshes for pipelines with irregular corrosion defects. For realistic defects, mapping the corroded region and its respective remaining wall thickness is necessary.

Figure 4.2 - Mesh created automatically using the PIPEFLAW system for a realistic defect: (a) Mesh discretization and (b) Cross section of the pipe in the center of the defect.

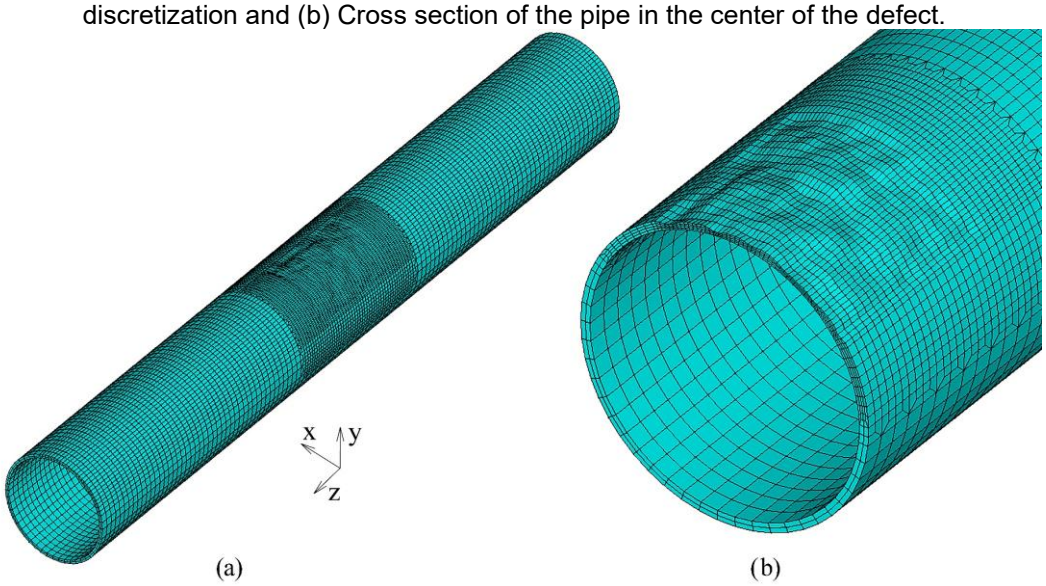

Source: The Author (2025).

The mapping of the corroded zone is normally provided in a spreadsheet that contains the value of the remaining thickness of the pipeline wall and the positions of the points in the longitudinal and circumferential directions. This paper uses synthetic cases based on real corrosion profiles. Section 4.4.1 describes the methodology for generating the mapping of corroded regions of synthetic defects.

4.3.2 Material Properties

The Modified Ramberg-Osgood (R-O), described in Eq. (25), provides the stress-strain relationship of steel pipelines (Gong; Wang; Yuan, 2020):

$$\varepsilon = \frac{\sigma}{E}\left(1 + \frac{3}{7}\left|\frac{\sigma}{\sigma_y}\right|^{n-1}\right) \tag{25}$$

where ε denotes the uniaxial strain, σ represents the uniaxial stress, E is Young's modulus, σ_y strands the effective yield stress, and n is the R-O strain hardening parameter. Particularly, the Eq. (25) is only applicable to the strain level of less than 0.015. According to Gong, Wang, and Yuan (2020), for strain values greater than 0.015, a linear variation is adopted as below:

$$E' = \left.\frac{d\sigma}{d\varepsilon}\right|_{\varepsilon=0.015} = E\left(1 + \frac{3}{7}n\left|\frac{\sigma}{\sigma_y}\right|^{n-1}\right)^{-1} \quad (26)$$

where E' is the material's modulus of hardening.

4.3.3 Load and boundary conditions

The primary design load of ultra-deep pipelines is the external hydrostatic pressure (Kyriakides; Lee, 2021). So, here FE simulations are subjected to external pressure only. Figure 4.3 illustrates the load application and boundary conditions in the FE model used in the present work. The displacement in the longitudinal direction (Fix Z) is constrained at all nodes on one side of the model. Additionally, the displacement at the angular cylindrical coordinate (Fix θ) is restricted at two nodes on one end to eliminate rigid body motion (rotation).

Figure 4.3 - Load and boundary conditions of the FE model

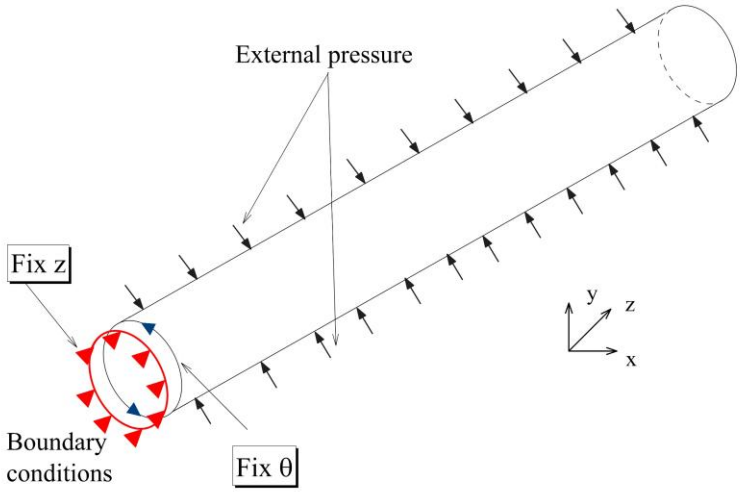

Source: The Author (2025).

4.3.4 Failure criterion

For onshore pipelines, the von Mises criterion defines burst pressure as the point at which the von Mises equivalent stress across the remaining wall thickness reaches the material's reference stress value, typically 80% of the true ultimate tensile strength (Velázquez *et al.*, 2022).

On the other hand, offshore pipelines generally operate under conditions where the external pressure exceeds the internal pressure, resulting in differential pressure across the pipeline wall (Nogueira; Mckeehan, 2005). In deepwater and ultra-

deepwater, the external hydrostatic pressure becomes the dominant load condition and is the main factor determining the minimum pipeline wall thickness (Novitsky; Gray, 2003).

As a result, plastic collapse is the most widely adopted failure criterion for thick-walled subsea pipelines under external pressure. In this study, collapse occurs when the pipe can no longer sustain the applied load due to progressive plastic deformation of its cross-section.

Collapse behavior is sensitive to severe geometric nonlinearities and structural instability (Gong *et al.*, 2020, 2021; Gong; Li, 2015; Xu; Gong; Hu, 2016). For this reason, in this paper, the external pressure is applied in small increments, and the Riks method (Riks, 1972) is used for the collapse simulation. The Riks method is typically employed to prevent structures' instability and geometrically nonlinear collapse. In this context, structural instability and collapse are understood to occur when the first limit point is reached. The limit point is the moment in the response history when the tangent instability matrix becomes singular, indicating that the structure has lost its stability. Accordingly, the collapse criteria consider that failure occurs when the conditions described in Eq. (27) and (28) are satisfied (Olatunde *et al.*, 2023):

$$\left|\frac{\partial \bar{I}^n}{d\bar{u}^m}\right| = |\mathbb{K}^{nm}| = 0 \tag{27}$$

$$\Delta\lambda_i < 0 \tag{28}$$

where $\bar{I}^n$ are the internal forces, $\bar{u}^m$ are nodal displacements $\bar{u}$, K^{nm} is the tangent stiffness of the assembly, n and m are the degree of freedom of the internal forces and displacements, respectively, and $\Delta\lambda_i$ is the increment in load proportionality factor λ_{i-1} towards the next load increment.

4.3.5 FE analysis validation

As mentioned previously, for assessment purposes, corrosion defects can be irregular (complex geometry) or idealized shaped. The idealized geometries of corrosion defects are usually constant-depth or elliptical shapes. The cross sections of the pipelines with complex shaped, constant-depth, and elliptical shapes are shown in Figure 4.4 where D is the nominal outer diameter, t is the thickness of the pipe, d_{max}

is the maximum depth of the realistic shape, c is the corrosion circumferential width, and φ is the half angle denoting the corrosion width.

Figure 4.4 - Geometry of pipe cross-section with three types of corrosion shapes: (a) Realistic shaped, (b) Constant-depth, and (c) Elliptical.

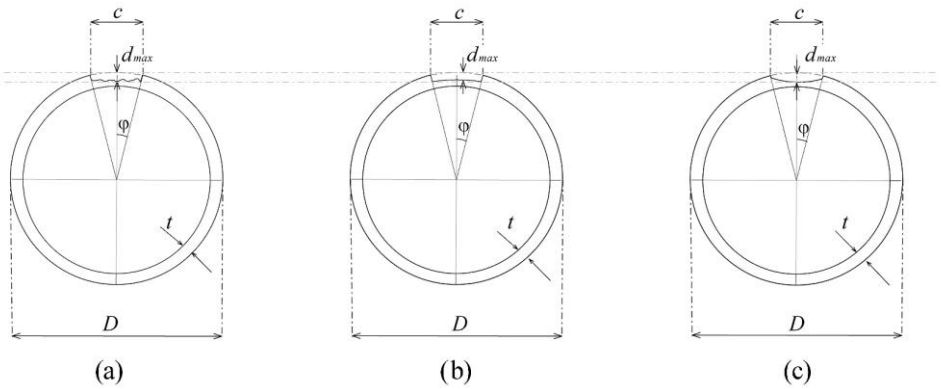

Source: The Author (2025).

The FE results from the current FE models are compared with previous experimental and numerical results by Gong *et al.* (2021) for subsea pipelines with a single isolated corrosion defect. Gong *et al.* (2021) tested specimens with different sizes of elliptical and rectangular defects under external pressure only.

The properties of the material used by Gong *et al.* (2021) are as follows: E = 200 GPA, σ_y = 198.2 MPa, n = 8.9, E' = 2400 MPa, $\sigma_{0.5}$ = 252.8 MPa (yield stress at a strain of 0.5 %). The modified R-O model of the material is also plotted in Figure 4.5.

Figure 4.5 - Stress-strain material curve adopted.

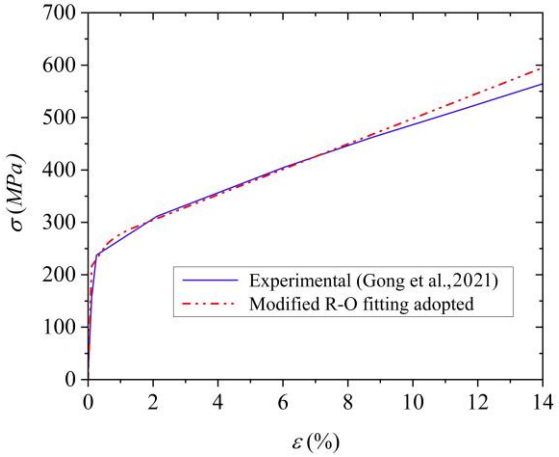

Source: Adapted by Gong *et al.* (2021).

Table 4.2 presents the dimensions of the studied pipelines and the geometric properties of defects, where l, c, and d are the length, circumferential width, and depth of the defect. The initial ovality of the tube cross-section (Δ_0 = 0.1 %) is the one considered in the experimental tests (Gong *et al.*, 2021). Table 4.2 also summarizes the experimental and numerical results of collapse pressure, and Figure 4.6 shows the

relative error for all cases. The relative error between the two results is calculated using Eq. (29).

$$Relative\ Error\ (\%) = \frac{\left|P_{cor}^{exp} - P_{cor}^{FE}\right|}{P_{cor}^{exp}} \times 100\ \% \tag{29}$$

where, P_{cor}^{exp} is collapse pressure obtained during experiments, while P_{cor}^{FE} is the collapse pressure from FE models.

Table 4.2 - Geometric properties and comparison of collapse pressure between experimental tests and FE analyses.

Specimen	Defect Shape	D (mm)	t (mm)	$\frac{l}{D}$	$\frac{d}{t}$	$\frac{c}{\pi D}$	P_{cor}^{exp*} (MPa)	P_{cor}^{FE*} (MPa)	P_{cor}^{FE} - PIPEFLAW (MPa)
TD1	Elliptical	89.08	4.50	1.0	0.3	0.05	22.40	22.31	21.75
TD2	Elliptical	89.01	4.50	1.0	0.4	0.05	21.78	21.60	21.32
TD3	Elliptical	88.89	4.50	1.0	0.5	0.05	19.87	20.33	20.34
TD4	Elliptical	89.00	4.50	1.0	0.6	0.05	18.29	18.68	18.41
TD5	Elliptical	89.12	4.50	1.0	0.7	0.05	16.80	17.01	16.44
TD6	Elliptical	88.97	4.50	0.5	0.6	0.05	21.55	21.27	21.58
TD7	Elliptical	88.99	4.50	1.5	0.6	0.05	16.71	17.19	16.88
TD8	Elliptical	89.04	4.50	2.0	0.6	0.05	16.20	16.34	16.00
TD9	Elliptical	88.94	4.50	1.0	0.6	0.025	20.13	19.92	19.89
TD10	Elliptical	89.00	4.50	1.0	0.6	0.075	17.19	17.79	17.24
TD12	Rectangular	89.03	4.50	1.0	0.3	0.05	20.45	20.54	20.92

*Gong *et al.* (2021).

Source: The Author (2025).

The results obtained using the PIPEFLAW demonstrate better accuracy and precision, with less error variation among the specimens, compared to those obtained by the FE model of Gong *et al.* (2021), especially for elliptical defects. The maximum error computed by the PIPEFLAW FE simulations is approximately 3 % for TD1, as shown in Figure 4.6.

Figure 4.6 - Error of predicted collapse pressure using FE model generated in PIPEFLAW.

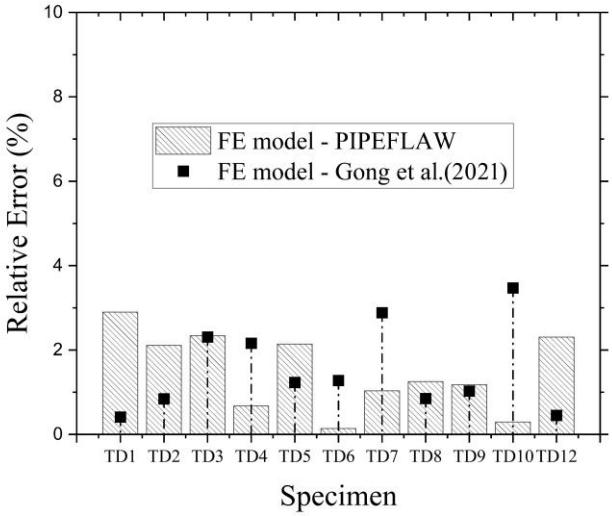

Source: The Author (2025).

Figure 4.7 illustrates the von Mises stress distribution and the deformed configuration after the collapse for specimen TD12 obtained using the PIPEFLAW system.

Figure 4.7 - FE result for specimen TD12 obtained using the PIPEFLAW: (a) Von Mises stress distribution, and (b) Deformed configuration after collapse.

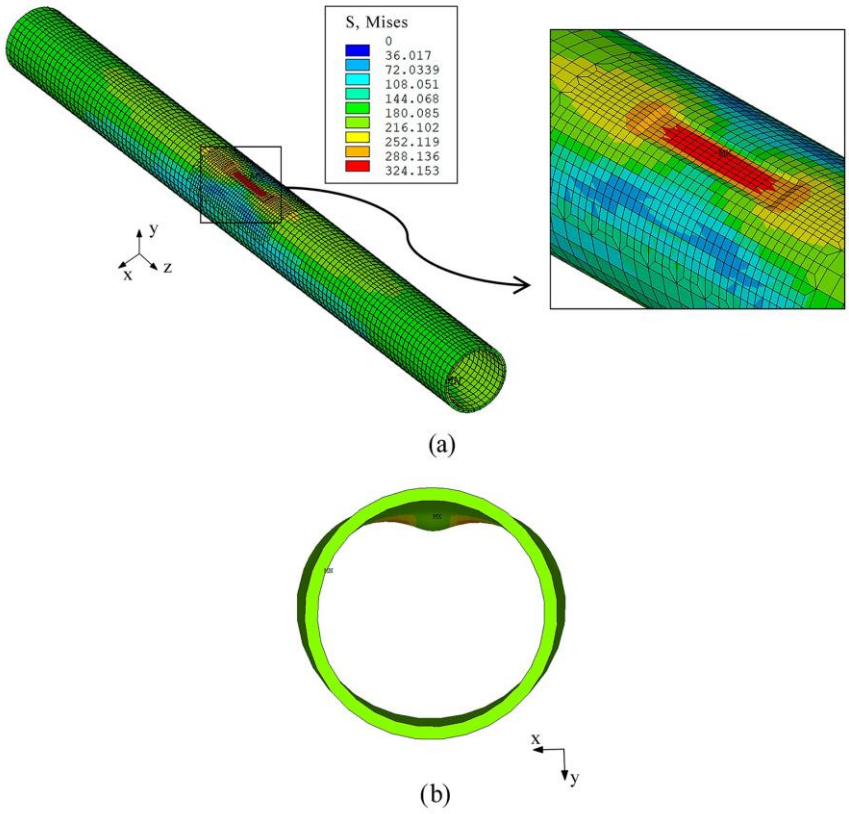

Source: The Author (2025).

The collapse shape is consistent with those observed numerically and experimentally by Gong *et al.* (2021). The results predicted by PIPEFLAW are in excellent agreement with the experimental data and can reliably predict the collapse behaviors of corroded pipelines.

4.4 REALISTIC CORROSION DEFECTS

This section describes the proposed procedure to predict the collapse pressure of subsea pipelines with realistic corrosion defects. As already mentioned, realistic corrosion defect profiles are defined from a three-dimensional mapping of the remaining pipeline wall thickness in the longitudinal and circumferential directions. Previous studies validated the FE models of pipes with realistic corrosion defects generated by the PIPEFLAW system using five real pipe segments removed from the field and tested to obtain the burst pressure (Ferreira *et al.*, 2021; Pimentel *et al.*, 2020).

4.4.1 Synthetic corrosion profiles

This paper uses synthetic corrosion profiles with realistic properties to create FE models and assess the accuracy of the proposed method for predicting the collapse pressure of corroded subsea pipelines, to be shown next. The use of synthetic corrosion profiles is motivated by the limited availability of experimental data and the need for a large dataset to ensure robust validation of the proposed method. The methodology adopted to generate synthetic corrosion profiles is based on previous research (Ferreira *et al.*, 2021; Ferreira; Willmersdorf; Afonso, 2024).

Synthetic profiles are generated using a random field model with a spacial correlation between mapped depth points. Studies on the statistical nature of corrosion show that extreme value analysis can be used to extrapolate inspection data (Benstock; Cegla, 2017; Cui; Liang; Bharadwaj, 2021; Melo *et al.*, 2020; Shibata, 1994). So, in the present study, the two-dimensional stochastic field is created using the generalized extreme value distribution given by Eq. (30) and (31) (Smirnov; Ma; Volchenkov, 2020; Zhang; Lian, 2018).

$$f(x|k,\mu,\sigma) = \left(\frac{1}{\sigma}\right)\exp\left[-\left(1+k\frac{x-\mu}{\sigma}\right)^{-\frac{1}{k}}\right] + \left(1+k\frac{x-\mu}{\sigma}\right)^{-1-\frac{1}{k}} \text{ for } k \neq 0 \quad (30)$$

$$f(x|k,\mu,\sigma) = \left(\frac{1}{\sigma}\right)\exp\left(-\exp\left(-\frac{(x-\mu)}{\sigma}\right) - \frac{(x-\mu)}{\sigma}\right) \text{ for } k \to 0 \quad (31)$$

where μ, σ and k are the location parameter, the scale parameter, and the shape parameter, respectively.

The stochastic field generated represents the corroded zone on the pipe surface, where each point (x, y) has a random depth. Coordinates x and y indicate the corrosion longitudinal and circumferential positions on the pipe, respectively.

Random data sets usually present excessive variations between adjacent points. Therefore, an analytical spatial covariance function, shown in Eq. (32), is used to correlate the remaining thickness data of the corroded region. In previous studies, the correlation function has already been used to generate complex defects (Ferreira *et al.*, 2021; Ferreira; Willmersdorf; Afonso, 2024).

$$cov(x,y) = \sigma\exp\left(\frac{-|x_1-y_1|}{co_1}\right)\exp\left(\frac{-|x_2-y_2|}{co_2}\right) \quad (32)$$

where x and y are the coordinates of the mapped points of remaining thickness of the defect region, co_1 and co_2 are the correlation lengths, and σ is the variance. Figure 4.8 shows the result of a synthetic random depth profile generated.

Figure 4.8 - Correlated remaining thickness data of corroded.

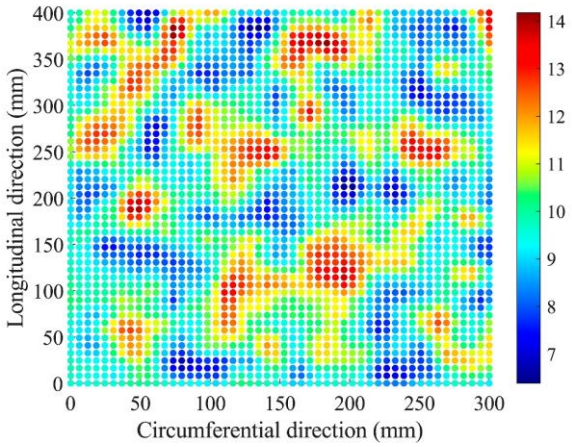

Source: The Author (2025).

The abrupt change in the remaining thickness of the points that delimit the corroded zone, compared to the nominal thickness of the pipe, combined with the lack

of a smooth geometric transition between the corroded and non-corroded areas, can result in distorted elements in the mesh, causing stress concentrations around the defect. Thus, after generating the correlated depths, the following conditions are added, according to the methodology by Ferreira *et al.* (2021) and Ferreira, Willmersdorf, and Afonso (2024):

- **Corroded area delimitation:** It is assumed that the thickness values of all points that delimit the running zone are equal to the nominal value of the pipeline thickness.
- **Transition smoothing:** The points close to the edge of the defect are smoothed from a curve fit using the $\sin^2(x)$ function.
- **Consistency checking:** Checks are performed to ensure that the remaining thickness does not exceed the nominal pipeline thickness, and that the corrosion does not completely penetrate the pipeline wall.

For example, Figure 4.9 illustrates a synthetic defect generated at the end of the procedure after the adjustment conditions described above. Ferreira *et al.* (2021) describe more details of this process.

Figure 4.9 - Example of a synthetic defect generated: (a) Synthetic corrosion data; (b) Synthetic corrosion contour map; (c) Synthetic corrosion A-A section map; (d) Synthetic corrosion B-B section map.

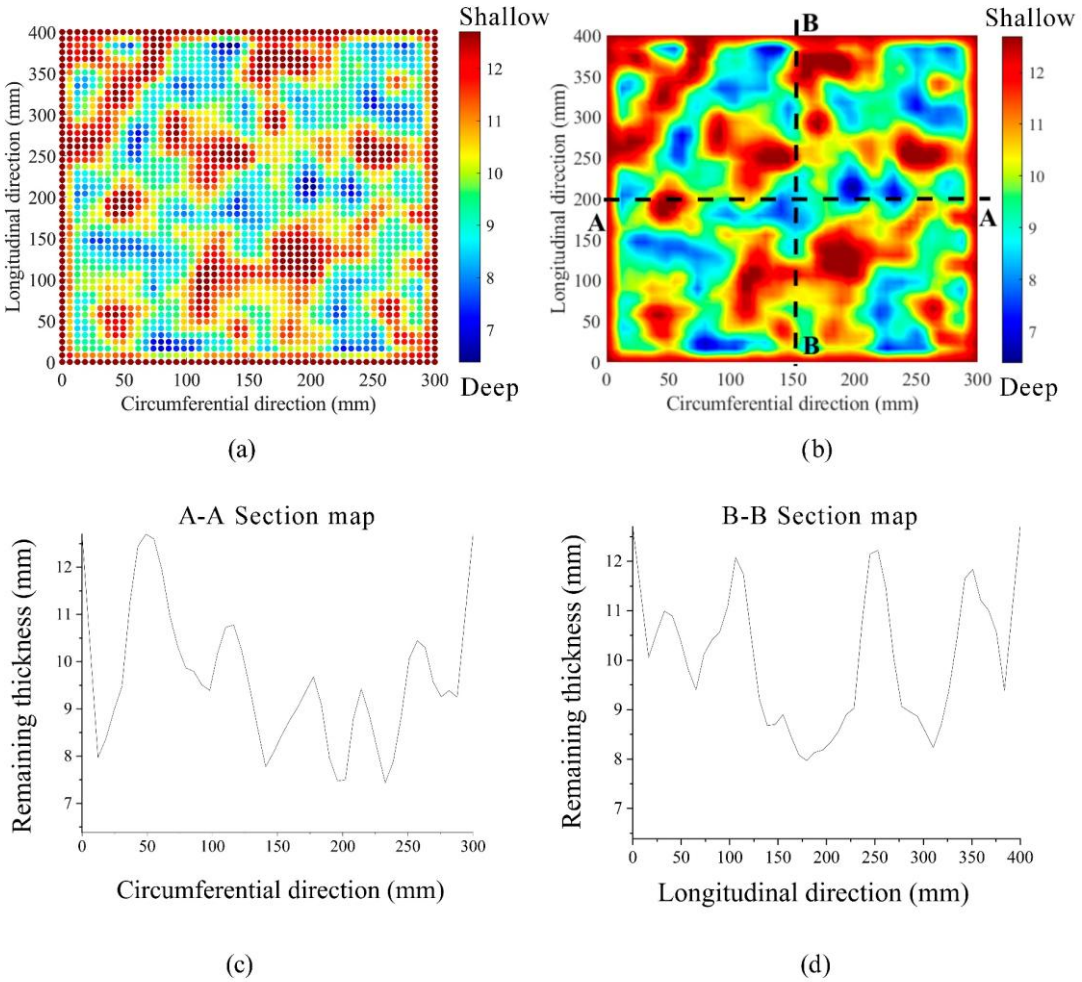

Source: The Author (2025).

4.4.2 Proposed method

As mentioned in the introduction section, the collapse of subsea corroded pipelines has been studied extensively in the last decades. However, both semi-empirical and FE-based assessment methods available in literature consider only idealized-shaped defects, whereas detailed realistic data on the defect shapes are not taken into account.

The literature includes methods for evaluating pipelines with complex defects subjected to internal pressure, defined as level 2 assessment methods, such as DNV-RP-F101(DNV, 2017) and the Effective Area Method (Vieth and Kiefner, 1993). Although widely adopted for internal pressure scenarios, these methods are tailored

for burst pressure estimation and do not account for the hydrostatic collapse mechanisms of corroded subsea pipelines under external pressure.

DNV-RP-F101(DNV, 2017) and the Effective Area Method (Vieth; Kiefner, 1993) consider axisymmetric defects based on a river bottom profile (RBP). An RPB is a detailed two-dimensional projection of the remaining wall thickness along the pipeline's length. However, axisymmetric models are not suited for the collapse assessment of corroded pipelines as they lead to inaccurate results, as the defect's circumferential width is also an essential parameter for the collapse response.

The proposed method is based on the surface mapping of the complex corrosion zone into equivalent defects, here named sub-defects, with varying dimensions, including the whole corrosion zone itself. For each sub-defect, its volume is calculated, and an equivalent uniform depth is obtained (that gives the same volume loss). All combinations of local metal loss, or sub-defect, are evaluated in this way. Figure 4.10 shows some sub-defects from a typical complex corrosion profile.

The collapse pressure for each equivalent defect is determined using any semi-empirical method available in literature. In this work, the semi-empirical method detailed in Section 4.2 is the one used. The critical collapse pressure is then defined as the lowest value among all the collapse pressures calculated for the individual defects. The detailed proposed procedure is described below.

Step 1 - Interaction among the corroded points. The corroded section of the pipeline must be subdivided into sub-defects based on the points measured on the corroded region (mapping). Here, all combinations of sub-defects are evaluated. The total number of sub-defects (N) can be computed as:

$$N = n_x \times \frac{(n_x - 1)}{2} \times n_y \times \frac{(n_y - 1)}{2} \tag{33}$$

where n_x is the number of points in the circumferential direction and n_y is the number of points in the longitudinal direction. Figure 4.10 shows an example to illustrate this process. For each sub-defect, an equivalent corrosion defect with equivalent depth (d_{eq}), equivalent width (c_{eq}), and equivalent length (l_{eq}) is analyzed.

In Figure 4.10, the synthetic corrosion defect is discretized into $n_x = 50$ points in the circumferential direction and $n_y = 50$ points in the longitudinal direction, resulting in a set of $N = 1{,}500{,}625$ sub-defects. The sub-defects are delimited by the initial and final coordinates i_0 and i_f (longitudinal direction) and j_0 and j_f

(circumferential direction). For each sub-defect (k), an equivalent corrosion defect with equivalent depth (d_{eq}), equivalent width (c_{eq}), and equivalent length (l_{eq}) is analyzed.

Figure 4.10 - Example of four sub-defects from a typical complex corrosion: (a) Sub-defect $\boldsymbol{k}$ **=1**, (b) Sub-defect $\boldsymbol{k}$ **= 2**, and (c) Sub-defect $\boldsymbol{k} = \boldsymbol{m}$.

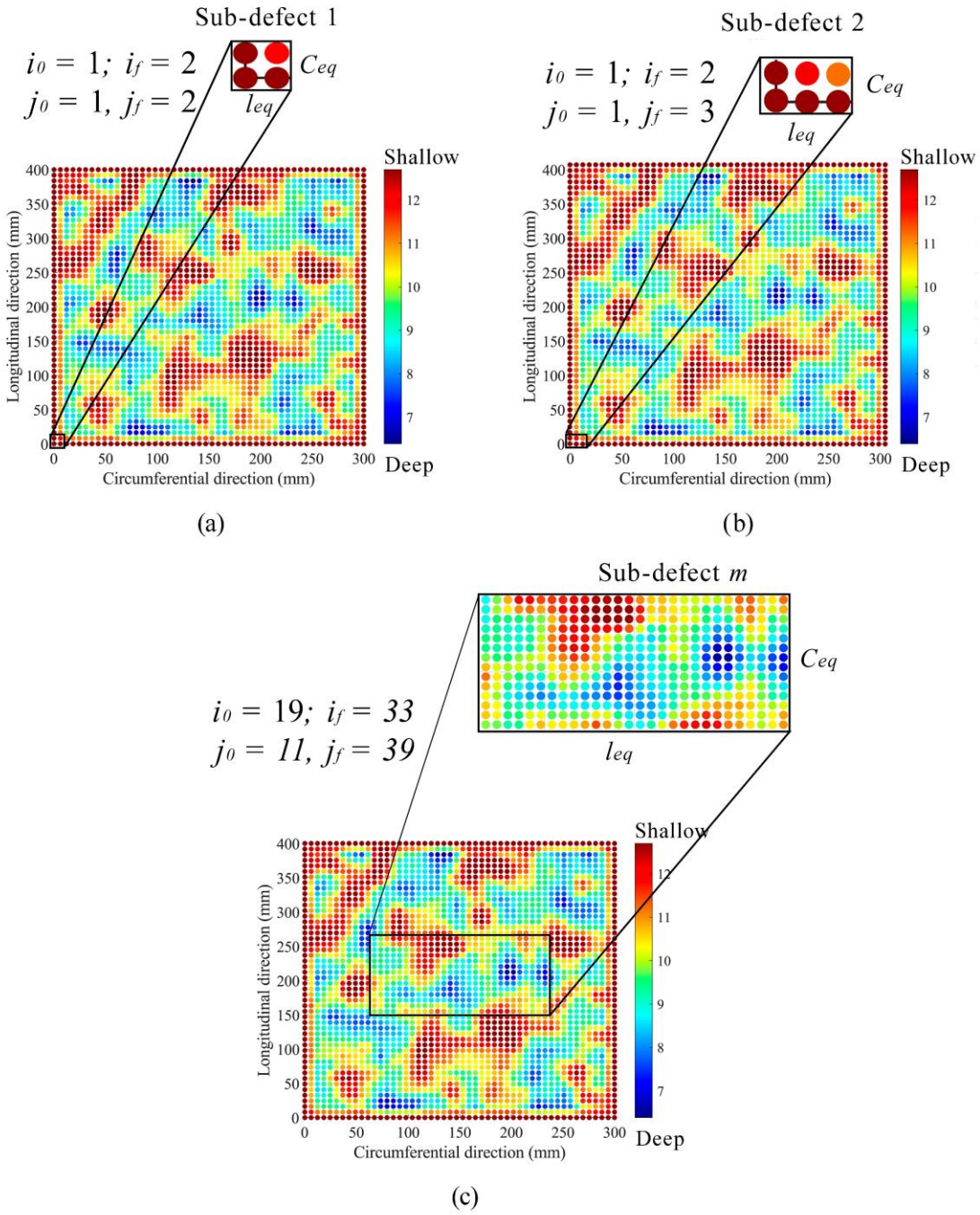

Source: The Author (2025).

Step 2 - Compute the equivalent depth of each sub-defect. The equivalent depth is calculated from the volume of metal loss for each sub-defect, according to Eq. (34):

$$d_{eq} = \frac{V_{eq}}{l_{eq} \times c_{eq}} \tag{34}$$

where V_{eq} is the equivalent volume of the sub-defect, computed as described below.

The sub-defect is composed of a rectangular set of depth points from the corroded zone mapping. Thus, V_{eq} is the summation of the volume of m sets of four depth points that form the equivalent profile.

$$V_{eq} = \sum_{i=1}^{i=m} V_i \tag{35}$$

The volume V_i of a generic set of four points from the corroded zone mapping is given by:

$$V_i = \frac{z_1 + z_2 + z_3 + z_4}{4} \times d_x \times d_y \tag{36}$$

in which z represents the corrosion depths, d_x and d_y are, respectively, the circumferential and longitudinal distances between the points. For example, Figure 4.11 illustrates sets of points used in the calculation of the effective volume of a sub-defect.

Figure 4.11 - Illustration of sets of four depth points that form a sub-defect.

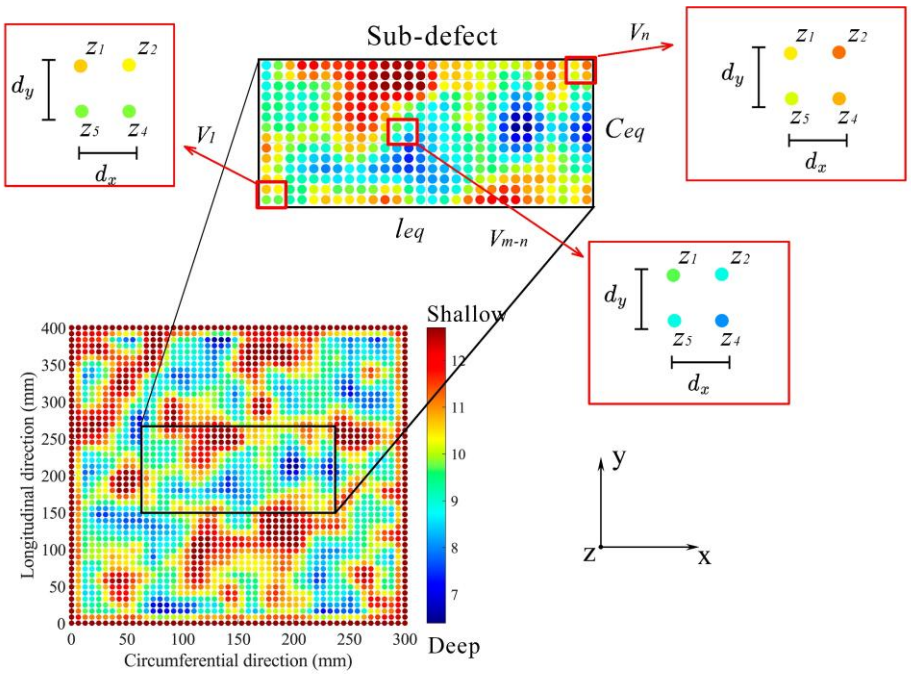

Source: The Author (2025).

Step 3 – Calculate the collapse pressure of the realistic defect. The critical collapse pressure of the realistic corrosion defect is assumed to be the smallest among all the calculated collapse pressures in the N sub-defects. The collapse pressure of all sub-defects is determined using the calculated equivalent depth (d_{eq}), equivalent length (l_{eq}), and equivalent width (c_{eq}) in the equation proposed by Netto (2009, 2010), described in Section 4.2 (Eq. (21)).

The pseudo-code to compute the collapse pressure considering all sub-defect combinations can be seen in Algorithm 1 (Table 4.3).

Table 4.3 - Algorithm 1.

Input: mapping of the complex corrosion zone (X, Y, Z), D, t, P_{co} .

Output: $\boldsymbol{P_{cor}}$

1. Set n_x, n_y and $N = n_x \times \frac{(n_x - 1)}{2} \times n_y \times \frac{(n_y - 1)}{2}$ Eq. (33)

2. Compute $L_{eq}(k)$, $C_{eq}(k)$ and $d_{eq}(k)$ # Equivalent length, width and depth of defect

```
k = 0
for i_0 = 1 to (n_y − 1) # initial longitudinal coordinate
    for i_f = (i_0 + 1) to n_y # final longitudinal coordinate
        for j_0 = 1 to (n_x − 1) # initial circumferential coordinate
            for j_f = (j_0 + 1) to n_x # final circumferential coordinate
                k = k + 1
                L_eq(k) = Y(i_f) − Y(i_0)
                C_eq(k) = X(j_f) − X(j_0)
                x ← [X(i_0 to i_f)] # is a vector
                y ← [Y(j_0 to j_f)] # is a vector
                z ← [Z(i_0 to i_f, j_0 to j_f)] # is a matrix
                V_eq(k) = equivalent_volume (i_0, i_f, j_0, j_f, x, y, z)  Eq. (35) and (36)
                d_eq(k) = V_eq(k) / (L_eq(k) × c_eq(k))  Eq. (34)
            end
        end
    end
end
```

3. Solve $P_{cor\,(k)} = \left[\frac{1-\frac{d_{eq}(k)}{t}}{1-\frac{d_{eq}(k)}{t}\left(1-\left(\frac{C_{eq}(k)}{\pi D}\right)^{0.4}\left(\frac{L_{eq}(k)}{10D}\right)^{0.4}\right)}\right]^{2.675} \times P_{co}, \forall\, k$ Eq. (21)

4. Return $P_{cor} = \min\left(P_{cor}(k)\right),\ k = 1,2,\ldots,N$

Source: The Author (2025).

In Algorithm 1, equivalent_volume$\left(i_0, i_f, j_0, j_f, x, y, z\right)$ is a function that computes the volume of metal loss (V_{eq}) for the individual sub-defect (k). The sub-defect (k) is

defined by all the points in the rectangular region $\{(i_0, j_0);\ (i_0, j_f);\ (i_f, j_0);\ (i_f, j_f)\}$ – and their respective depths $z(i, j)$ – on the corrosion mapping.

For the corrosion profile given as an example, the equivalent defect shown in Figure 4.12 is the most critical, as it presented the lowest calculated collapse pressure.

Figure 4.12 - Critical equivalent defect corresponding to realistic corrosion shown in Figure 4.10.

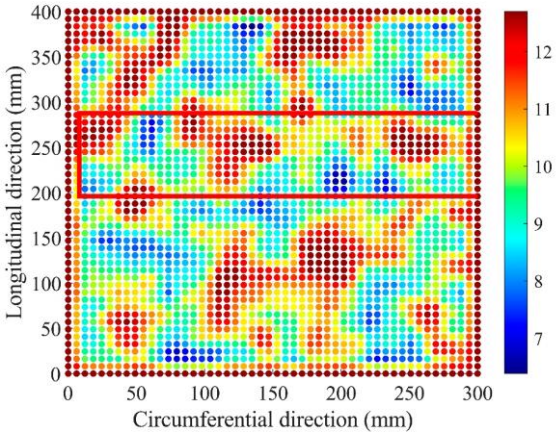

Source: The Author (2025).

4.4.3 Comparative study

In this section, initially the collapse pressure of pipes with realistic corrosion defects predicted by 3D FE simulations conducted by the PIPEFLAW system are compared with the novel approach described in Section 4.4.2. The objective is to verify the accuracy of the proposed method.

Initially, the collapse response of six subsea pipes with synthetic corrosion defects is analyzed. A representative pipe steel grade (i.e., X65) is selected for the comparative study, as used in previous studies (D'Aguiar; Motta; Afonso, 2024; Gong *et al.*, 2020, 2021). The geometric parameters of the pipes and the material properties adopted are summarized in Table 4.4.

The corrosion defects are generated using the methodology of creating synthetic corrosion profiles with realistic properties described in Section 4.4.1. The fixed geometric parameters of corrosion defects are: $c/\pi D = 0.3$, $l/D = 1.0$.

Table 4.4 - Pipe dimensions and the material features.

D (mm)	t (mm)	Δ_o (%)	E (GPa)	E' (MPa)	σ_y (MPa)	$\sigma_{0.5}$ (MPa)	N
400	12.7	0.5	207	3047	410	450	13

Source: The Author (2025).

Figure 4.13 - Corrosion contour maps of different synthetic corrosion profiles: (a) Case 1, (b) Case 2, (c) Case 3, (d) Case 4, (e) Case 5, and (f) Case 6.Figure 4.13

shows the corrosion contour maps from the corroded region of the six synthetic profiles.

Figure 4.13 - Corrosion contour maps of different synthetic corrosion profiles: (a) Case 1, (b) Case 2, (c) Case 3, (d) Case 4, (e) Case 5, and (f) Case 6.

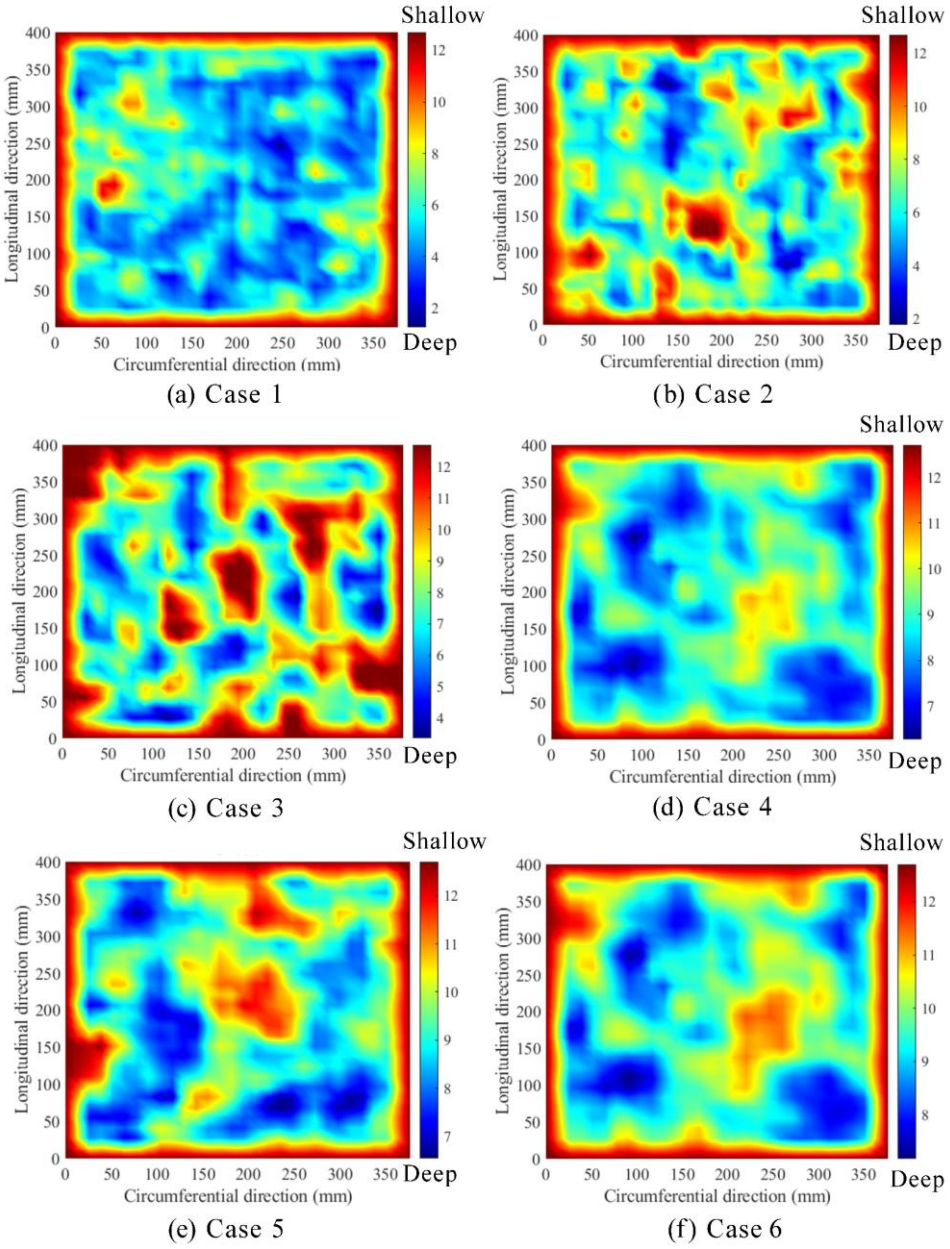

Source: The Author (2025).

Figure 4.14 shows the maximum and the mean depth of the realistic corrosion profiles evaluated. As can be seen, the greatest mean depth computed is approximately 0.50 t (Case 1) and the smallest is approximately 0.20 t (Case 6).

Figure 4.14 - The maximum depth ($d_{\max}$) and the mean depth (d_{mean}) of synthetic corrosion profiles.

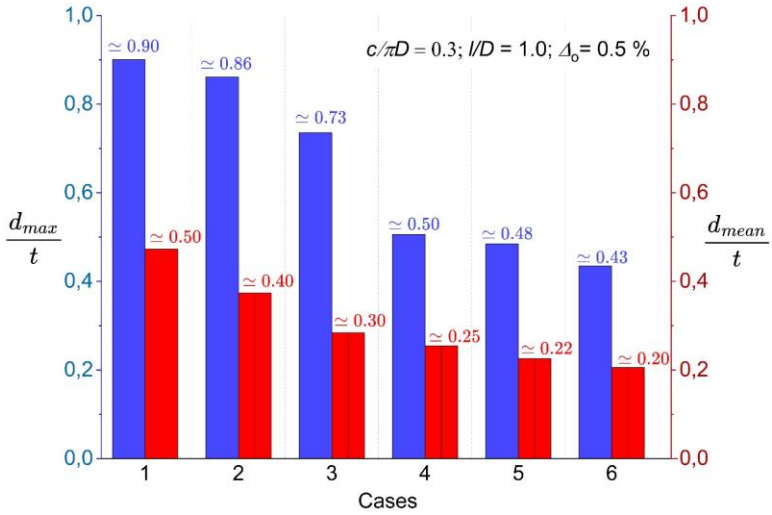

Source: The Author (2025).

Figure 4.15 illustrates the FE models generated using the PIPEFLAW system for Cases 3 and 6.

Figure 4.15 - Finite element mesh at different defect arrangements: (a) Case 3, and (b) Case 6.

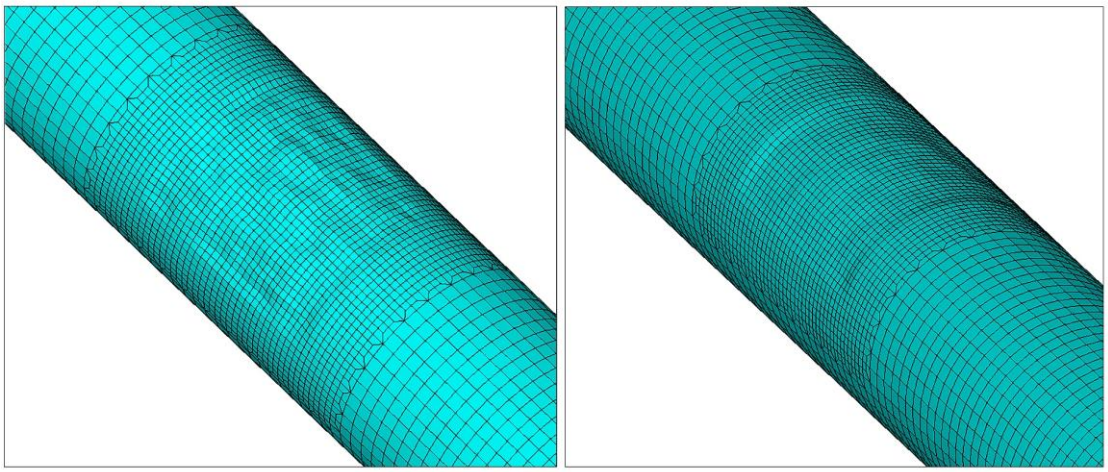

(a) Case 3 (b) Case 6

Source: The Author (2025).

Figure 4.16 and Figure 4.17 show the deformed configuration of the pipe cross-section, obtained numerically via FEA, after the collapse in Cases 3 and 6, respectively. In general, defects with idealized geometry present symmetrical collapse modes. The collapse modes illustrated in Figure 4.16 and Figure 4.17 for the realistic defects analyzed are asymmetric because the depths are not uniform. Additionally, these collapse modes are influenced by the ratio between the mean depth and the maximum depth of the corrosion defect.

Figure 4.16 - Cross-sectional of deformed configuration at collapse for Case 3.

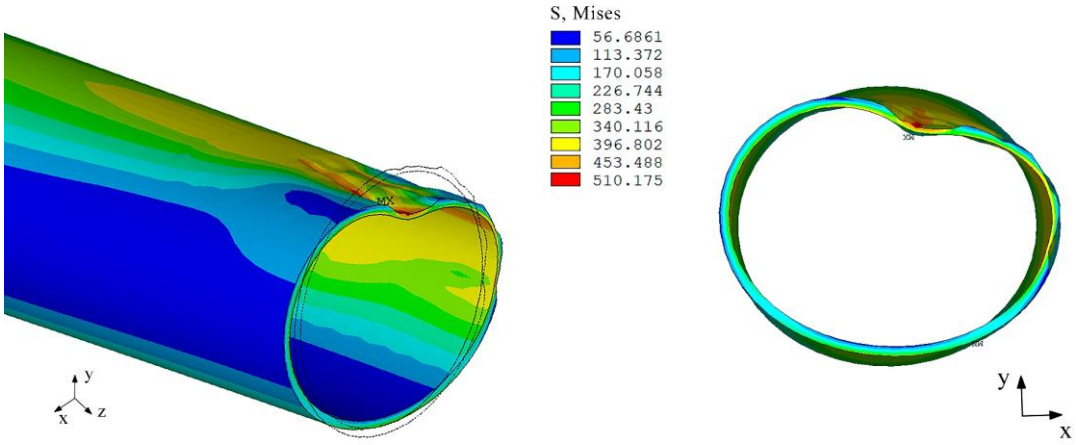

Source: The Author (2025).

Figure 4.17 - Cross-sectional of deformed configuration at collapse for Case 6.

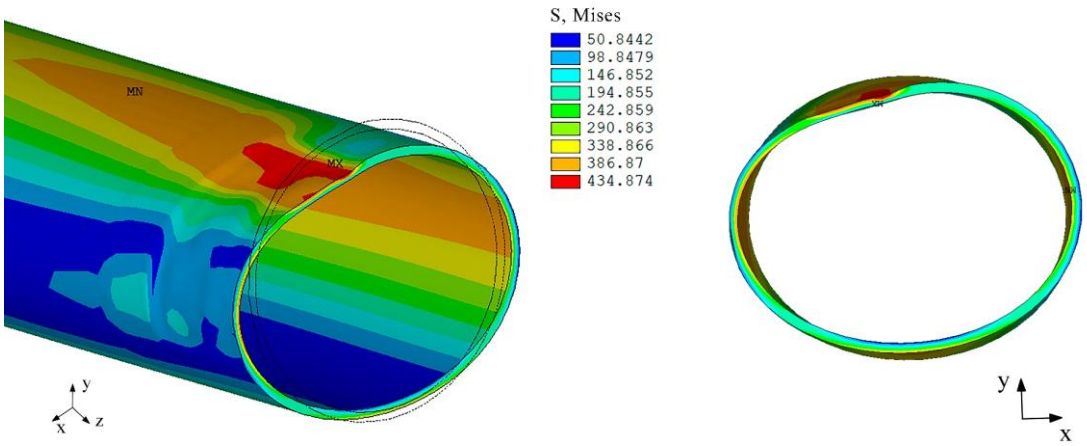

Source: The Author (2025).

Figure 4.18 presents a compilation of collapse pressure results obtained through 3D FEA, the results from the semi-empirical equation based on maximum depth (d_{max}) and the mean depth (d_{mean}) of the realistic corrosion profiles, and the results using the proposed method.

As expected, the semi-empirical results obtained considering d_{max} are extremely conservative, and its use may lead to premature shutdown of the offshore pipelines. In contrast, although more accurate, the collapse pressure based on d_{mean} may give non-conservative results. This can be seen in Case 2, where the reported collapse pressure exceeds the reference value from the FE model by approximately 17 %. The proposed method, on the other hand, produces results aligned with those from FE model simulations while maintaining an acceptable level of conservatism.

Figure 4.18 - Comparison of normalized collapse pressure obtained from: 3D FE models, semi-empirical approach based on d_{max}, d_{mean}, and the proposed method.

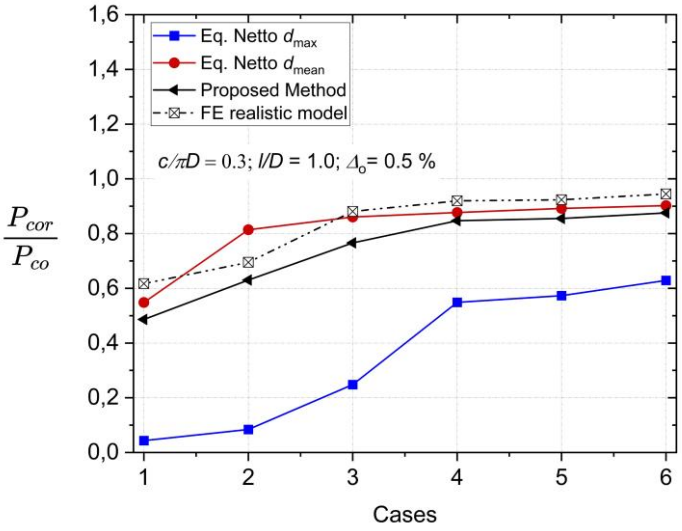

Source: The Author (2025).

Next, a larger dataset (100 cases) of numerical results generated using the advanced simulation software PIPEFLAW is employed. The geometric parameters of pipes and the material properties for these examples are identical to those presented in Table 4.4. The defects were generated with random parameters, according to the methodology described in Section 4.4.2, considering the following application range: $0.3 \leq c/\pi D \leq 0.4$, $1.0 \leq l/D \leq 2.0$, $0.4 \leq \frac{d_{max}}{t} \leq 0.9$, and $0.05 \leq \frac{d_{mean}}{t} \leq 0.5$.

Figure 4.19 shows the predicted collapse pressures for the dataset evaluated. Figure 4.20 presents the mean and dispersion of the relative error between the semi-empirical methods (based on the maximum depth, mean depth, and the proposed method) and the reference results obtained by the finite element method.

Figure 4.19 - Comparison of the semi-empirical approaches and numerical analysis results.

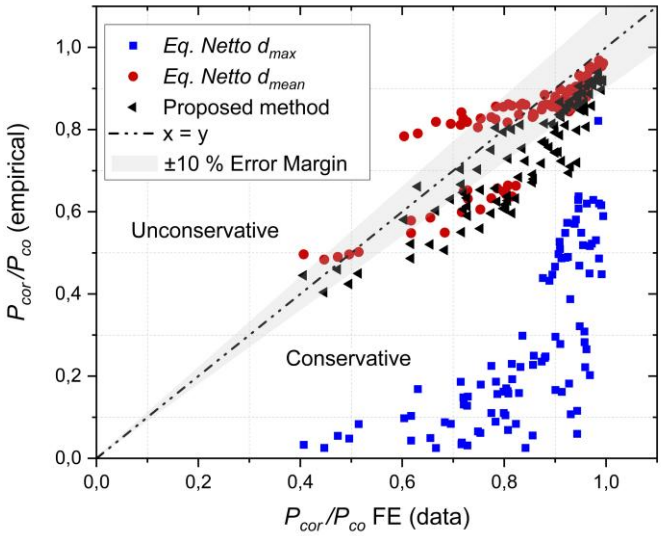

Source: The Author (2025).

Figure 4.20 - Relative errors between semi-empirical approaches and numerical analysis results.

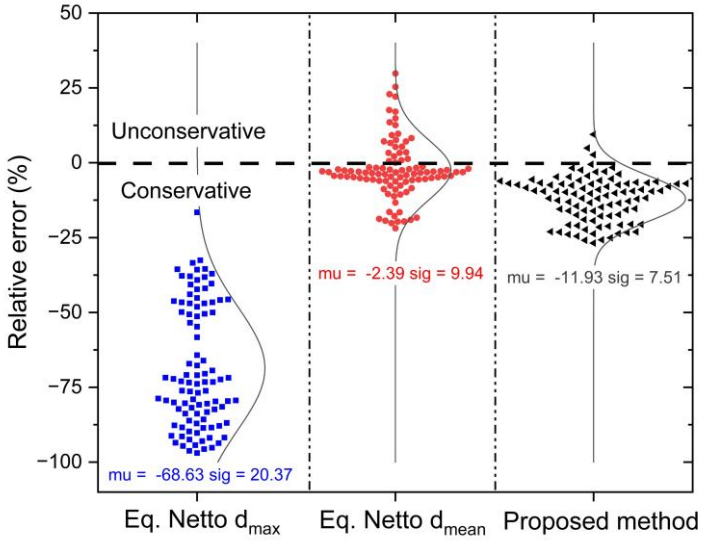

Source: The Author (2025).

The results, plotted in Figure 4.19 and Figure 4.20, highlight that the semi-empirical approach based on maximum depth tends to overestimate defect severity significantly. This leads to overly conservative predictions, with an average error of approximately -68%.

The semi-empirical method based on mean depth may underestimate the severity of the defect, leading to results that exceed the reference value (FE results) by approximately 25 %. Figure 4.20 shows a more considerable fluctuation in predictions based on mean depth, with a standard deviation of 9.94%. This high level of uncertainty renders this approach unreliable for accurate defect assessment. Consequently, its applicability is limited, particularly for larger defects where more precise and robust assessment methods are essential.

The proposed method has the smallest standard deviation relative error of 7.51 %, indicating low variability in the results. Furthermore, the average error is -11.93 %, demonstrating an acceptable level of conservatism in the estimates, which includes the conservatism of Netto's Equation. As a result, the proposed method yields reliable outcomes and significant practical applicability.

Figure 4.21 shows the probability density distribution obtained by Kernel Density Estimation (KDE) of relative errors for the traditional approach, based on the Netto equation using the maximum depth (d_{max}) and the proposed method. The traditional method presents a significantly wider 80% confidence interval (CI), ranging approximately from -95% to 35%, which reflects a greater dispersion of errors and, therefore, a lower precision in the estimates. In contrast, the proposed method displays

a distribution with less dispersion, characterized by a narrower 80% CI, situated between approximately -20% and -2%. This characteristic indicates a lower variability of errors, evidencing that the proposed method provides greater consistency and reliability in the variations.

Figure 4.21 - Probability density distribution of relative errors obtained by Netto Equation (Traditional approach) and by the Proposed Method.

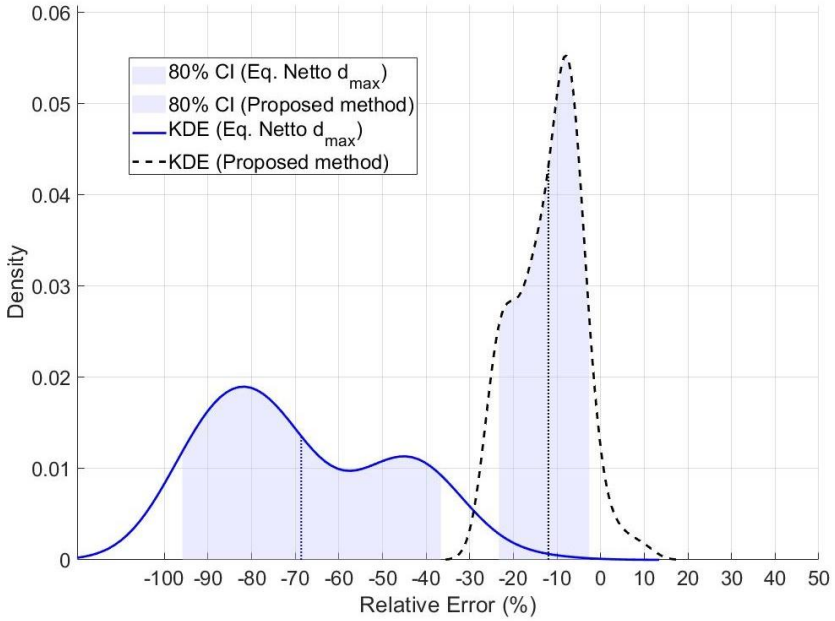

Source: The Author (2025).

In addition, Table 4.5 compares the proposed methodology and 3D finite element analysis (FEA), based on four main criteria: mean error, computational time, and relative speed.

Table 4.5 - Comparation proposed method and 3D Finite Element Analysis (FEA).

Criterion	Proposed Method	FEA
Average Error (%)	-11.93 % (conservative)	Baseline (reference method)
Computation Time	~2 seconds	~4 minutes
Relative Speed	$\approx 120 \times$ faster	-

Source: The Author (2025).

The novel approach demonstrates significantly lower computational cost compared to 3D finite element analysis (FEA). The FEA simulation for a typical pipeline considered in this study takes about 4 minutes, using the automatic advanced tool described, on a standard desktop computer (i7 CPU–2.5 GHz/32 GB RAM). In contrast, the computational time required for the collapse pressure prediction using the proposed method is almost instantaneous, requiring around 2 seconds - making it approximately 120 times faster than 3D finite element simulations. This drastic

reduction in time makes the novel approach a highly attractive tool for practical applications.

4.4.4 Practical implications and limitations

The proposed method offers practical implications for assessing the integrity of subsea pipelines with corrosion defects. Its main application is the integration with existing inspection routines, functioning as a complementary tool to traditional methods. This integration is especially beneficial in analysis with large data volumes, where the computational cost of full simulations is prohibitive.

Corroded pipelines under internal pressure, particularly when buried, are typically assessed through methodologies organized by complexity and detail, following technical standards such as DNV-RP-F101 (DNV, 2017) and the Effective Area Method (Vieth; Kiefner, 1993). The choice of the approach depends on the defect type, boundary and load conditions, and the required data (Motta *et al.*, 2021). Level 1 employs a simplified representation of the defect, requiring minimal data and resulting in conservative yet often restrictive assessments. Level 2, on the other hand, uses more refined semi-empirical models, which consider the complex profile of the corrosion or colonies of corrosion defects. Although more precise, these methods demand more detailed data and analytical effort.

In subsea pipelines, a standard assessment procedure based on the realistic geometry of corrosion damage was lacking. As previously mentioned, Netto's solution (Netto, 2009; 2010), widely applied in simplified analyses, is limited to scenarios with isolated, uniform defects. Recent empirical methods have attempted to address interacting corrosion defects (Wu *et al.*, 2022, 2023) but there is still no consensus on its practical applicability.

The methodology presented in this paper addresses this gap by providing an alternative Level 2 assessment for subsea pipelines, based on real thickness data obtained through inspection. The results underscore the efficiency and robustness of the proposed approach. Its key advantage is the reduction of conservatism compared to traditional semi-empirical methods, which can help avoid unnecessary interventions and provide stronger technical support for decisions on maintaining pipeline operations.

Another relevant aspect of the methodology proposed is its possible adaptability to different loading and operating conditions. The core idea of subdividing a complex defect into sub-defects can be applied widely, provided an appropriate solution is available in the literature for isolated defects. However, broadening the use of this approach will require additional studies, including real field data.

It is also essential to recognize methodological limitations. The accuracy of the results is directly tied to the quality of inspection data. Incomplete or imprecise data can lead to inaccurate collapse pressure estimates, highlighting the need for more reliable inspection technologies.

Moreover, like Level 2 assessment methods commonly applied to onshore pipelines, the approach proposed here relies on simplified assumptions about the behavior of corrosion defects. Consequently, it is important to note that the proposed method does not account for the interaction effects between sub-defects, which may affect the nonlinear buckling behavior. Therefore, caution is required when extrapolating the results.

In summary, the results demonstrate the potential of the methodology as an intermediate alternative between simplified approaches and complex simulations, facilitating more balanced technical decisions that weigh operational safety against economic feasibility.

4.5 CONCLUSIONS

This work presents a novel approach to assessing the integrity of subsea pipelines with realistic corrosion defects. The proposed methodology decomposes realistic defects into sub-defects with equivalent depths, widths, and lengths. The critical collapse pressure is then determined as the lowest collapse pressure obtained among all sub-defect computed pressures. A semi-empirical method is used for the collapse pressure computations for each sub-defect. The accuracy of the proposed method, compared against alternative approaches based on maximum and mean defect depth, is verified through numerical results obtained from 3D finite element analyses. The main conclusions of this paper are as follows:

- The semi-empirical method based on the mean depth approach has considerable dispersion in the results and errors that can exceed the reference values by up to 25% (non-conservative). In contrast, the traditional

semi-empirical method based on the maximum depth presents excessively conservative results, resulting in an average error of approximately -68%.

- The novel approach exhibits an average error of approximately -12%. Compared to the traditional method based on maximum defect depth, the standard deviation of the average error decreases from 20% to about 7%. So, the proposed approach significantly reduces the conservatism associated with the traditional method and exhibits a smaller dispersion of results, providing greater precision and accuracy.
- The significant reduction in computational time compared to finite element analysis makes this novel approach a valuable tool for the oil and gas industry, enabling faster assessments of pipeline structural integrity. Specifically, the proposed approach is approximately 120 times faster than 3D finite element simulations, further enhancing its practicality for real-world applications.

Thus, the methodology developed in this work represents a significant advance in assessing the integrity of corroded subsea pipelines, combining greater precision, reduced computational time (up to 120 times faster), and high potential for practical application in the offshore industry.

5 ADVANCES IN RESEARCH

This chapter presents some advances following the development and validation of the innovative semi-analytical approach described in Chapter 4.

5.1 SUBSEA PIPELINES WITH REALISTIC CORROSION DEFECTS

This section conducts an extensive parametric study to investigate the influence of metal loss volume on the hydrostatic collapse of subsea pipelines with realistic corrosion defects using the novel approach presented in Chapter 4. This approach involves mapping and subdividing the complex corrosion zone into equivalent defects with equivalent depths, widths, and lengths, as described in Section 4.4.2.

5.1.1 Effect of metal loss volume on collapse response

The methodology for the parametric study presented in this chapter involves generating synthetic corrosion profiles using a random field model with spatial correlation between the mapped depth points, as described in Section 4.4.1. This model allows for a realistic representation of the variability and distribution of corrosion defects in subsea pipelines.

The fixed input parameters for generating profiles include the defect's length and width. In this study, three different defect sizes are used, as described in Table 5.1.

Table 5.1 – Defects sizes in parametric study

Small defects	Moderate defects	Larger defects
$\left(\frac{c}{\pi D} = 0.07, \frac{l}{D} = 0.2\right)$	$\left(\frac{c}{\pi D} = 0.15, \frac{l}{D} = 0.5\right)$	$\left(\frac{c}{\pi D} = 0.3, \frac{l}{D} = 1.0\right)$

Source: The Author (2025).

A total of 700 synthetic profiles (field of depth) are applied to each defect size, categorized as small, moderate, and large, resulting in 2,100 corrosion defects. The depth points within each defect are randomly mapped, respecting the spatial correlation imposed by the random field model.

Figure 5.1 illustrates the relationship between the volume of metal loss due to corrosion (V_{loss}) and the total volume of the intact defect region (V_{total}) for all defects generated, considering three different defect sizes, shown in Table 5.1. The average

and the standard deviation of V_{loss}/V_{total} remains approximately constant (~0.26 and ~0.15, respectively) for all configurations analyzed. Therefore, despite the different defect geometries, the fraction of volume loss follows a similar statistical behavior.

Figure 5.1 - Distribution of V_{loss}/V_{total} for different corrosion defect geometries

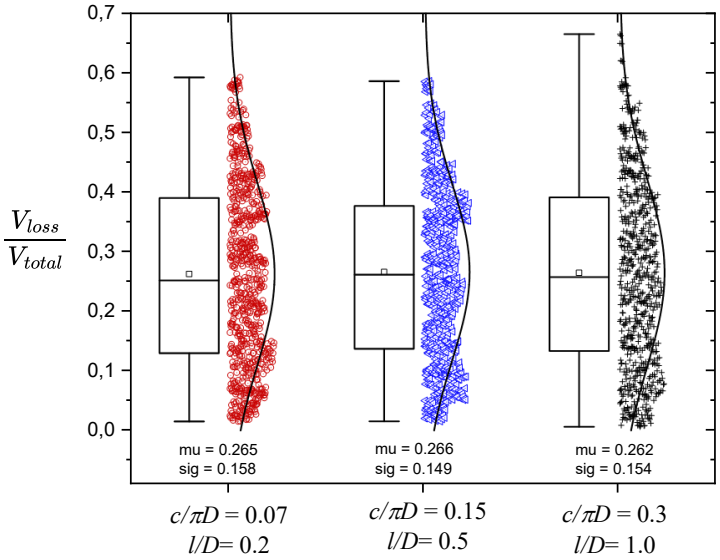

Source: The Author (2025).

The parametric analysis then evaluates how the volume of metal loss influences the collapse response of subsea pipelines, considering the same pipeline geometric and material properties used in the comparative study presented in Chapter 4 (Table 4.4). So, for all corrosion profiles shown in Figure 5.1, the collapse pressure is calculated using the proposed method described in Section 4.4.2.

Figure 5.2 shows the normalized collapse pressure of a corroded subsea pipeline versus the fraction of volume loss, considering different defect sizes. The y-axis represents the ratio of the collapse pressure of the corroded pipeline (P_{cor}) to the collapse pressure of the intact pipeline (P_{co}). When the ratio P_{cor}/P_{co} is approximately equal to 1, the influence of corrosion on the collapse capacity is minimal.

Figure 5.2 – Normalized collapse pressure against V_{loss}/V_{total} for different defect sizes.

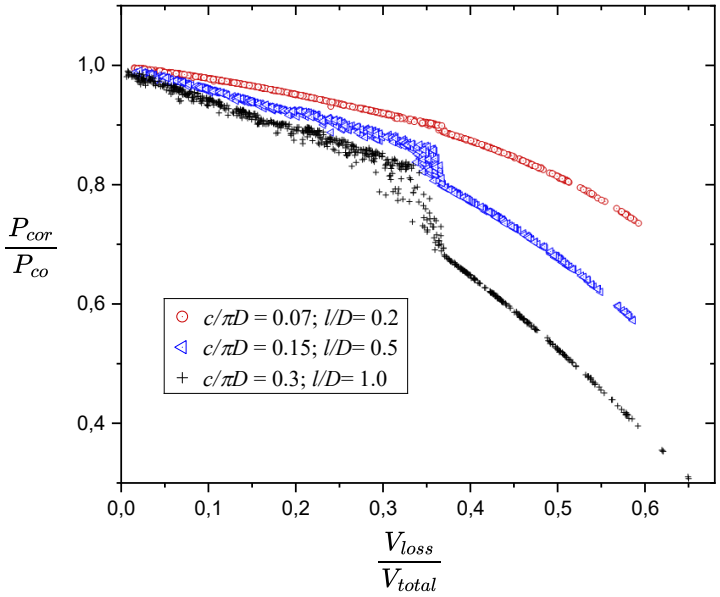

Source: The Author (2025).

As expected, the collapse capacity decreases with the increase of the fraction of volume loss (V_{loss}/V_{total}). This indicates that material loss due to corrosion progressively reduces the ability of the pipeline to carry external loads before collapse.

In addition, the Figure 5.2 illustrates that for a given value of V_{loss}/V_{total}, cases with larger and wider defects ($c/\pi D$ =0.3, l/D =1.0) exhibit a more significant reduction in collapse pressure. In contrast, smaller defects ($c/\pi D$ =0.07, l/D =0.2) have a less severe impact and maintain higher P_{cor}/P_{co} values.

Finally, as shown in Figure 5.2, when V_{loss}/V_{total} exceeds 0.3, the reduction in collapse capacity is significant. These results indicate that the pipeline's structural integrity is seriously compromised at high levels of corrosion. In the most extreme case ($c/\pi D$ =0.3, l/D =1.0), the collapse pressure can drop to less than 50% of the original value, which is critical for operational safety.

5.2 SUBSEA PIPELINES WITH INTERACTING CORROSION DEFECTS

The novel approach described in Section 4.4.2 can predict collapse pressure relatively accurately for realistic corrosion defects. Here, based on numerical analyses, a parametric study is developed to prove that the present approach can be applied to predict the collapse pressure of subsea pipelines with interacting corrosion defects.

5.2.1 Extending the application range of novel approach

The finite element models of pipelines with two corrosion defects, as rigorously validated in Section 3.4, are used to verify the applicability of the novel approach proposed and described in Section 4.4.2 for subsea pipes with interacting corrosion defects. The pipe attributes of the pipeline are presented in Table 5.2. The fixed geometric parameters of corrosion defects are: $c/\pi D$ =0.3, l/D =1.0. Here, two different defect depths are used: d/t =0.3 (shallow defect) and d/t =0.5 (deep defect).

Table 5.2 – Material properties and geometric parameters of the pipe.

E (GPa)	E' (MPa)	σ_y (MPa)	$\sigma_{0.5}$ (MPa)	N	D (mm)	D/t	Δ_o (%)
207	3047	410	450	13	323.85	20.4	0.1

Source: Adapted by Gong *et al.* (2020).

This section focuses on dual identical corrosion defects (rectangular geometric) aligned longitudinally, circumferentially, and diagonally on the pipe's external surface, respectively, as shown in Figure 5.3. Table 5.3 presents the corrosion defect configuration with three categories of alignments. The normalized distances between defects, S_l/t (longitudinal distance) and $S_c/\pi D$ (circumferential distance), are specified for each configuration.

Table 5.3 – Corrosion defect configuration with different alignment.

Specimen	Aligned type	S_l/t	$S_c/\pi D$
SL1	Longitudinal	20	-
SL2	Longitudinal	40	-
SC1	Circumferential	-	0.1
SC2	Circumferential	-	0.3
SD1	Diagonal	20	0.1
SD2	Diagonal	20	0.3

Source: The Author (2025).

In addition, the novel approach results are compared against the ones obtained by the equation proposed by Netto (2009, 2010) to predict the collapse pressure for a pipeline with a single corrosion defect (Eq. (9) in Section 2.2.1), and those obtained by the formulation developed by Wu *et al.* (2022) for a pipeline with identical dual corrosion defects (Eq. (10) in Section 2.2.2). In Netto's equation, the corrosion defects are simplified into a single equivalent corrosion defect, as illustrated in Figure 5.3. The collapse pressure of the intact pipeline (P_{co}) for all cases is calculated from the equation proposed by DNV (2013), described in Section 2.1 (Eq. (6)).

Figure 5.3 - Simplification scheme for combining two corrosion defects into a single equivalent corrosion defect, considering various alignments: (a) longitudinal, (b) circumferential, and (c) diagonal.

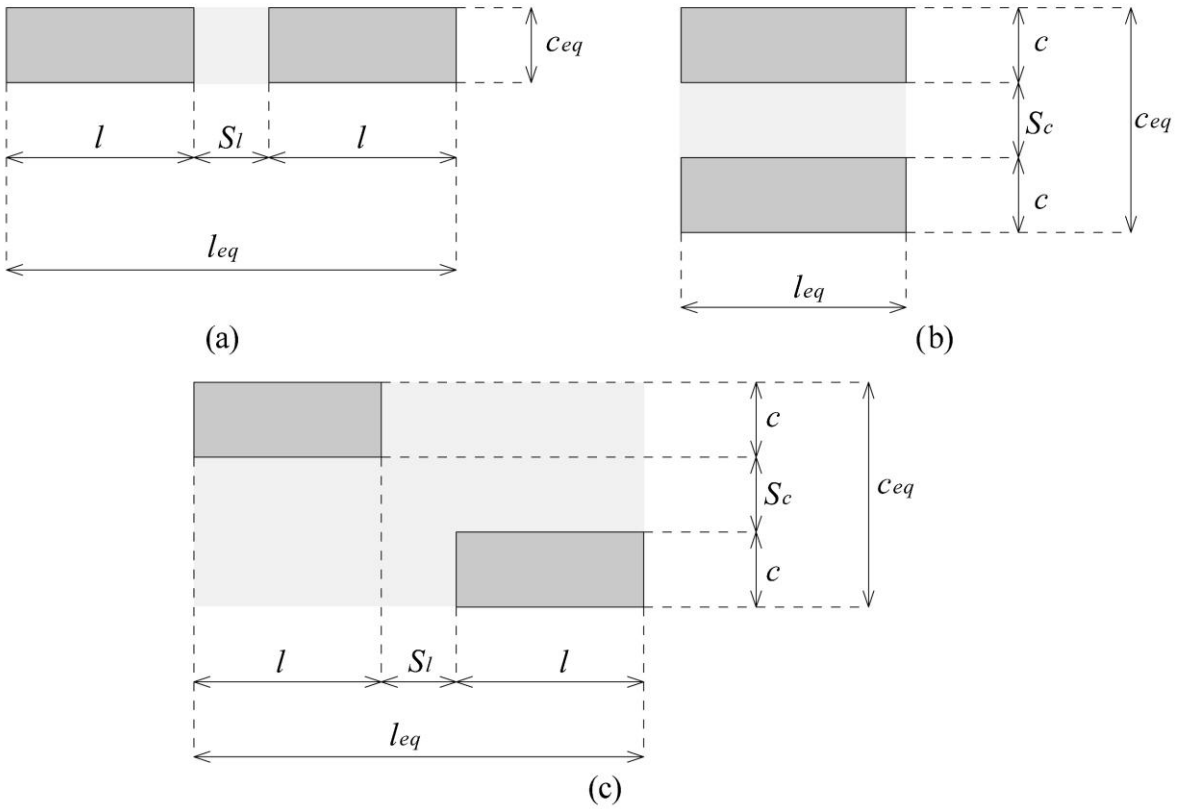

Source: The Author (2025).

Figure 5.4 presents a comparison of the collapse pressure obtained using FE numerical simulations via PIPEFLAW (reference) and the collapse pressures predicted by the different semi-empirical approaches and the novel approach proposed in this work. This latter provides estimates closer to the numerical results, especially for cases with more severe defects (Figure 5.4 (b)).

The results obtained using the expressions proposed by Netto (2009, 2010) and Wu *et al.* (2022) tend to be more conservative. Figure 5.4 (b) shows that Netto's equation underestimates collapse pressure more significantly as defect depth increases (d/t = 0.6), indicating its potential sensitivity to defect geometry. In this situation, it has a steeper decreasing trend than other approaches, particularly for SC and SD specimens, suggesting an overestimation of defect severity.

Figure 5.4 - Comparison of semi-empirical methods and the FE analyses for predicting the collapse pressure of pipelines with two corrosion defects: (a) $d/t = 0.3$ and (b) $d/t = 0.6$.

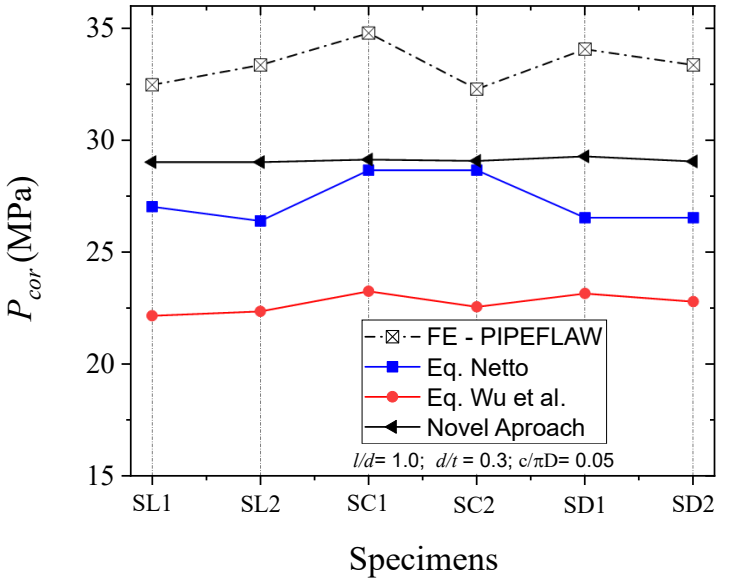

(a) $d/t = 0.3$

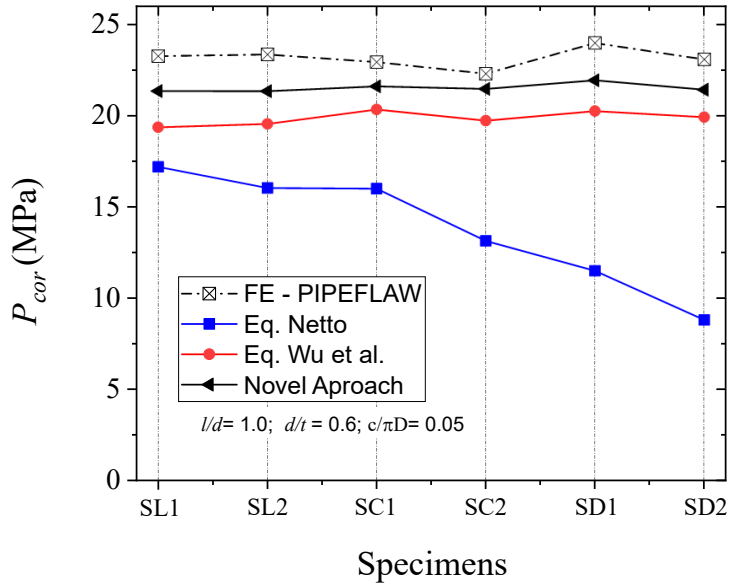

(b) $d/t = 0.6$

Source: The Author (2025).

Figure 5.5 shows the distribution of the relative error for the three methods for assessing the collapse capacity of pipelines with corrosion defects. The relative error is calculated based on the reference results obtained via numerical simulations (3D FE – PIPEFLAW). The box plot allows for comparing the accuracy and dispersion of the relative errors of the evaluated approaches.

Figure 5.5 - Distribution of Relative Error for the analyzed methods.

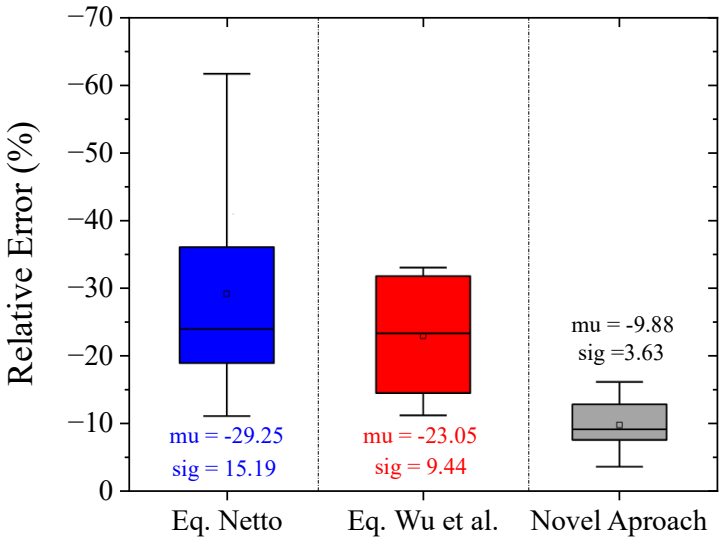

Source: The Author (2025).

As previously noted, the semi-empirical equations of Netto (2009, 2010) and Wu *et al.* (2022) underestimate the collapse pressure, with mean percentage error values of -29.25% and -23.05%, respectively. In addition, both methods exhibit a significant dispersion of the results, evidenced by the standard deviations: 15.19% (Netto, 2009, 2010) and 9.44% (Wu *et al.*, 2022).

In contrast, the novel approach proposed in this study showed superior performance, with an average percentage error of −9.88% and low dispersion (standard deviation of 3.63%). These results demonstrate precision and accuracy in estimating the collapse capacity compared to traditional methods. The results show that the novel approach effectively predicts the collapse pressure in pipelines with interacting corrosion defects, highlighting its high potential for the assessment of pipelines with multiple defects in arbitrary corrosion configurations.

5.3 FINAL REMARKS

This chapter highlighted the practical applicability of the novel approach proposed in this work for predicting the collapse pressure in subsea pipelines with corrosion defects. Due to the significant reduction in computational time compared to FEA, an extensive analysis was conducted to evaluate how metal volume loss affects the collapse capacity of subsea pipelines. The results confirmed that the pipelines'

collapse capacity decreases sharply with the increase in volume loss fraction, evidencing the impact of corrosion on the integrity of these structures.

In addition, the methodology demonstrated excellent performance in scenarios with interacting defects, significantly expanding its field of application. These findings underscore the potential of this approach as an accurate and robust tool for evaluating pipeline integrity in offshore environments.

6 CONCLUSIONS

The main objective of this thesis was to develop a methodology for assessing the structural integrity of subsea pipelines with corrosion defects under external pressure. Throughout this work, significant contributions were made to understanding the collapse behavior of corroded subsea pipelines and improving prediction methods available in the literature.

The interaction between multiple corrosion defects was investigated through extensive FE numerical analyses (Chapter 3), considering different geometries, arrangements, and operational conditions, such as initial ovality and temperature variation. The results revealed that both the size and spacing between defects directly influence the collapse pressure. Furthermore, the results proved that the initial ovality and the temperature variation affect the collapse response of subsea pipelines with single and multiple corrosion defects. So, it is necessary to consider such effects in integrity assessments. As a practical contribution, two adjustment factors were developed to incorporate these effects in predicting the collapse pressure, providing a more accurate alternative to traditional approaches.

Subsequently, a novel approach for predicting the collapse pressure of subsea pipelines with realistic corrosion defects was presented (Chapter 4). The proposed approach decomposes the complex corrosion defect into equivalent defects, and the collapse pressure for each equivalent defect is determined using a semi-empirical method available in the literature. Comparisons with traditional methods showed that the novel approach offers a more accurate estimate of the collapse pressure, significantly reducing the conservatism and dispersion of the results. Additionally, the computational performance of this method, when compared to 3D finite element analyses, demonstrates its practical applicability in the oil and gas industry.

Chapter 5 complemented previous advances by applying the novel methodology to parametric studies involving realistic defects with different material volume losses, including cases with dual interacting defects. The results confirmed the effectiveness of the proposed approach even in different scenarios, expanding its field of application. Besides that, the results indicated that the volume loss significantly affects collapse capacity, making it crucial to factor this parameter into integrity assessments.

Therefore, the results obtained in this research provide relevant technical support for improving engineering practices focused on the integrity of submarine pipelines, contributing to safer and more efficient decisions in the offshore context.

6.1 FUTURE WORK

This research's findings demonstrate the proposed approach's potential to assess the structural integrity of corroded submarine pipelines under external pressure. However, several possibilities for developing and deepening the work can still be investigated. As directions for future studies, the following suggestions stand out:

- Establish the novel approach's application to different defect geometries, types of materials, and operational and loading conditions.
- Include additional tests for other corrosion defect arrangements, i.e., colonies of interacting corrosion defects with different longitudinal and circumferential spacing between defects.
- The proposed methodology should be extended to account for internal corrosion defects, which pose a significant risk to subsea pipelines. While the current study and experimental and numerical investigations primarily address external corrosion, internal corrosion frequently occurs due to the characteristics of transported fluids and the influence of external protective coatings. Future adaptations should assess the applicability of the approach for simulating internal defects and verify their accuracy in these scenarios.
- Use optimization techniques based on numerical results from FE simulations to improve the semi-empirical equations available in the literature. This strategy aims to increase the accuracy of the collapse pressure estimates and make the methodology proposed in this thesis more useful for practical engineering.
- Conduct studies involving reliability analysis based on the approach developed in this thesis to quantify the influence of the main random variables involved in determining the collapse pressure. Such analysis can provide more realistic probabilistic estimates of pipeline structural safety and support risk management decisions.

- Integrate the proposed approach into automated evaluation systems, aiming to apply it in real-time during inspections and field operations. This application can expand the methodology's use in operational contexts, contributing to fast and accurate decision-making.
- A computational framework with an interactive user interface that incorporates the proposed methodology for assessing the structural integrity of corroded subsea pipelines under external pressure. This tool would enable practical application of the approach by engineers and professionals in the field, facilitating the entry of geometric and operational data, the execution of numerical and/or semi-empirical analyses, integration with reliability models, and the automated generation of results and recommendations for decision-making.

REFERENCES

AL-OWAISI, S. S; BECKER, Adib A.; SUN, Wei. Analysis of shape and location effects of closely spaced metal loss defects in pressurised pipes. **Engineering Failure Analysis**, v. 68, p. 172–186, 2016.

ANP. Boletim da Produção de Petróleo e Gás Natural. 2023. Disponível em: https://www.gov.br/anp/pt-br/centrais-de-conteudo/publicacoes/boletins-anp/boletins/arquivos-bmppgn/2023/boletim-setembro.pdf. Acesso em: 1 ago. 2023.

ANP. VII Workshop de Segurança Operacional e Meio Ambiente (VII Soma). 2019. Disponível em: https://www.gov.br/anp/pt-br/assuntos/exploracao-e-producao-de-oleo-e-gas/seguranca-operacional/workshop-soma/vii-workshop-de-seguranca-operacional-e-meio-ambiente-vii-soma. Acesso em: 1 ago. 2023.

ANSYS. Ansys Release 12.0 Documentation: operations guide (Chapter 3) and structural guide (Chapter 8). 2020.

BAI, Yong; BAI, Qiang. **Subsea Pipelines and Risers**. 2005.

BAI, Yong; HAUCH, Soren. Analytical collapse capacity of corroded pipes. In: **ISOPE International Ocean and Polar Engineering Conference**. 1998. p. 182–188.

BARDAL, Einar. **Corrosion and Protection**. 1. ed. Springer London, 2004-. ISSN 1619-0181.

BENJAMIN, Adilson C *et al.* Burst tests on pipeline containing interacting corrosion defects. In: **24th International Conference on Offshore Mechanics and Arctic Engineering**. 2005. p. 403–417.

BENJAMIN, Adilson C. *et al.* Interaction of corrosion defects in pipelines - Part 1: Fundamentals. **International Journal of Pressure Vessels and Piping**, v. 144, p. 56–62, 2016a. Doi: http://dx.doi.org/10.1016/j.ijpvp.2016.05.007.

BENJAMIN, Adilson C. *et al.* Interaction of corrosion defects in pipelines – Part 2: MTI JIP database of corroded pipe tests. **International Journal of Pressure Vessels and Piping**, v. 145, p. 41–59, 2016b.

BENJAMIN, Adilson C; CUNHA, Divino J S. Assessment of hydrostatic collapse of submarine pipelines: historical review of the classic methods. In: **International Pipeline Conference**. American Society of Mechanical Engineers, 2012a. p. 65-74

BENJAMIN, Adilson C; CUNHA, Divino J S. Assessment of hydrostatic collapse of submarine pipelines: the classical approach revisited. In: **International Conference on Offshore Mechanics and Arctic Engineering. American Society of Mechanical Engineers**, 2012b. p. 685-694.

BENJAMIN, Adilson C; CUNHA, Divino J S. Structural assessment of corroded deepwater pipelines subjected to dominant external Pressure – part 1: New assessment method. In: **Rio Oil & Gas Expo and Conference,** Rio de Janeiro, 2014a.

BENJAMIN, Adilson C; CUNHA, Divino J S. Structural assessment of corroded deepwater pipelines subjected to dominant external Pressure – part 2: Comparative study of four assessment methods. In: **Rio Oil & Gas Expo and Conference,** Rio de Janeiro, 2014b.

BENJAMIN, Adilson C; CUNHA, Divino J.S. New Method for the Prediction of the Hydrostatic Collapse Pressure of Submarine Pipelines. In: **Proceedings of the XXXVI Iberian102 Latin-American Congress on Computational Methods in Engineering**, Rio de Janeiro. 2015

BENSTOCK, Daniel; CEGLA, Frederic. Extreme value analysis (EVA) of inspection data and its uncertainties. **NDT&E International**, v. 87, p. 68–77, 2017.

BHARDWAJ, U.; TEIXEIRA, A. P.; GUEDES SOARES, C. Failure assessment of corroded ultra-high strength pipelines under combined axial tensile loads and internal pressure. **Ocean Engineering**, v. 257, p. 111438, 2022.

BHARDWAJ, U.; TEIXEIRA, A. P.; SOARES, C. Guedes. Reliability assessment of a subsea pipe-in-pipe system for major failure modes. **International Journal of Pressure Vessels and Piping**, v. 188, p. 104177, 2020.

BRUÈRE, Vivianne Marie *et al.* Failure pressure prediction of corroded pipes under combined internal pressure and axial compressive force. **Journal of the Brazilian Society of Mechanical Sciences and Engineering**, v. 41, n. 4, p. 1–10, 2019. Doi: https://doi.org/10.1007/s40430-019-1674-2.

BRUSCHI, R. *et al.* Pipe technology and installation equipment for frontier deep water projects. **Ocean Engineering**, v. 108, p. 369–392, 2015.

CABRAL, Rodolfo M.S. *et al.* Assessment by finite element modeling of pipelines with corrosion defects based on River-Bottom Profile model. **Engineering Structures**,v. 261, 2022.

CABRAL, Hélder L. D. *et al.* Development of Computational Tools for Automatic Modeling and FE Analysis of Corroded Pipelines. **International journal of modeling and simulation for the petroleum industry**, v. 1, n. 1, p. 9–22, 2007.

CABRAL, Hélder L.D. *et al.* The development of a computational tool for generation of high quality FE models of pipelines with corrosion defects. **Journal of the Brazilian Society of Mechanical Sciences and Engineering**, v. 39, n. 8, p. 3137–3150, 2017.

CHEN, Yanfei *et al.* Buckling analysis of subsea pipeline with idealized corrosion defects using homotopy analysis method. **Ocean Engineering**, v. 234, 2021a.

CHEN, Yanfei *et al.* Collapse failure and capacity of subsea pipelines with complex corrosion defects. **Engineering Failure Analysis**, v. 123, 2021b.

CHEN, Yanfei *et al.* Failure analysis of high strength pipeline with single and multiple corrosions. **Materials and Design**, v. 67, p. 552–557, 2015.

CHOUCHAOUI, B. A.; PICK, R. J. Behaviour of longitudinally aligned corrosion pits. **International Journal of Pressure Vessels and Piping**, v. 67, n. 1, p. 17–35, 1996.

COSHAM, A.; HOPKINS, P.; MACDONALD, K. A. Best practice for the assessment of defects in pipelines - Corrosion. **Engineering Failure Analysis**, v. 14, n. 7, p. 1245–1265, 2007.

CUI, Xiaofei; LIANG, Xiaoxia; BHARADWAJ, Ujjwal. A framework for corrosion assessment in metallic structures, from data analysis to risk based inspection. **Eksploatacja i Niezawodnosc – Maintenance and Reliability**, v. 23, n. 1, p. 11–20, 2021.

CUNHA, Divino J. S. *et al*. Hydrostatic collapse tests of full-scale pipeline specimens with thickness metal loss. In: **International Pipeline Conference**. American Society of Mechanical Engineers, 2020. Doi: https://doi.org/10.1115/IPC2020-9562

D'AGUIAR, Savanna C. M.; MOTTA, Renato de S.; AFONSO, Silvana M. B. An investigation on the collapse response of subsea pipelines with interacting corrosion defects. **Engineering Structures**, v. 321, 2024.

D'AGUIAR, Savanna C. M.; MOTTA, Renato de S.; FERREIRA, Adriano D. M., AFONSO, Silvana M. B. Novel approach of collapse pressure prediction for subsea pipelines with realistic corrosion defects. **Ocean Engineering**, v. 337, 2025.

D'Aguiar Savanna. C. M, Motta, Renato de S; Afonso, Silbana. M. B. Collapse of subsea pipelines: Numerical study on the interaction of corrosion defects with different geometrical properties. In: **27th COBEM – International Congress of Mechanical Engineering**. Florianópolis, Brasil, 2023.

D'AGUIAR, Savanna C. M.; MOTTA, Renato de S.; FERREIRA, Adriano D. M., AFONSO, Silvana M. B. An investigation on the collapse pressure prediction of subsea pipelines with realistic corrosion defects. In: **XLV Ibero-Latin American Congress on Computational Methods in Engineering**. Maceió, Brasil, 2024.

DNV, (Det Norske Veritas). DNV-OS-F101 Submarine Pipeline Systems. 2013.

DNV, (Det Norske Veritas). DNV-ST-F101 Submarine pipeline systems. 2021.

DNV, (Det Norske Veritas). Recommended practice DNVGL-RP-F101 - corroded pipelines. 2017.

DRUMOND, Geovana P. *et al.* Pipelines, risers and umbilicals failures: A literature review. **Ocean Engineering**, v. 148, p. 412–425, 2018.

DURET-THUAL, C. Understanding corrosion: Basic principles. In: **Understanding Biocorrosion: Fundamentals And Applications**. p. 3–32. 2014.

EASTVEDT, Daniel; NATERER, Greg; DUAN, Xili. Detection of faults in subsea pipelines by flow monitoring with regression supervised machine learning. **Process Safety and Environmental Protection,** v. 161, p. 409–420, 2022.

FAN, Zhiyuan *et al.* Effect of axial length parameters of ovality on the collapse pressure of offshore pipelines. **Thin-Walled Structures**, v. 116, p. 19–25, 2017.

FENG, Chunjian; WU, Hang; LI, Xin. Buckling Analysis of Corroded Pipelines under Combined Axial Force and External Pressure. **Metals**, v. 12, n. 2, 2022.

FERREIRA, Adriano D. M. *et al.* Stochastic assessment of burst pressure for corroded pipelines. **Journal of the Brazilian Society of Mechanical Sciences and Engineering,** v. 43, n. 4, 2021.

FERREIRA, Adriano D. M.; WILLMERSDORF, Ramiro B.; AFONSO, Silvana M.B. Corroded pipeline assessment using neural networks, the Finite Element Method and discrete wavelet transforms. **Advances in Engineering Software**, v. 196, 2024.

FRALDI, M. *et al.* An improved formulation for the assessment of the capacity load of circular rings and cylindrical shells under external pressure. Part 2. A comparative study with design codes prescriptions, experimental results and numerical simulations. **Thin-Walled Structures**, v. 49, n. 9, p. 1062–1070, 2011.

FRALDI, M.; GUARRACINO, F. An improved formulation for the assessment of the capacity load of circular rings and cylindrical shells under external pressure. Part 1. Analytical derivation. **Thin-Walled Structures**, v. 49, n. 9, p. 1054–1061, 2011.

GERE, James M.; TIMOSHENKO, Stephan P. **Theory of elastic stability**. McGrawHill Book Co, v. 3, p. 91–126, 1961.

GONG, Shunfeng *et al.* Buckle propagation of sandwich pipes under external pressure. **Engineering Structures**, v. 175, p. 339–354, 2018.

GONG, Shunfeng *et al.* On the collapse of thick-walled pipes with corrosion defects under external pressure. **Marine Structures**, v. 76, 2021.

GONG, Shunfeng *et al.* On the influence of interacting dual defects on the collapse pressure of pipes under external pressure. **Thin-Walled Structures,** v. 157, 2020.

GONG, Shunfeng; LI, Gen. Buckle propagation of pipe-in-pipe systems under external pressure. **Engineering Structures**, v. 84, p. 207–222, 2015.

GONG, Shunfeng; WANG, Xipeng; YUAN, Lin. On the arresting performance of welded-ring buckle arrestor for subsea pipelines. **Ships and Offshore Structures**, v. 15, n. 10, p. 1057–1069, 2020.

GUO, Boyun *et al.* **Offshore Pipelines: Design, Installation, and Maintenance**. Second Editioned.Elsevier, 2014.

HAAGSMA, S. C; SCHAAP, D. Collapse resistance of submarine lines studied. **Oil and Gas Journal**, v. 79, p. 86–90, 1981.

HAQ, M Masood; KENNY, S. Lateral buckling response of subsea hthp pipelines using finite element methods. In: **International Conference on Ocean**. American Society of Mechanical Engineers, 2013.

HE, Tong; DUAN, Menglan; AN, Chen. Prediction of the collapse pressure for thick-walled pipes under external pressure. **Applied Ocean Research**, v. 47, p. 199–203, 2014.

IDRIS, Nurul Neesa *et al.* Burst capacity and development of interaction rules for pipelines considering radial interacting corrosion defects. **Engineering Failure Analysis**, v. 121, 2021.

KAISER, Mark J. **The Offshore Pipeline Construction Industry.** Elsevier, 2020.

KAMALARASA, S; CALLADINE, C. R. Buckle Propagation in Submarine Pipelines. **International Journal of Mechanical Sciences**, v. 30, p. 217–228, 1988.

KARA, Fuat; NAVARRO, Josef; ALLWOOD, Robert L. Effect of thickness variation on collapse pressure of seamless pipes. **Ocean Engineering**, v. 37, n. 11–12, p. 998–1006, 2010.

KYRIAKIDES, Stelios; CORONA, Edmundo. **Mechanics of offshore pipelines**. 2007.

KYRIAKIDES, Stelios; LEE, Liang-Hai. On the Propagation Pressure of Pipelines. In: **Mechanics Of Offshore Pipelines**, **Volume 2**. Elsevier, 2021. v. 2, p. 37–77.
LI, Xin *et al.* Effect of interaction between corrosion defects on failure pressure of thin wall steel pipeline. **International Journal of Pressure Vessels and Piping**, v. 138, p. 8–18, 2016.

LI, Songling *et al.* Research on remaining bearing capacity evaluation method for corroded pipelines with complex shaped defects. **Ocean Engineering**, v. 296, 2024.

LI, Ruoxuan; CHEN, Baiqiao; GUEDES SOARES, C. Design equation for the effect of ovality on the collapse strength of sandwich pipes. **Ocean Engineering**, v. 235, 2021.

LI, Ruoxuan; CHEN, Bai Qiao; SOARES, C. Guedes. Effect of Ovality Length on Collapse Strength of Imperfect Sandwich Pipes Due to Local Buckling. **Journal of Marine Science and Engineering**, v. 10, n. 1, 2022.

LI, Tao; XIE, Peng; LIU, Shicheng. Collapse of pipes with non-uniform corrosion defects under external pressure: A reverse inversion modeling method. **Engineering Failure Analysis**, v. 153, 2023.

LIU, Xiuquan *et al.* Multi-level optimization of maintenance plan for natural gas pipeline systems subject to external corrosion. **Journal of Natural Gas Science and Engineering**, v. 50, p. 64–73, 2018.

MAHMOODIAN, Mojtaba; LI, Chun Qing. Failure assessment and safe life prediction of corroded oil and gas pipelines. **Journal of Petroleum Science and Engineering**, v. 151, p. 434–438, 2017.

MARQUARDT, Donald W. An algorithm for least-squares estimation of nonlinear parameters. **Journal of the society for Industrial and Applied Mathematics**, v. 11, p. 431–441, 1963.

MELO, Carlos *et al.* Extreme value modeling of localized internal corrosion in unpiggable pipelines. **International Journal of Pressure Vessels and Piping**, v. 182, 2020.

MONDAL, Bipul Chandra; DHAR, Ashutosh Sutra. Interaction of multiple corrosion defects on burst pressure of pipelines. **Canadian Journal of Civil Engineering**, v. 44, n. 8, p. 589–597, 2017.

MOTTA, Renato de S. *et al.* Comparative studies for failure pressure prediction of corroded pipelines. **Engineering Failure Analysis**, v. 81, n. July 2016, p. 178–192, 2017.

MOTTA, Renato de S.; *et al.* Reliability analysis of ovalized deep-water pipelines with corrosion defects. Marine Structures, v. 77, 2021.

MOTTA, Renato de S.; Ferreira, Adriano D. M.; AFONSO, Silvana M. B. Probabilistic assessment of complex corrosion in pipelines considering River-Bottom Profile information. **Engineering Failure Analysis**, v. 165, 2024.

MURPHEY, C. E; LANGNER, C. G. Ultimate pipe strength under bending, collapse, and fatigue. In: **Proc. of the 4th International Offshore Mechanics and Arctic Engineering Conference** (OMAE 85). p. 467-477, 1985.

MUTHUKUMAR, N. Petroleum Products Transporting Pipeline Corrosion-A Review. In: **The Role of Colloidal Systems in Environmental Protection**. Elsevier Inc., 2014. p. 527–571.

NETTO, T. A. A simple procedure for the prediction of the collapse pressure of pipelines with narrow and long corrosion defects - Correlation with new experimental data. **Applied Ocean Research**, v. 32, n. 1, p. 132–134, 2010.

NETTO, T. A. On the effect of narrow and long corrosion defects on the collapse pressure of pipelines. **Applied Ocean Research**, v. 31, n. 2, p. 75–81, 2009.

NETTO, T. A.; FERRAZ, U. S.; BOTTO, A. On the effect of corrosion defects on the collapse pressure of pipelines. **International Journal of Solids and Structures**,v. 44, n. 22–23, p. 7597–7614, 2007.

NOGUEIRA, André C; MCKEEHAN, David S. **Handbook of Offshore Engineering**. 2005.

NOVITSKY, Adriano; GRAY, Fin. Flexible and Rigid pipe solutions in the development of ultra-deepwater fields. In: **22nd International Conference on Offshore Mechanics and Arctic Engineering**, p. 755-770, 2003.

OLATUNDE, Michael *et al.* An investigation on the effect of widespread internal corrosion defects on the collapse pressure of subsea pipelines. **Ocean Engineering**, v. 287, 2023.

PAPADAKIS, George. Buckling of thick cylindrical shells under external pressure: A new analytical expression for the critical load and comparison with elasticity solutions. **International Journal of Solids and Structures**, v. 45, n. 20, p. 5308–5321, 2008.

PATRAN. MSC Patran Library (PCL Manuals) and MSC. Acumen Library (Develop Manuals). 2012.

PENGCHAO, Chen. Advancements and future outlook of safety monitoring, inspection and assessment technologies for oil and gas pipeline networks. **Journal of Pipeline Science and Engineering**, 2025

PHMSA, Pipeline and Hazardouss Materials Safety Administration. **Pipeline Safety Research and Development Plan for FY 2021/2022**. 2022. Disponível em: https://www.phmsa.dot.gov/. Acesso em: 14 nov. 2023.

PIMENTEL, Júlio Tenório *et al.* New procedure of automatic modeling of pipelines with realistic shaped corrosion defects. **Engineering Structures**, v. 221, 2020.

PYTHON. Python. Tutorial and library reference manual. 2011.

QIN, Guojin; CHENG, Y. Frank. A review on defect assessment of pipelines: Principles, numerical solutions, and applications**. International Journal of Pressure Vessels and Piping**, v. 191, 2021.

RIKS, E. The Application of Newton's Method to the Problem of Elastic Stability 1. **Journal of Applied Mechanics**, v. 39, n. 4, p. 1060–1065, 1972.

SAKAKIBARA, Naoto; KYRIAKIDES, Stelios; CORONA, Edmundo. Collapse of partially corroded or worn pipe under external pressure. **International Journal of Mechanical Sciences**, v. 50, n. 12, p. 1586–1597, 2008.

SHIBATA, Toshio. Application of Extreme Value Statistics to Corrosion. **Journal of Research of the National Institute of Standards and Technology**, v. 99, n. 4, 1994.

SILVA, R. C.C.; GUERREIRO, J. N.C.; LOULA, A. F.D. A study of pipe interacting corrosion defects using the FEM and neural networks. **Advances in Engineering Software**, v. 38, n. 11–12, p. 868–875, 2007.

SMIRNOV, Veniamin; MA, Zhuanzhuan; VOLCHENKOV, Dimitri. Extreme events and emergency scales. **In: Mathematical Methods in Modern Complexity Science.** Cham: Springer International Publishing, p. 99-128, 2021.

SOARES, Elder *et al.* Structural integrity analysis of pipelines with interacting corrosion defects by Multiphysics modeling. **Engineering Failure Analysis**, v. 97, n. January, p. 91–102, 2019.

SULAIMAN, Nurul Sa'aadah; TAN, Henry. Third party damages of offshore pipeline. **Journal of Energy Challenges and Mechanics**, v. 1, n. 1, p. 14, 2014.

SUN, Jialin. Development of Finite Element-based Models for Defect Assessment on Pipelines. 2020. 196 f. – Thesis – University of Calgary, Graduate Program in Mechanical and Manufacturing Engineering, Calgary, 2020.

SUN, Jialin; CHENG, Y. Frank. Assessment by finite element modeling of the interaction of multiple corrosion defects and the effect on failure pressure of corroded pipelines. **Engineering Structures**, v. 165, p. 278–286, 2018.

SUN, Jialin; CHENG, Y. Frank. Modeling of mechano-electrochemical interaction between circumferentially aligned corrosion defects on pipeline under axial tensile stresses. **Journal of Petroleum Science and Engineering**, v. 198, 2021.

TAN, Mike Yongjun. **Localized Corrosion in Complex Environments**. John Wiley & Sons. 2023.

TIAN, Haifeng *et al.* The effect of corrosion defects on the collapse pressure of submarine pipelines. **Ocean Engineering**, v. 310, 2024.

TORSELLETTI, Enrico *et al.* Minimum Wall Thickness Requirements for Ultra Deep-Water Pipelines. In: **International Conference on Offshore Mechanics and Arctic Engineering. Cancun**, México, p. 647–660. 2003.
VELÁZQUEZ, J. C. *et al.* Failure pressure estimation for an aged and corroded oil and gas pipeline: A finite element study. **Journal of Natural Gas Science and Engineering**, v. 101, 2022.

VIETH, P H; KIEFNER, J F. **RSTRENG2 user's manual. Final report**. American Gas Association, Inc., Arlington, VA (United States). Pipeline Research Committee; Kiefner and Associates, Inc., Worthington, OH (United States), 1993.

WANG, Huakun *et al.* Effect of 3D random pitting defects on the collapse pressure of pipe — Part I: Experiment. **Thin-Walled Structures**, v. 129, p. 512–526, 2018a.

WANG, Huakun *et al.* Effect of 3D random pitting defects on the collapse pressure of pipe — Part II: Numerical analysis. **Thin-Walled Structures**, v. 129, p. 527–541, 2018b.

WU, Hang *et al.* Buckling response of subsea pipeline with irregular corrosion defect under external pressure. **Ocean Engineering**, v. 280, 2023.

WU, Hang *et al.* Experimental and numerical studies on collapse of subsea pipelines with interacting corrosion defects. **Ocean Engineering**, v. 260, 2022.

XIE, Ying; MENG, Jin; CHEN, Diwen. Wax deposition law and OLGA-Based prediction method for multiphase flow in submarine pipelines. **Petroleum**, v. 8, n. 1, p. 110–117, 2022.

XU, Lei *et al.* The research progress and prospect of data mining methods on corrosion prediction of oil and gas pipelines. **Engineering Failure Analysis**, v. 144, 2023.

XU, Quanbiao; GONG, Shunfeng; HU, Qing. Collapse analyses of sandwich pipes under external pressure considering inter-layer adhesion behaviour. **Marine Structures**, v. 50, p. 72–94, 2016.

XUE, Jianghong; GAN, Neng. A comprehensive study on a propagating buckle in externally pressurized pipelines. **Journal of Mechanical Science and Technology**, v. 28, n. 12, p. 4907–4919, 2014.

XUE, J.; HOO FATT, M. S. Buckling of a non-uniform, long cylindrical shell subjected to external hydrostatic pressure. **Engineering Structures**, v. 24, n. 8, p. 1027–1034, 2002.

XUE, Jianghong; HOO FATT, Michelle S. Symmetric and anti-symmetric buckle propagation modes in subsea corroded pipelines. **Marine Structures**, v. 18, n. 1, p. 43–61, 2005.

YAN, Sun Ting; SHEN, Xiao Li; JIN, Zhi Jiang. On instability failure of corroded rings under external hydrostatic pressure. **Engineering Failure Analysis**, v. 55, p. 39–54, 2015.

YE, Hao; YAN, Sunting; JIN, Zhijiang. Collapse of corroded pipelines under combined tension and external pressure. **PLoS ONE**, v. 11, n. 4, 2016.
YEH, M. K.; KIRIAKIDES, s. On the Collapse of Inelastic Thick-Walled Tubes Under External Pressure. **J. Energy Resour. Technol**, v. 108(1), p. 35–47, 1986.

YU, Jianxing *et al.* Computation of plastic collapse capacity of 2D ring with random pitting corrosion defect. **Thin-Walled Structures**, v. 119, p. 727–736, 2017.

YU, Jianxing *et al.* Research progress of buckling propagation experiment of deep-water pipelines. **Transactions of Tianjin University**, v. 22, n. 4, p. 285–293, 2016.

ZHANG, Xinhu; CHEN, Baiqiao; GUEDES SOARES, C. Effect of non-symmetrical corrosion imperfection on the collapse pressure of subsea pipelines. **Marine Structures**, v. 73, 2020.

ZHANG, Xinyan; LIAN, Jinguo. Analysis of Extreme Value at Risk to Amazon Stocks. **International Journal of Engineering Research and Development**, v. 14, n. 2, p. 62–71, 2018.

ZHANG, Xinhu; PAN, Guang. Collapse of thick-walled subsea pipelines with imperfections subjected to external pressure. **Ocean Engineering**, v. 213, 2020.

ZHOU, Rui *et al.* Finite element analysis of the failure of high-strength steel pipelines containing group corrosion defects. **Engineering Failure Analysis**, v. 136, 2022.

ZHOU, Libei *et al.* Theoretical analysis of the collapse behaviour of subsea pipelines with corrosion defects under external pressure. **Ocean Engineering**, v. 307, 2024.

ZHU, Xian Kui. A comparative study of burst failure models for assessing remaining strength of corroded pipelines. **Journal of Pipeline Science and Engineering**, v. 1, n. 1, p. 36–50, 2021.

ZHU, Xian-Kui. Assessment methods and technical challenges of remaining strength for corrosion defects in pipelines. In: **Pressure Vessels and Piping Conference.** American Society of Mechanical Engineers, 2018.